# SEISMIC SHEAR DEMAND IN REINFORCED CONCRETE CANTILEVER WALLS

by

Jeffrey Scott Yathon

B.Sc., University of Calgary, 2008

A THESIS SUBMITTED IN PARTIAL FULFILLMENT OF
THE REQUIREMENTS FOR THE DEGREE OF

MASTER OF APPLIED SCIENCE

in

The Faculty of Graduate Studies

(Civil Engineering)

THE UNIVERSITY OF BRITISH COLUMBIA
(Vancouver)

April 2011

# ABSTRACT

This thesis addresses the issue of seismic shear force demand in reinforced concrete cantilever walls, and specifically the dynamic amplification of shear force due to higher mode effects. Current design codes either do not account for this phenomenon, or vary considerably in the approach they take. In order to determine the reason for the variation, previous research is first examined, and it is found that the conclusions reached are not consistent with each other. It is identified that a major source of the problem is a lack of a comprehensive analysis of the problem.

To attempt to address this issue, the analysis portion of the thesis starts by performing response spectrum analysis on structures with heights ranging from 5 to 70 storeys. It is shown that when a pin is placed at the bottom of the structure to simulate yielding, the moment is limited but the shear can still increase. A simple relationship between the fixed base and pinned base shear is found. Reduction in the shear stiffness, possible yielding higher in the structure, and the effect of the spectrum are also issues examined.

The next two chapters deal with both linear and nonlinear time history analyses performed using OpenSees. Linear time history analysis is used to demonstrate the issues with ground motion scaling in tall structures. It is then shown that the shear at the base of the structure from a nonlinear analysis is more than the code predicts, as is the moment higher up in the structure. Furthermore, the shear at the base of the structure remains relatively constant no matter how the rest of the structure yields. A possible model is then proposed which adds the pinned response spectrum analysis results to the reduced shear. This model is compared to the nonlinear results and it is found to agree well.

Finally, a chapter is devoted to factors which may complicate the results. They are separated into two sections: choice of hysteretic model, and the influence of the shear capacity on the demand. It is determined that further research is needed in these areas.

# TABLE OF CONTENTS

# LIST OF TABLES

# LIST OF FIGURES

# ACKNOWLEDGEMENTS

First and foremost I would like to thank my supervisor, Dr. Perry Adebar, for his support and contributions. I also appreciate the input of my colleagues, and specifically Stephen and Ehsan, who have provided different perspectives. My thanks to Dr. Ken Elwood for his input whenever I had a question about some specific bit of analysis, and for being my second reader. Without the generous funding from NSERC and UBC I would not be able to be lucky enough to live in beautiful Vancouver, so many thanks to those organizations. And finally, I would like to thank my friends and family, and in particular my parents, for being there when I needed to think about things other than this thesis.

# 1 INTRODUCTION

Throughout the world, one of the most common seismic force resisting systems is the reinforced concrete cantilever shear wall. In western Canada it is by far the most common system used in high rise construction, and generally is used in one of the principle directions as part of a rectangular box (called the core), the other direction being comprised of coupled shear walls to allow for access openings. However despite being so widely used some aspects of the seismic response of cantilever shear walls are still not well understood, in particular the question of how to determine the design shear force. This thesis will attempt to address this issue.

Current design philosophy, as detailed in the National Building Code of Canada 2005 (NRC, 2005) and in other design codes around the world, links the shear force over the height of the wall to the base moment. In other words, it is assumed that whatever relationship exists between the two in the elastic system will remain constant when the structure becomes inelastic. This is represented in the code by the ductility factor $R_d$, by which both the elastic shear force and elastic bending moment are divided to obtain the inelastic design forces. The implicit assumption is that when yielding occurs at the base of the structure, it will limit the shear force in the same way that it limits the moment. Unfortunately, due to the fact that the modal contributions to the shear and the moment are not identical, the picture is not that simple. Previous research has shown that the shear force tends to be larger than predicted, a phenomenon known as “dynamic shear amplification”. Some design codes recognize that this problem exists (SEAOC, 2009; CEN, 2004), and attempt to account for this amplification by multiplying the shear force by some factor.

So then, if methods for correcting the mistake of tying the shear to the moment already exist, why is further research necessary? It turns out that not only do the various methods disagree with each other (in that they predict different levels of amplification), but they vary to a surprising extent. Furthermore, not only do the predictions vary, but so does the basic methodology, including which parameters are used to calculate the amplification. For example, the most basic method uses only the number of storeys as a parameter, while some of the more complex methods use the modal results from a response spectrum analysis along with ductility factors. Finally, researchers have developed these methods for application in different codes, meaning that often it is unclear

whether they are meant to be applied to the static or dynamic results from a code analysis. This has led to cases where corrections developed for use with the static method have been applied to results from the dynamic method, without investigation into whether this is appropriate.

To this end, the objectives of this study are twofold: first to understand the phenomena of shear amplification, and then to develop a model to predict the appropriate level of shear amplification. By understanding qualitatively how shear amplification occurs, and why it is inappropriate to link the shear to the moment, a solid rational base can be developed to use when quantifying the problem. Furthermore, this understanding should reveal the reason for the differences in the proposed methods of previous researchers. Ideally, the method developed in this study would use common design parameters, and would be simple enough to be implemented (perhaps with minor modifications) in any modern design code. However, because this study takes place within the context of the Canadian design community, the terminology used will be that of NBCC 2005.

In order to meet these objectives, this main body of this study has been organized into chapters two through five, with the final proposed model and comparisons to existing models appearing at the end of chapter five. A brief outline of the goals of each chapter follows.

It has been mentioned already that there has been work on the topic of shear amplification in the past. Chapter 2 summarizes the previous papers in the field, from the original work done on the subject in 1975 to more refined work done recently, and includes a section on some distinctly Canadian approaches. In the chapter, the papers are arranged not chronologically, but instead by the method that they chose to try to quantify the phenomena. This enables the reader to see clearly the associations between works. Perhaps the most important parts of Chapter 2 are the final two, where the historic methods are applied to a number of model structures of varying heights. This enables graphical comparisons, and furthermore using the data generated from these calculations a number of issues are identified. For example, these include questions about which parameters are important, and whether different spectra should result in different amplifications. Lastly, the chapter concludes with a brief analysis of where some of the previous research may have diverged, and what the individual studies seemed to have lacked.

A preamble to the major analysis work of this thesis is found in Chapter 3, where the analysis parameters are defined. The biggest contribution of this chapter is defining the example structures which are then used for the remainder of the thesis. As well, Chapter 3 goes into detail with regards to spectra, ground motions, damping, hysteretic behaviour, and other issues needed to perform both response spectrum analyses and nonlinear time history analyses.

The analysis part of this thesis starts in Chapter 4, where a comprehensive response spectrum analysis (RSA) study is carried out. RSA is central to work in the topic of shear amplification because it enables the user to perform a simple analysis on a number of structures, and, critically, to separate out the modal contributions. Analysis is first carried out the example structures, ranging from five to seventy storeys, and there is some discussion about the significance of the modal contributions.

Chapter 3 then continues on to perform a number of RSA with the base of the structure pinned (a soft spring is used to simulate this condition), which is interesting because a full set of results is generated. The idea is to attempt to represent the nonlinear yielding of the base of the wall in a linear RSA model. Using the results, the causes of the shear amplification phenomenon can be explored, and furthermore possibilities for applying the pinned base data to potential models can be examined. Also discussed within the chapter are what happens to the results when the shear stiffness is reduced (simulating cracking), and the effects of different spectral shapes on the curves. The power using simple methods is demonstrated in a short case study concerning issues with the NBCC 2005 spectrum leveling off after 4.0s.

However, using RSA has its limitations, the first and foremost being that it cannot predict the nonlinear response of a structure without assumptions being made (such as that the shear is linked to the moment). Because of this, any study dealing concerning itself with nonlinear phenomena must employ a more detailed method, and in Chapter 5, the structures are analyzed by nonlinear time history analysis (NLTHA).

Chapter 5 then starts with a brief section on linear time history analysis (LTHA), with the goal of examining the differences between RSA and LTHA and examining first whether any differences exist, and second whether these contribute towards any shear amplification. The issues of ground motion

selection and scaling can be best addressed by considering the LTHA results, so a discussion on those issues is also found. The central part of the chapter is then analyzing the structures when they go into the nonlinear range. Data from the many nonlinear analyses carried out are organized into both maximum absolute value sets, and also full time history sets, and using both of these representations of the response, the shear amplification phenomenon is discussed. It is the goal with these discussions to both sharpen the understanding of how shear amplification happens, but also to try and see if any useful information is obtained to the end of trying to create a model.

Ultimately, the approach this thesis is attempting to take when creating a model for the maximum shear force is to minimize the amount of empirical fitting of lines, and instead to attempt to use the basic concepts gained from previous parts of the thesis to construct a model which can then be compared to the NLTHA. In chapter five, this goal is accomplished by combining some rational parts from chapter three as well as using some empirical data to generate a full model to predict the maximum shear. This model can then be compared to both the NLTHA results and the predictions of previous models.

At this point in the thesis, one of the main objectives will be complete – creating a model to predict the maximum shear. However, while Chapters 4 and 5 have contributed significantly to understanding the phenomenon, there are still some questions that remain. Providing full answers to these questions are outside the scope of this thesis, mainly because they are full topics within themselves. Despite this, it is possible to do some preliminary investigation into each area, and Chapter 6 summarizes this work.

The two main issues addressed are hysteretic models, and multiple shear peaks. Typically the hysteretic models used in previous research have employed a bilinear backbone curve, and this work is no exception. However, recent work has provided a trilinear moment-curvature relationship specifically designed for use with high rise cantilever shear walls. Some preliminary NLTHA results from this work are compared to the results from this thesis, with a focus on how both the moment and shear demands change based on the ductility level.

Lastly, the idea of looking at multiple shear peaks is raised. In general, and in most of this thesis, only the maximum shear is considered, with the assumption that the structure will fail in a brittle

manner once this shear is reached. However, this is not true, and it is conceivable that a structure would not actually fail with only a very short pulse of high shear. Therefore, some work will be done on attempting to capture how many large cycles of shear the structure will see, and also some brief discussion on how many of these cycles it would take to fail a wall.

# 2 LITERATURE REVIEW

Research on shear amplification in cantilever concrete walls began in 1975, and continues to the present day, with more sophisticated models and methods advancing the state of the art. Many of the methods developed have been implemented in building codes across the world, with the Canadian Concrete Code (CSA, 2004) being one of them. Unfortunately, there is not currently a consensus among academics as to what is the correct approach, and many of the proposed methods contradict each other. Some researchers attempt to take a theoretical approach to the problem, while some rely on computer modeling, and yet others use small-scale tests of walls. Chapter 2 of this thesis will summarize and explain what has been done to date, compare the methods proposed, and discuss the papers critically with a view to explain discrepancies.

## 2.1 SUMMARY OF PREVIOUS PAPERS

The summary of papers is not organized chronologically, but into subsections that describe approximately the approach each author took, from basic parametric studies to methods that attempt to explicitly use the results from a modal analysis.

### 2.1.1 PARAMETRIC APPROACHES

**Blakely, Cooney & Megget (1975)**

The first paper that addressed the problem of shear amplification was Blakely et al. (1975), published in New Zealand. Perhaps the most influential paper on the subject of shear amplification, the authors begin by emphasizing the importance of the problem – in order for a wall to dissipate energy in a flexural mode, brittle shear failure must not occur. This is consistent with the capacity design approach taken in most codes around the world, including CSA A23.3 (CSA, 2004) in Canada. They go on to show that while code static procedures usually assume a triangular load distribution (with some modifications), the influence of higher modes may result in larger shear forces at the base of the wall, and possibly flexural yielding higher up in the wall.

Blakely, et al. (1975) attempt to investigate the large shear forces in two ways. The first is to perform a response spectrum analysis on a 10-storey structure, and combine the modal forces in such a way as to cause flexural yielding at the base of the wall. However, instead of using modal combination techniques such as square-root-sum-of-the-squares (SRSS), they simply take the full second and third modes and determine what proportion of the first mode is required to initiate

yielding. Using this method they find that the base shear is much larger than predicted by a code static analysis, and that mid-height yielding can occur before base yielding. Whether these modal combinations are likely to occur simultaneously under an earthquake is unclear, and Blakely, et al. (1975) came to the conclusion that nonlinear analysis is preferable.

The nonlinear analyses they performed were on a 6 storey structure ($T_1$ = 0.45s), a 10 storey structure ($T_1$ = 0.81s) and a 20 storey structure ($T_1$ = 1.2s), under 5 different unscaled earthquake records. The program used was DRAIN-2D, with beam-column elements representing the shear wall, and concentrated plastic hinging allowed at the end of each element. The moment-curvature hysteretic behavior was assumed to be bilinear. Due largely to the difference in intensity between each of the records (for example Taft (1952) with a PGA of 0.16g vs. Pacoima Dam (1971) with a PGA of 1.2g) a large spread of base shear amplification factors was found, ranging from 0.83 to 3.35 times the static shear. Under the larger earthquakes it was also found that flexural yielding occurred further up the height of the structure, in addition to the base.

Finally, Blakely, et al. (1975) proposed a method to determine a modified shear envelope (based on the results of their nonlinear analysis), by first determining the shear envelope from the static code procedure, then applying an amplification factor to find the design shear forces. Their approach was codified in the New Zealand Design Standards (NZS, 1982), by the following equation:

$$\omega_v = 0.9 + \frac{n}{10} \; for \; n < 6 \tag{2-1}$$

$$\omega_v = 1.3 + \frac{n}{30} \leq 1.8 \; for \; n \geq 6 \tag{2-2}$$

Where $\omega_v$ is the dynamic shear amplification factor to be applied to the static analysis, and *n* is the number of storeys in the structure. Equations 2-1 and 2-2 propose an increase in amplification with building height, separated into two linear curves, and with an upper limit of 1.8 after 15 storeys. These factors were developed using only two of the five earthquakes under which the structures were analyzed (El Centro (1940) and simulated earthquake “B1”), and that the authors specifically state that if a larger level of seismic shaking were to be designed for the factors would have to be increased.

Possibly because it was the first paper on the topic, this approach has appeared in building codes and guidelines worldwide, including CSA A23.3-94 (CSA, 1994) and more recently the SEAOC Blue Book (2009), although the latter publication distinguishes between static and dynamic analyses, and proposes the following equation for amplifying the results of a dynamic analysis:

$$\omega_d = 1.2 + \frac{n}{50} \tag{2-3}$$

Where $\omega_d$ is the amplification factor to be applied to a linear dynamic response spectrum analysis. In contrast to Equations 2-1 and 2-2, there is no upper limit on Equation 2-3.

**Rutenberg & Nsieri (2006)**

The work of Rutenberg & Nsieri (2006) is somewhat a departure from more recent research on shear amplification, choosing to develop a parametric solution to the problem, as opposed to attempting to explicitly consider modal contributions (see Section 2.1.4). They use the results of simple nonlinear analyses performed on model structures with fundamental periods ranging from 0.3s to 3.0s to investigate both the shear at the base of the structure and the shear envelope. The nonlinear analyses were performed using Ruaumoko, assumed elastic perfectly plastic response, and for the seismic input used two suites of 20 ground motions each.

Rutenberg & Nsieri (2006) then proceeded to plot the mean base shear amplification factor versus the fundamental period for a range of "q" values – the ratio of the elastic strength to the actual strength ($R_d$ in Canada). In their paper the amplification factor $\omega_v$ is defined as the ratio of the maximum shear observed to the static shear $V_d$:

$$V_d = \frac{M_y}{\frac{2}{3}H\left(1 + \frac{1}{2n}\right)} \tag{2-4}$$

Where H is the building height, n is the number of storeys, and $M_y$ is the moment required to initiate yielding at the base of the wall. These ratios are compared to the Eurocode 8 (CEN,2004) approach to the problem, based on the work of Keintzel (1992) (see Section 2.1.3), and the Eurocode 8 approach is found to poorly estimate the amplification. However, it is important to note that the

amplification factor developed by Keintzel (1992) was intended to be applied to the results from a response spectrum analysis, so this may be an unfair comparison.

Given the apparent inadequacy of the Eurocode 8 (CEN, 2004) approach, Rutenberg & Nsieri (2006) choose to model the amplification curves linearly. Although there is some discrepancy between the linear equations and the curves, particularly at short periods, the overall fit is not unreasonable. The equation defining these lines is:

$$\omega_v = 0.75 + 0.22(T + q + Tq) \tag{2-5}$$

Where T is the fundamental period of the structure. Because the fundamental period of the structure is to an extent related to the number of storeys in the structure, compared to Blakely, et al. (1975), Rutenberg & Nsieri (2006) have added the ductility factor q (or $R_d$).

The authors also propose a different shape of the shear envelope than that from either static or response spectrum analysis, in order to capture the effects of the higher modes at the top of the structure. The method requires that the wall be designed for at least half of the base shear force the entire way up the structure, as shown in Figure 2.1 below:

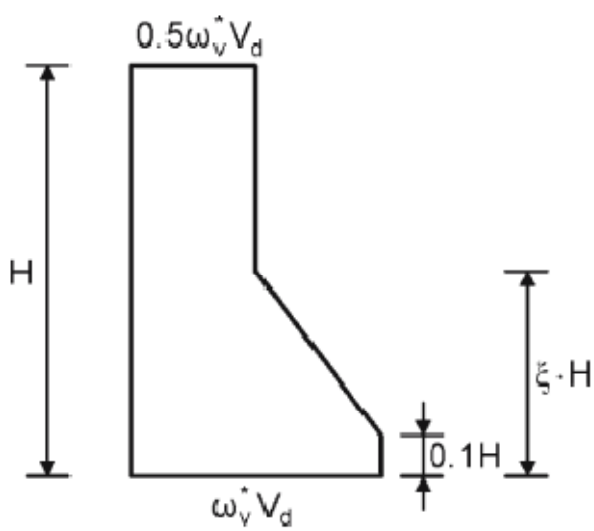


*Figure 2.1: Proposed shear force diagram from Rutenberg & Nsieri (2006), $\omega_v$ is from Equation 2-5, $V_d$ is from Equation 2-4*

Lastly Rutenberg & Nsieri (2006) briefly discuss the effect that allowing yielding to propagate higher up the structure would have on the base shear amplification. They find that it reduces the amplification, but the decrease is quite small relative to the shear demand. This is consistent with the findings of Babak (2009), who saw that the reduction in shear is much greater near the top than at the bottom.

### 2.1.2 The Ghosh Approach

The set of similar approaches called here "the Ghosh approach" were initially proposed by Kabeyasawa & Ogata (1985) for frame-wall systems, but Ghosh & Markevicius (1990) developed a similar equation for cantilever shear walls. The basic form of the approach is as shown in Equation 2-6 below:

$$V_{max} = V_s + D_m \cdot W \cdot PGA \tag{2-6}$$

Where $V_{max}$ is the maximum design base shear, $V_s$ is the static shear resulting from an inverted triangular force distribution causing flexural yielding at the base, $D_m$ is a coefficient usually around 0.25-0.30, *W* is the total weight of the structure, and *PGA* is the peak ground acceleration in terms of the acceleration due to gravity. Equation 2-6 is interesting because it can be interpreted as the sum of a first mode component (the static shear, $V_s$) and a component that represents the higher modes. However, whether the peak ground acceleration is the best indicator of the higher mode shear is debatable. As well, although all of the following papers promote Equation 2-6, it has yet to find its way into any building codes.

**Kabeyasawa & Ogata (1985) and Aoyama (1987)**

These two papers are concerned with the results from combined Japanese-US tests on a full-scale 7 storey frame-wall building. Although frame-wall systems can display significantly different behavior than a cantilever wall, the wall carried the majority of the increase in shear force due to dynamic amplification, and furthermore it was possible to somewhat separate the response of the wall from the total response. Aoyama (1987) shows that the column shears vary in phase with the (first mode dominated) displacement, whereas the wall shears do not.

The solution for the shear amplification problem developed in Kabeyasawa & Ogata (1985) and then repeated in Aoyama (1987) is developed using a mainly theoretical approach, with some assumptions coming from behaviour seen during the tests. Essentially the equation of motion is decomposed into modal contributions and the first mode is kept separate while the higher modes are lumped together. It is assumed (with some evidence from the tests) that the first mode distribution is an inverted triangle, and furthermore that the shear force time history is very similar to that of the input acceleration. These assumptions enabled Kabeyasawa & Ogata (1985) to express the higher mode accelerations as a product of the input acceleration and a response magnification factor, after further assuming that only the second mode is magnified. From there, an expression for $D_m$ can be developed, ranging from 0.27 at N = 5 storeys to 0.34 at N = infinity. The shear predicted was compared to results for 5 and 9 storey structures, as well as the aforementioned 7 storey structure, and Aoyama (1987) wrote that "the proposed estimate is a fair upper bound of dynamic base shear."

Although no equations were developed for the shear force in higher storeys, Aoyama (1987) states that it would be relatively simple to use a similar process to create equations that describe the shear envelope.

**Eberhard & Sozen (1993)**

The work by Eberhard and Sozen (1993) looks at a series of small scale shake table tests done on coupled-wall and frame-wall structures in the late 1970s, with the goal of quantifying the base shear. They begin by calculating the strength of the plastic collapse mechanism under an inverted triangular distribution and find that it underestimates the total shear, and in particular the shear in the wall, by a factor of up to 5.8. The authors show by modal decomposition that the force distribution after the structure has yielded is controlled by fluctuating higher modes.

Following Kabeyasawa & Ogata (1985) and Aoyama (1987), Eberhard & Sozen (1993) go on to adopt to determine the total base shear, and compare it to the experimental results. They plot the higher mode portion of the wall shear versus the PGA times the weight, normalized to the static shear, which results in a series of data points that they fit with a line that has a slope $D_m$. Although a fair amount of scatter is observed in the data, it is concluded that a value of $D_m$ of 0.30 provides a

"reasonable estimate of the shear demand for walls." Even in the case of a frame-wall system, Eberhard & Sozen (1993) recommend assigning all of the additional shear force to the walls.

**Ghosh & Markevicius (1990) and Ghosh (1992)**

Unlike the work of Kabeyasawa & Ogata (1985), Ghosh & Markevicius (1990) take an empirical approach to creating Equation 2-6, based on numerical simulations. Using the program DRAIN-2D, nonlinear time history analyses were performed on walls with fundamental periods ranging from 0.5-3.0 seconds under 5 different records with intensities modified for certain heights.

Similar to previous work, Ghosh & Markevicius (1990) found that the shear and moment varied somewhat independently, suggesting that it is inappropriate to assume a constant shear distribution to cause yielding, as a static analysis would. In order to see how the base shear varied with yield moment, the authors plotted the yield moment normalized by height and weight versus the maximum base shear normalized by weight. They found that it was still suitable to assume a first mode relationship between the maximum base shear and yield moment (i.e. a slope of 0.67), but that additional shear needed to be added. This additional shear could further be normalized by the peak ground acceleration to give a component equal to approximately 0.25 times the weight multiplied by the PGA ($D_m$ in Equation 2-6).

Ghosh & Markevicius (1990) also attempted to find out whether the term contributing additional shear depended at all on structural periods or wall height, but they could find no relationship. This seems to contradict the work in Section 2.1.1, but in practice Equation 2-6 still predicts larger shears for taller buildings. Taller buildings tend to be heavier, so the weight proportional term in the second part of Equation 2-6 will increase. Even if the increase in the period due to the heavier structure is account for (proportional to $\sqrt{W}$ ), the predicted shears will still be larger.

**Seneviratna & Krawinkler (1994)**

The work by Seneviratna & Krawinkler (1994) addresses the strength and displacements demands on a series of cantilever wall structures with a fundamental period of 0.22-2.05 seconds. The analyses were performed with a suite of 15 ground motions from "Western US" earthquakes, using the program DRAIN-2D and a bilinear moment-rotation hysteretic model with hinging confined to the base of the wall.

Seneviratna & Krawinkler (1994) observe that higher mode effects contribute largely to the base shear, and that assuming an inverted triangular distribution is unconservative. They also find that if modal analysis is used to determine the base shear, it is still underpredicted. Furthermore, it is primarily second mode contributions to the shear that cause this difference, and the shear amplification depends strongly on ductility.

In order to compare their results to Equation 2-6, Seneviratna & Krawinkler (1994) plotted the additional shear force versus the ductility demand. They find that for the 5 and 10 storey structures Equation 2-6 is a reasonable estimate of the shear, but for shorter structures it overestimates the demand and for taller structures underestimates the demand, due to the increased participation of higher modes as structural height increases. Large contributions from higher modes were also observed in the shear distribution up the height of the structure.

Seneviratna & Krawinkler (1994) also found that when hinging occurred only at the base of the wall, significant moment demands were seen higher up in the wall in the taller and more ductile structures. They repeated their analysis allowing the walls to yield, and found that yielding extended a considerable way up the wall for highly ductile structures, and that although the base shear demand was less, the reduction was not significant.

### 2.1.3 The Keintzel Approach

**Keintzel (1992)**

At the time that Keintzel (1992) wrote about the shear amplification problem, an amplification factor based on the work by Blakely, et al. (1975) was being used in many codes. Keintzel (1992) found, however, that the amplification did not vary linearly with the number of storeys, that the shear forces did not increase linearly with yield moment, and that the shear amplification is greater for higher seismic input level. The amplification Keintzel (1992) considered was not scaled to the code static procedure but to the linear response spectrum analysis results.

The analyses performed by Keintzel (1992) were on structures with 2-5 lumped masses, first periods varying from 0.2-1.6 seconds, and different ratios of flexural to shear stiffness. A set of 10 ground motions was used in the time history analysis, with records chosen that had most of their activity in the short periods, in order to better study the effects of higher modes. After plotting the

amplification in terms of the static shear, it was concluded that using a response spectrum analysis procedure modified to account for the increased effect of higher modes was more appropriate.

Keintzel (1992) proposed using a SRSS approach to combine modes, with a modification factor to calibrate the higher modes. He went on to modify this approach by assuming that only the second mode contributes significantly to the amplification, and that the second period is always on the constant acceleration portion of the design spectrum. These assumptions lead to Equation 2-7:

$$\omega_v = q\gamma\sqrt{\left(\frac{M_y}{qM_I}\right)^2 + 0.1\left(\frac{S_{a,max}}{S_a(T_1)}\right)^2} \leq q \tag{2-7}$$

Where $\omega_v$ is the amplification factor to be applied to a response spectrum analysis, $M_y$ is the base yield moment, $q$ is the ductility factor, $M_I$ is the base moment from the response spectrum analysis, $S_{a,max}$ is the maximum spectral acceleration, $S_a(T_1)$ is the spectral acceleration of the first period, and $\gamma$ is a correction factor normally equal to 1.0. Equation 2-7 is a two-term solution similar to Equation 2-6, but it is more explicit in the way it deals with the results from a modal analysis.

Lastly, Keintzel (1992) shows that at least part of the phenomenon can be explained by considering an elastic cantilever with a rotational spring at the base. When the spring is infinitely stiff, the model represents an elastic shear wall with a fixed base, but as the spring softens it begins to represent a post-yield wall, and it is instructive to examine the mode shapes. What Keintzel (1992) found was that although the first mode effectively disappears, the higher modes do not significantly change, giving credence to the idea of separating the first and higher modes.

**Fischinger, Rejec, & Isakovic (2010)**

The Keintzel approach was briefly discussed in the paper by Fischinger, et al. (2010), who attempted to clarify its usage in Eurocode 8 (CEN, 2004). While Equation 2-7 is typically applied to the results from response spectrum analysis (as stated above), they insist that the original intention of Keintzel was for the amplification factor to be applied to the base shear resulting from a first mode based analysis, such as the static code methods. This is an interesting interpretation, and it changes the way Equation 2-7 would predict shear amplification. However, then they go on to compare time

history results to shear forces amplified using Equation 2-7 in conjunction with response spectrum analysis (the supposedly unintended method) and find that the match is fairly good.

Unfortunately not many details of the analysis are provided – the authors write that the number of storeys ranged from 4 to 20, with the length of the wall, the overstrength ratios, and the wall-to-floor area ratio varying, but no details are given on the record selection or scaling, hysteretic model, or analysis program used. This information would be useful, because some of the analyses for the longer period structures appear to show large amplifications of up to 4.5.

### 2.1.4 Multi-Mode Approaches

While most conclude that it is the fluctuation of higher modes that causes the shear amplification effect, generally these higher modes are not taken into account explicitly, but are lumped together like in the Equation 2-6 or 2-7. Two recent papers have attempted to consider all the modes independently, with varying degrees of success.

**Priestly & Amaris (2003)**

The work by Priestly & Amaris (2003) is written as an extension of the work by Keintzel (1992) and attempts to more explicitly account for the actions of higher modes. The authors start by making the point that under current codes once a shear wall has been designed, the forces are unaffected by seismic intensity (i.e. ductility demand) as long as yielding has initiated. They then go on to perform nonlinear analysis on 6 structures with calculated first periods from 0.34-3.65 seconds, using the program Ruaumoko under 5 different records, scaled in intensity from 0.5 to 2.0. For a hysteretic model they use a modified Takeda relationship, and write that higher mode effects are sensitive to the hysteretic model chosen, although no comparisons are provided. The results of this analysis show that both the moment profile above the base of the wall and the shear profile over the entire height are very sensitive to seismic intensity, and that using response spectrum analysis results is unconservative.

Priestly & Amaris (2003) carry on to attempt to quantify the influence of the higher modes on the response. The method they develop depends on two assumptions – first that ductility limits primarily first mode response, an assumption also made by Keintzel (1992), among others. Second, Priestly & Amaris (2003) assume that (as seen in Keintzel (1992)) the inelastic higher modes will not

differ significantly from the elastic modes, meaning that it is not appropriate to apply a force reduction factor ($R_d$) to any mode past the first. This approach is summarized in Equation 2-8, applicable to shear forces up the entire height of the structure:

$$V_i = \sqrt{V_{1i}^2 + V_{2Ei}^2 + V_{3Ei}^2 + \cdots} \tag{2-8}$$

Where $V_i$ is the shear at level *i*, $V_{1i}$ is the shear corresponding to the development of a plastic hinge in the first mode at level *i*, and $V_{xEi}$ are the elastic modal shears at level *i* due to the $x^{th}$ mode. Equation 2-8 is deemed the "Modified Modal Superposition" (MMS) method.

Priestly & Amaris (2003) then compare the results from the MMS method with time history results. At seismic intensities scaled by a factor of 1.0 the results compare very well, however at double the seismic intensities the MMS method overestimates shears. It is also worth noting that the Keintzel (1992) recommendations as implemented in Eurocode 8 (CEN, 2004) are also presented for comparison, but it appears that the values are miscalculated, or the method is misapplied.

**Sullivan, Priestly & Calvi (2006)**

Partly, the work of Sullivan, et al. (2006) is an extension of the work done by Priestly & Amaris (2003) in that a similar method is developed to account for higher modes, except that it is meant to be applied to frame-wall structures instead of cantilever wall structures. However, like the work by Aoyama (1987), it is possible to extend the work to cantilever shear walls if the shear in the wall is isolated.

The paper begins by comparing the Eurocode 8 (CEN, 2004) approach, the MMS approach, and time history results using Ruaumoko from 5 frame-wall structures under 5 scaled records. For each of these methods two types of structures are analyzed – one that carries 50% of the shear in the wall, and one that carries 80% of the shear in the wall. For comparison to a cantilever wall the 80% case is clearly more useful. The results of the analysis show that the wall shear is overestimated by the MMS approach, but underestimated by the Eurocode 8 approach and the response spectrum analysis approach. However, the same concerns about the application of the Eurocode 8 method found in Priestly & Amaris (2003) are also present here.

Sullivan, et al. (2006) then introduce the interesting idea of "transitory inelastic modes" (TIMs) to describe what is happening to the structure once the base of the wall has yielded. Similar to Keintzel (1992), they argue that once the structure has yielded the moment-curvature relationship is essentially flat, so it is more reasonable to use modal forces from a response spectrum analysis with a soft spring at the base of the structure. This also takes into account the lengthening of the periods that occurs when the structure yields (the given reason for the inaccuracy in the MMS method). Together with the assumption that it is solely first mode behavior that is related to developing a plastic hinge, this method can be described by Equation 2-9:

$$V_i^* = \sqrt{(V_{i1}^o)^2 + (V_{iTIM2})^2 + (V_{iTIM3})^2 + \cdots} \tag{2-9}$$

Where $V_i^*$ is the capacity design wall shear at level *i*, $V_{i1}^o$ is the overstrength shear related to a first mode hinging at the base of the wall at level *i*, and $V_{iTIMx}$ is the shear at level *i* from mode *x* of an analysis of the structure with a very soft spring at the base (transitory inelastic modes).

Sullivan, et al. (2006) investigate how well their method compares to the average results of the time history analyses they performed, and find that for the case where the wall is taking 50% of the shear the match is quite good, but when the wall is taking 80% of the shear the TIMs approach underestimates the shear, particularly as height (and structural period) increases. This suggests that the method may be less suitable for cantilever concrete walls than dual systems.

### 2.1.5 Other Canadian Approaches

Along with the papers already covered, there have been some attempts to solve the problem from a Canadian code perspective, and one paper that does not address the topic directly but still provides some interesting data. In general, these approaches not only address the issue of higher modes causing larger shear demand, but also take into account the increase in shear due to overstrength effects. These papers are important, but do not fit well into the parametric to modal trend outlined in 2.1.1 to 2.1.4, so they are covered here.

**Filiatrault, D'Aronco & Tinawi (1994)**

The work of Filiatrault, et al. (1994) is interesting not only because it was done with a Canadian perspective in mind, but also because they looked at structures in 3 different seismic regions of

Canada. The three regions chosen were selected based on the frequency content across the spectrum, with Montreal ($Z_a$>$Z_v$) having the most energy in the short periods, Prince Rupert ($Z_a$<$Z_v$) having the most energy in the long periods, and Vancouver ($Z_a$=$Z_v$) falling in between. The nonlinear analyses were done using DRAIN-2D with 5 structures, each designed somewhat differently based on the region, with records selected and scaled to match the appropriate spectrum.

The structures were designed using the static procedure, and the shear demand from the nonlinear analysis is compared to the probable shear resistance from the static analysis. Trends from this calculation are interesting; Filiatrault, et al. (1994) find that the shear amplification is greater for a region where the energy is concentrated in the shorter periods (as expected), but also find that the amplification reduces as height increases, contradicting most previous papers. In order to take into account both shear amplification and overstrength, they proposed to replace $R_d$ with a new factor for shear, "$R_v$", used as follows:

$$V_d = \frac{V_e}{R_v} \qquad \begin{aligned} R_v &= 1.00 \;\; if \; Z_a \geq Z_v \\ R_v &= 1.50 \;\; if \; Z_a < Z_v \end{aligned} \tag{2-10}$$

Where $V_d$ is the design shear, $V_e$ is the elastic shear from a static analysis, and $R_v$ is the force reduction factor for shear. As stated before, the authors did not find any dependence on structural height, so it does not appear in the equations.

**Chaallal & Gauthier (2000)**

Chaallal & Gauthier (2000) are unique in the set of papers on the topic of shear amplification because theirs is the only paper devoted explicitly to coupled walls. Their study involved performing nonlinear analysis on 10 different coupled shear walls with first periods ranging from 0.68-3.62 seconds using the program DRAIN-2D. 10 records were selected, 2 for each of 5 PGA/PGV targets. They found that in most cases, the maximum shear force occurred after yielding of the wall.

The code static loading was also calculated, and a base shear dynamic amplification factor equal to the maximum shear force from the nonlinear analysis divided by the static shear times the overstrength was calculated. It is important to note that this factor depended heavily on whether the shear resistance was calculated from the compression or the tension wall. When calculated

with the shear resistance of the compression wall, it was found that the amplification never rose about 1.0, whereas with the tension wall the maximum amplification was 2.03. Similar to Filiatrault, et al. (1994), Chaallal & Gauthier (2000) express the amplification in terms of a shear reduction factor "$R_v$" that takes into account dynamic amplification and overstrength. They found that $R_v$ should vary as follows in plastic zones:

$$R_v = 2.0 \;\; if \; Z_a > Z_v$$
$$R_v = 2.0 \;\; if \; Z_a > Z_v \qquad (2\text{-}11)$$
$$R_v = 1.0 \;\; if \; Z_a < Z_v$$

This is the opposite of the recommendation made by Filiatrault, et al. (1994), and implies that if the majority of the energy is in the short periods of the earthquake there will be less dynamic amplification. As well, these values are derived from the data in a very conservative way – the $R_v$ values suggested by the majority of the data are greater than the ones adopted by Chaallal & Gauthier (2000).

**Panneton, Leger & Trembley (2006)**

Another Canadian paper of interest is the work of Panneton, et al. (2006), published in order to demonstrate the use of NBCC 2005. An 8 storey example building located in Montreal was analyzed using the programs SAP2000 and ETABS, and was found to have a fundamental period of roughly 1.2 seconds. Three different seismic analyses were then performed: a code static analysis, a response spectrum analysis, and a nonlinear time history analysis using the program Ruaumoko under 3 records scaled to the Montreal spectrum.

Results of the analysis showed that both the NBCC static and the response spectrum analysis procedures underestimate the shear forces over the height of the structure. Interestingly, the static procedure provides better estimates of the forces than the response spectrum analysis, because the code calculation for the period is very conservative. The mean dynamic amplification factor calculated for all walls and cores was found to be 2.57, defined as the shear from the nonlinear analysis divided by the probable shear from the other analyses. Panneton, et al. (2006) acknowledge that this value assumes no degradation of the shear strength or stiffness of the walls.

Lastly it was also seen that plastic hinging occurred above the base of the structure in several cases, leading to large curvature demands.

**Boivin & Paultre (2010)**

Similar to the work by Panneton, et al. (2006), Boivin & Paultre (2010) explored the seismic performance of an example 12 storey core wall structure located in Montreal. The walls were designed according to CSA A23.3-04 and NBCC 2005, and were analyzed using both the program Ruaumoko and the program EFiCoS under two historical and six simulated ground motions, some linearly scaled and some fitted to the design spectrum. The choice of damping was an important parameter in this study, and both 1% and 2% damping models were considered, as opposed to the 5% damping assumed by the code.

Results from the analyses performed showed minimal shear amplification and very little inelastic action overall. This is because although the wall was designed with an $R_d$ of 3.5, minimal reinforcement requirements raised the flexural strength considerably, so that the effective $R_d$ was much less than 3.5. Boivin & Paultre (2010) observe some shear amplification in the structure, however they determine that at least part of it is due to the discrepancy between the damping assumed in the code spectrum and that assumed by the analysis. They finish by saying that even with the very small amount of inelastic action observed, some shear amplification exists due to the effects of inelastic higher modes, but no attempt is made to quantify or explain this portion of the shear. Lastly it is interesting that Boivin & Paultre (2010) only observe plastic hinging at mid-height in the Ruaumoko analysis of the wall, and attribute it to issues related to lumped plasticity modeling rather than as a result of a real physical phenomenon.

## 2.2 Comparison of Methods

From the summary of previous papers on shear amplification, it can be seen that opinions are divided as to the correct approach, and the difference between methods can be quite large. Therefore it is important to compare methodologies and comment on the reasons for the differences, and discuss possible shortcomings.

### 2.2.1 Application of Methods to Model Structures

One way to compare the different methods is to apply them all to a series of example structures. More details of the example structures can be found in Section 3.1, but for the purposes of this comparison they are 8 structures with first periods ranging from 0.5-7.0 seconds. This upper range of 7.0 seconds is larger than any of the structures previous studies have considered, but it is not unrealistic for a tall building in Canada.

Normalizing all of the methods is also important if they are to be compared, since some of the methods have developed amplification factors to modify code static procedures, some for response spectrum analyses, and some simply give the shear force without any other analysis necessary. In order to facilitate evaluation of the methods, response spectrum analyses were performed on all of the model structures under both the Vancouver and Montreal uniform hazard spectra, and all the methods were normalized to these values to give an "equivalent amplification". Ductility factors of $R_d$ = 2.0 and 3.5 were used, and no overstrength was considered, so a value of 1.0 would be equal to $V_e/R_d$. The base shear from various methods is compared below:

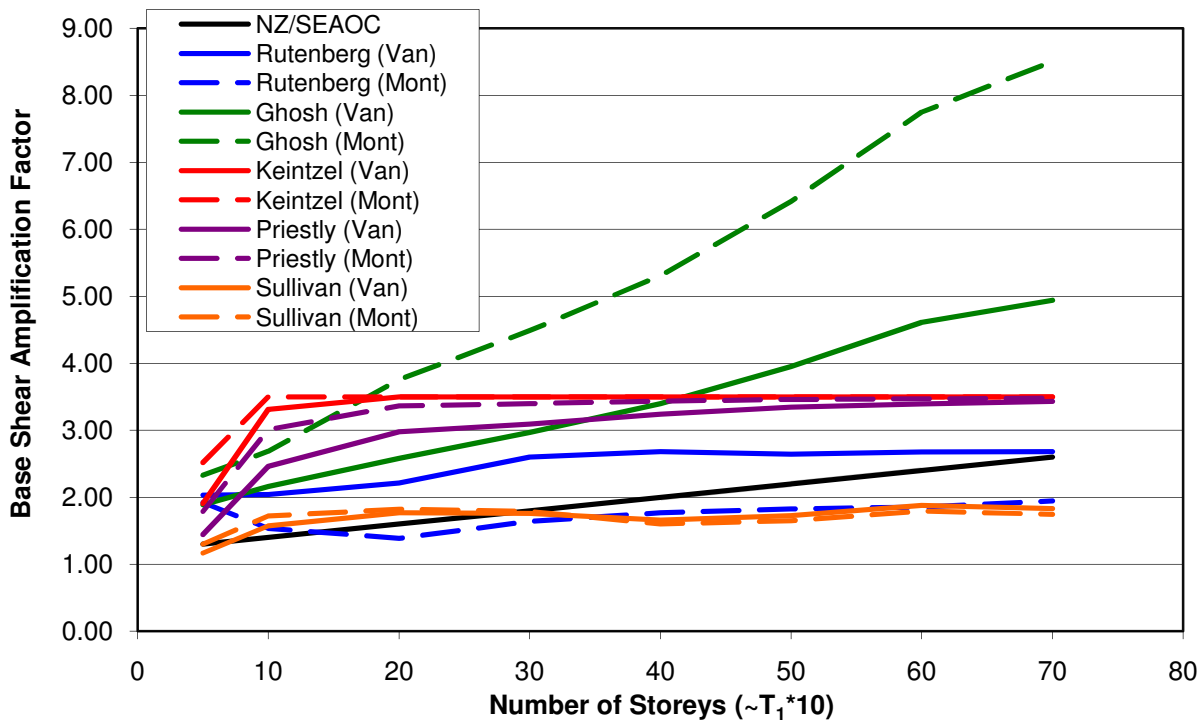


*Figure 2.2: Amplification factors (defined as predicted base shear divided by RSA base shear) for Vancouver (Van) and Montreal (Mont) spectra with $R_d$ = 3.5*

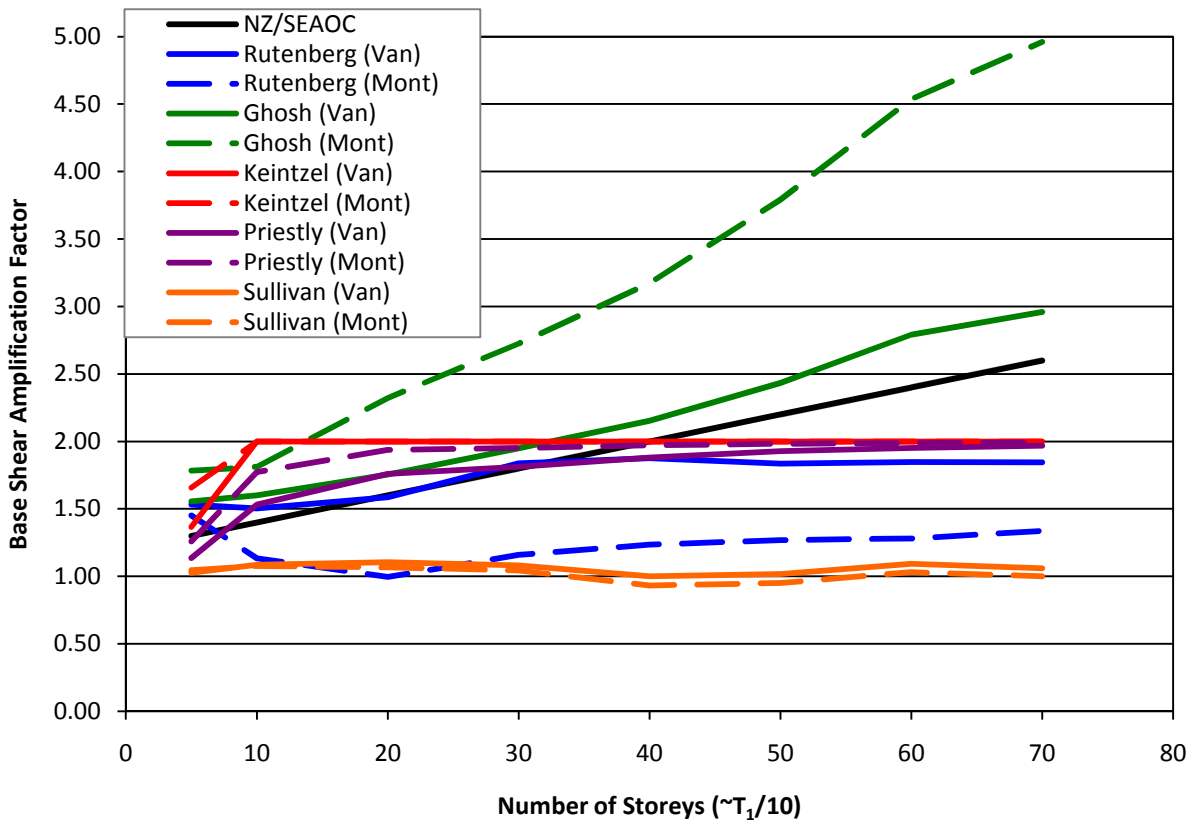


*Figure 2.3: Amplification factors (defined as predicted base shear divided by RSA base shear) for Vancouver (Van) and Montreal (Mont) spectra with $R_d$ = 2.0*

Not plotted is the method of Filiatrault, et al. (1994), because it would appear as a straight line at 2.0 or 3.5 for $R_d$ = 2.0 and 3.5 respectively, independent of whether the Vancouver or Montreal spectrum is used.

Immediately one sees that the methods are quite scattered at all structural heights – they do not agree around 5-30 storeys (the heights for which they were developed) and further diverge as the first period becomes large. For example, at 20 storeys (2.0 second first period) there are a range of amplification factors from 1.6-3.5 for Vancouver and 1.4-3.8 for Montreal. This suggests that there are significant problems with at least some, if not all, of the methods proposed. Some useful questions can be asked by looking at the data in Figures 2.2 and 2.3, which are discussed as follows.

**Can the maximum shear be greater than the elastic shear?**

The shear force obtained by applying Equation 2-6 is clarified considerably by plotting it as an amplification factor. Because there is no upper limit on the shear in this method, it can extend past what would be expected from an elastic analysis (3.5 in Figure 2.2) and does so under both the Vancouver and Montreal spectra. Is this possible? Keintzel (1992) explicitly, and Priestly & Amaris (2003) implicitly, limit the shear to less than that from an elastic analysis. The New Zealand/SEAOC method and the Rutenberg & Nsieri (2006) methods do not limit the shear force, but neither do they predict values larger than the elastic for this range of structures.

This partly calls into question the accuracy of a response spectrum analysis relative to a time history analysis. It is generally assumed that using the modal combination rules gives a good estimate of the maximum response. However, this may not be completely true, and Chopra (2007) states that in situations where higher modes are important the modal combination rules can be unconservative. Section 5.1 considers this question further.

It is conceivable that even if a response spectrum analysis is correct in predicting maximum moment and shear, in an inelastic structure where yielding has occurred there could be a situation where the shear would exceed that of the elastic due to the fluctuating higher modes. However, the method of Sullivan, et al. (2006) suggests that due to structural softening and period lengthening the shear is unlikely to exceed that of the elastic.

**Should the Montreal amplification be greater than the Vancouver amplification?**

The reason for choosing the Montreal and Vancouver spectra, other than that they represent two common places in Canada where cantilever wall buildings could be found, is that they have different spectral frequency content. In the Montreal spectrum most of the energy is concentrated in the short periods, and the spectral acceleration in the long periods is very small. Conversely the Vancouver spectrum, while having significant energy in the short periods, also displays considerable energy in the long periods. For comparison, the value $S_a(0.2)/S_a(2.0)$, indicating to what extent the short periods dominate the energy content, is 14.4 for Montreal, but only 5.5 for Vancouver.

It can be seen in Figures 2.2 and 2.3 that the Ghosh method, the Keintzel method, and Priestly & Amaris (2003) all predict larger amplifications for Montreal, the New Zealand/SEAOC method is

independent of spectral shape, the Sullivan, et al. (2006) method predicts very similar amplifications, and Rutenberg & Nsieri (2006) actually predicts lower amplifications for Montreal. In all cases this difference is implicit – in fact both the Ghosh approach and Rutenberg & Nsieri (2006) give shear forces directly without considering the spectral shape. Only when the methods are converted to an amplification factor do the differences become apparent.

An argument can more easily be made for the Montreal amplification being greater than vice versa. Considering that most agree that the cause of dynamic amplification is the fluctuating nature of the higher modes, a spectrum that has more energy content in the shorter periods would excite these modes more and lead to a greater amplification. As well, if yielding at the base does serve primarily to limit first mode forces, as many of the papers suggest, then a structure which has lower first mode contributions in the elastic range will see less of an effect when these forces are limited. This phenomenon will be investigated more extensively in Chapter 4.

**What are the parameters that are most important in dynamic shear amplification?**

Figure 2.2 shows that two important factors many researchers have attempted to take into account are structural height (and more importantly period) and spectral shape. These have not always been expressed explicitly – for example in Ghosh & Markevicius (1990) the authors state that they could find no relationship in the higher mode term to structural height (or first period). Yet because the weight of a structure is tied to its periods, the second weight dependent term in Equation 2-6 acts as a proxy for the periods, and therefore the height.

The one factor that is implied in most equations and is explicitly expressed in Keintzel (1992) and Rutenberg & Nsieri (2006) and may not be represented adequately in the plots is the ductility. It is possible, however, to compare the shapes of Figures 2.2 and 2.3 and draw some conclusions. For example, most of the methods predict lower amplification factors when the ductility factor is lower. Although generally the ductility factor is used to establish capacity rather than demand, to some extent it can be thought of as representative of the seismic intensity. So finding lower amplification factors with lower ductility factors is consistent with the research done by Priestly & Amaris (2003), who found that greater seismic intensity resulted in larger amplifications. It is only the New Zealand/SEAOC method that does not predict varying shear amplification based on ductility,

although the original paper by Blakely, et al. (1975) did anticipate that different factors would be needed for larger earthquakes.

### 2.2.2 Missing Pieces

In addition to raising the previous questions, Figures 2.2 and 2.3 make it clear that most, if not all, of the methods previously proposed must be incomplete or incorrect in some way. If this were not the case, it would be expected that they would arrive at the same conclusions. So then what are the factors that have led previous researchers on the subject to arrive at such different conclusions?

Ultimately, what seems to be missing is that none of the researchers have taken a comprehensive view of the problem. This can mean several things, and in many of the previous papers shows up in different ways. For example, one of the main problems has been a lack of robustness in the nonlinear analysis. Many of the researchers only use a small set of ground motions (Blakely et al., 1975; Ghosh & Markevicius, 1990; Keintzel, 1992; Priestly & Amaris; 2003, Sullivan et al., 2006; Boivin & Paultre, 2010), and often these ground motions are scaled in ways that may be inappropriate (scaling around one period) or even in different ways depending on the situation. The result of using such a small set of motions is that the results may not be an accurate reflection of the seismic response – because the response varies quite considerably from record to record, it may be that the ones selected just happen to all cause a certain type of response, and a whole subset of responses may be missed.

Another problem can be that the structures and the cases the researchers select do not represent a full range of possible structures. None of the researchers choose structures with a fundamental period greater than about 3.5s, and so may miss out on how the amplification varies after that, or even if it does at all. The series of tests done on scale models (Kabeyasawa & Ogata, 1985; Aoyama, 1987; Eberhard & Sozen, 1993), while instructive, are by nature a very limited set of structures, none being taller than 9 storeys. Keintzel (1992) assumed that structures with mass distributed in 5 discrete locations (essentially a 5 storey structure) would be indicative of the behaviour of structures of any height.

Many of the researchers appear to fail to take into account the differences between spectral shapes (Priestly & Amaris, 2003; Rutenberg & Nsieri, 2006), even if their proposed method does actually

imply a difference. All of this points to a failure to consider the entire problem from the outset, carefully studying which factors are important.

Although not something that one can fault any researcher for, as mentioned in Section 2.2.1 many of the methods calculate their shears in very different ways. This can obfuscate the results of the analysis, particularly when the methods are based on local codes. With some difficulty the meaning can be extracted, although as Fischinger et al. (2010) show, it is then never entirely clear how the method was originally intended to be applied.

Finally, there are really no papers with the exception of Blakely et al. (1975) that attempt to look at the problem in a systematic way. In other words, most of the researchers will jump into doing nonlinear analysis right away without considering what can be learned from simpler procedures. While it is true that only nonlinear analysis can provide the actual shear force, it will be seen in Chapter 4 that even ordinary response spectrum analysis can give important insight as to the important parameters that affect the phenomenon of shear amplification.

# 3 ANALYSIS PARAMETERS

Chapter 2 has shown that the shear amplification phenomenon requires a consistent and robust analysis. In particular, if many types of analyses are used (for example response spectrum analysis (RSA), and nonlinear time history analysis (NLTHA)), they must all use identical inputs. To this end, the first two sections of Chapter 3 deal with the example structures and the spectra that will be used for all of the analyses. The later sections deal with issues specific to the analysis of structures by NLTHA – hysteretic shape, ground motions, damping, and the specifics of the computer program.

## 3.1 EXAMPLE STRUCTURES

Given that the goal of this study is to find a simple way to quantify shear amplification, it follows that the structures chosen for analysis should be practical, but also represent a wide range of possibilities. To this end, eight structures of varying heights (and therefore periods) were designed to a level of sophistication great enough to determine the critical parameters for the analyses, such as the stiffnesses and masses.

Each structure is based around a central "core" of shear walls, coupled in one direction and cantilevered in the other. For the purposes of this study the coupled direction was ignored, and in the cantilevered direction the dimensions of the wall were chosen with three restrictions. The first is that the section be realistic, as determined by experienced practicing engineers (personal communication, DeVall, R. & Mutrie, J., August 2009). This narrowed considerably the choices as to the ratio of the flexural and shear rigidities. Secondly, the ratio $h_w/L_w$ (height of wall/length of wall) was kept below 12, so that they would not be too slender, which influenced the taller structures considerably. Thirdly, the rigidities of the walls (determined from the thickness and width) and weight of the structure (determined from the floor plate size) were chosen such that the first period of the structure was approximately equal to the number of stories divided by ten – again a common design choice made by practicing engineers. Figure 3.1 below shows the general layout of the cores.

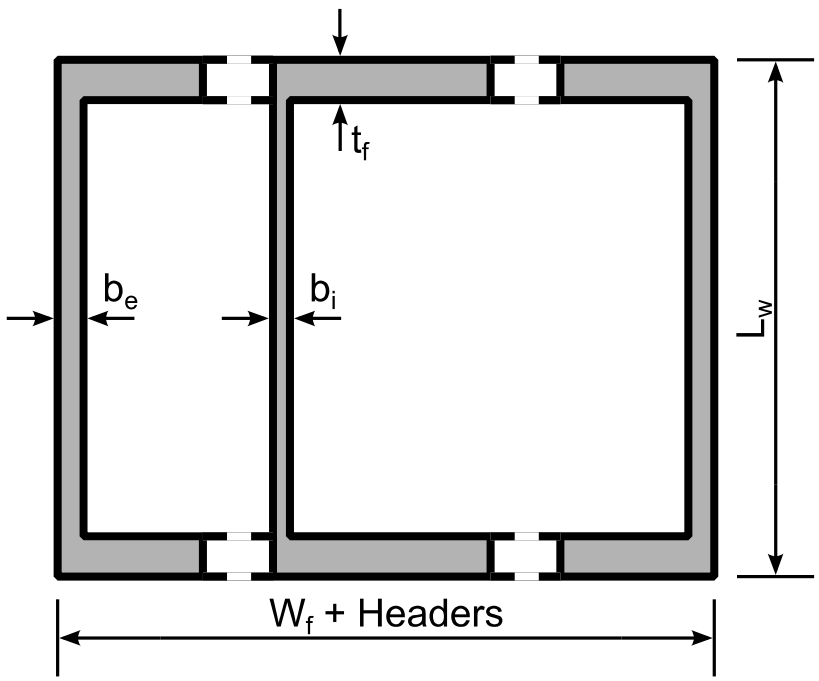

*Figure 3.1: General layout of example cores*

Where $L_w$ is the length of the wall, $W_f$ is the total width of the flanges (headers are not included in $W_f$, but are shown in Figure 3.1 for the sake of realism), $b_e$ is the width of the exterior walls, $b_i$ is the width of the interior walls, and $t_f$ is the thickness of the flanges. In Table 3.1 the total width of all the walls is combined into one value, called $\sum b$.

The structural height was chosen based on typical floor-to-floor heights in condominium buildings, with the first storey lobby being 4.5 metres (14'9") tall, and each typical floor after that being 2.8 metres (9'2") tall, which includes a 200mm (8") flat plate slab. Column and wall weights were lumped together with the floor mass to create an idealized mass at each floor. Table 3.1 below summarizes the basic dimensional properties of the cores for each of the sample structures, while Table 3.2 includes information about the stiffness, mass, axial load, and periods.

*Table 3.1: Dimensional design data for sample structures*

| Number of Floors | Flange Thickness $t_f$ (m) | Web Width $\sum b$ (m) | Flange Width $W_f$ (m) | Wall Length $L_w$ (m) | Wall Height $h_w$ (m) | $h_w/L_w$ |
|---|---|---|---|---|---|---|
| 5 | 0.3 | 0.6 | 4.6 | 4.6 | 15.7 | 3.4 |
| 10 | 0.45 | 0.6 | 6.0 | 5.5 | 29.7 | 5.4 |
| 20 | 0.55 | 0.9 | 8.0 | 7.5 | 57.7 | 7.7 |
| 30 | 0.7 | 1.2 | 9.0 | 9.0 | 85.7 | 9.5 |
| 40 | 0.8 | 1.4 | 11.5 | 10.75 | 113.7 | 10.6 |
| 50 | 0.85 | 1.6 | 13.5 | 13.75 | 141.7 | 10.3 |
| 60 | 0.925 | 1.8 | 16 | 16 | 169.7 | 10.6 |
| 70 | 1.0 | 1.9 | 19.25 | 18.25 | 197.7 | 10.8 |

*Table 3.2: Other design data for sample structures*

| Number of Floors | $E_cI_{eff}$ ($x10^{12}$ $Nm^2$) | $G_cA_{v,eff}$ ($x10^{10}$ N) | Storey Weight (kN) | Fundamental Period (s) | f'c (MPa) | $P/f'cA_g$ |
|---|---|---|---|---|---|---|
| 5 | 0.25 | 2.6 | 5400 | 0.5 | 30 | 0.035 |
| 10 | 0.68 | 3.4 | 5700 | 1.0 | 30 | 0.059 |
| 20 | 2.4 | 7.5 | 6300 | 2.0 | 35 | 0.087 |
| 30 | 5.2 | 13 | 6900 | 3.0 | 40 | 0.101 |
| 40 | 12 | 19 | 8900 | 4.0 | 45 | 0.114 |
| 50 | 27 | 29 | 13400 | 5.0 | 50 | 0.127 |
| 60 | 49 | 40 | 17400 | 6.0 | 55 | 0.136 |
| 70 | 87 | 50 | 22800 | 7.0 | 60 | 0.146 |

It can be seen in Table 3.2 that the criteria of having the fundamental period be the number of storeys divided by ten was met. The axial load at the base of the structure ($P/f'cA_g$), while large in the case of the tall structures, is still significantly less than the code allows.

Preliminary response spectrum analyses using the NBCC 2005 (NRC, 2005) design spectrum for Vancouver were performed on the structures in order to determine some basic structural responses so as to compare them to accepted standards. These properties are shown below:

*Table 3.3: Important response parameters, from analysis run under the Vancouver spectrum*

| No. of Floors | Global Drift Ratio | Shear Stress v,c (MPa) |
|---|---|---|
| 5 | 0.35% | 1.17 |
| 10 | 0.41% | 1.22 |
| 20 | 0.44% | 0.90 |
| 30 | 0.51% | 0.74 |
| 40 | 0.46% | 0.75 |
| 50 | 0.58% | 0.85 |
| 60 | 0.69% | 0.89 |
| 70 | 0.81% | 1.07 |

Table 3.3 shows that the drift ratios are all less than 1%, and the shear stress is reasonable. Additional properties of the example sections are described in Appendix A, including drawings of the cores of each structure.

## 3.2 CHOICE OF SPECTRUM

Along with the structural characteristics, the second input parameter needed to perform a response spectrum analysis is the spectrum itself. A response spectrum captures two important characteristics of an earthquake – the overall magnitude and the energy content across different frequencies. Ideally, spectra should be chosen that are both realistic in their magnitude, but vary enough that the effect of the shape is not lost.

To meet these requirements, two spectra were chosen – the uniform hazard spectra for Vancouver and Montreal with an exceedance probability of 2% in 50 years, from the Geological Survey of Canada report (Adams & Halchuk, 2003) on which the NBCC 2005 (NRC, 2005) values are based. Because the spectral accelerations given in this report stop at a period of 2.0 seconds, some assumptions were made about the remainder of the spectrum. The acceleration at 4.0 seconds was chosen to be half of the acceleration at 2.0 seconds, based on the assumption of constant velocity in that portion of the spectrum (acceleration falls off proportional to 1/T). Note that this is the same assumption that is made for the code values in NBCC 2005. After 4.0 seconds, it is unclear what the correct procedure should be, so guidance was taken from the ASCE 7 (ASCE, 2005) spectrum for Seattle. In this spectrum, the acceleration continues to decline proportional to 1/T until 6.0 seconds, and then at $1/T^2$ afterwards. This is considerably different than NBCC 2005, which chooses to level the spectrum off after 4.0 seconds, assuming constant acceleration. Section 4.5 shows that

this assumption is questionable, and is not compatible with the analysis required by this thesis. Figure 3.2 shows the Vancouver and Montreal spectra used:

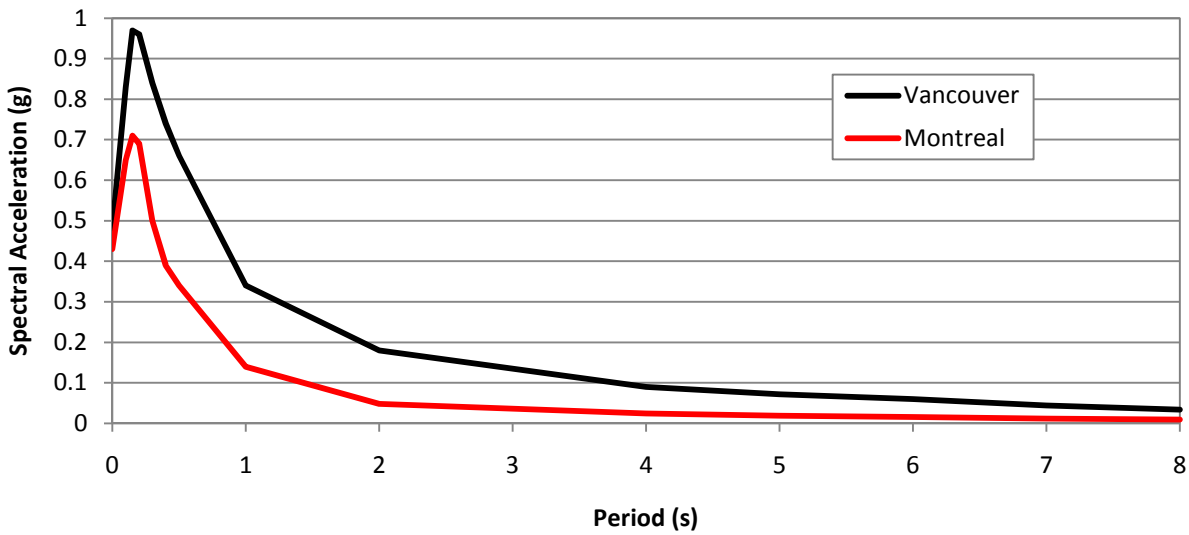


*Figure 3.2: Vancouver and Montreal spectra used for study*

The choice of using the uniform hazard curves may seem questionable, given that it is well known that these curves do not represent real earthquakes. However, the magnitude of the spectrum (and hence the ground motion) is not a critical factor in a linear analysis like this, since the structural response will simply scale in direct proportion to the accelerations. Even in a non-linear analysis, where higher magnitudes may impose higher ductility demands and therefore different structural response, because the amount of yielding is proportional to the elastic, magnitude has no effect. In both analyses, design is done using a ductility factor chosen beforehand to attempt to account for the nonlinearity of the structure, and this is constant.

More important is how the spectral accelerations vary with the period, because the response of the example structures is expected to depend considerably on the higher modes. The difference in frequency content between the Montreal and Vancouver spectra is significant enough to capture this effect – more extreme spectra could be chosen, but it is unnecessary for most of the analysis. Figure 3.2 shows that while the Vancouver spectrum is greater over all periods, proportionally is has much more energy in the longer periods. A ratio used by the code to represent the differences is

Sa(0.2)/Sa(2.0), and the larger the ratio is, the more energy is in the short periods. For example, the Vancouver spectrum has an Sa(0.2)/Sa(2.0) of 5.5, while for Montreal it is 14.4.

## 3.3 Analysis Program and Implementation

The open source program OpenSees (UC Berkeley, 2009), developed by researchers in the United States, will be used for the time history analyses. The advantage of the program is that the user has a large amount of control, in comparison to other structural analysis programs designed for use by the practicing engineer. For example, it is easy to quickly run a large parametric study, or to create new material models. As well, it has been developed primarily for nonlinear analysis of structures under earthquake loads, and so is appropriate for this study. The freedom in inputs and in the way that the analysis is run can present a problem, however, in that many parameters not normally considered must be set, and convergence issues sometimes arise.

The implementation of the sample structures in OpenSees involves using beam-column elements, which provides the connectivity between nodes, and uniaxial sections, which provide the material rigidity properties. Compounded together, and by assigning mass at the nodes, this models the dynamic characteristics of the structure. The iteration technique used was the modified Newton method, and the integration technique used was the Newmark method, with a gamma of 0.5 and a beta of 0.25.

## 3.4 Hysteretic Model

In the simplified model used, no variation in axial load is considered, and there are no P-Delta effects – a reasonable assumption for a core wall structure. Furthermore, the relationship between applied shear force and shear strain is assumed to be linear. This is not accurate (Gerin, 2003), but the softening in shear expected when diagonal cracking, or even yielding of the shear reinforcing, occurs is discussed in Chapter 4 at length.

All of the nonlinearity, therefore, was assumed to occur in the moment-curvature model. The hysteretic curve selected was a bilinear elastically perfectly plastic (EPP) model, with a nominal post-yield slope to ensure numerical stability. This type of bilinear model is both consistent with work done by previous researchers and with the common assumption of equal displacement, and its relationship to ductility factors. While the seismic design portion of codes such as CSA A23.3-04

(CSA, 2004) are often written assuming a more complicated relationship (e.g. trilinear) in mind, these codes are difficult to use in a research context that does not follow a design procedure. Specifically, relating the ductility of a concrete wall to the factor $R_d$ is simplest when using a bilinear model with a well defined yield point.

Another advantage of using the EPP model is the simplicity with which it is defined and the ease in changing parameters. Only two pieces of data are necessary – the yield point and the initial slope. In the analyses that follow, the initial slope of the EPP model is chosen to be 70% of the initial flexural rigidity, $EI_G$. This value is both consistent with the code and seems to be a reasonable approximation for the reduction in stiffness due to cracking. The yield point (also the nominal strength) was selected by using the response spectrum analysis (RSA) results and dividing by the strength reduction factor $R_d$. Theoretically if one were to attempt to apply a consistent ductility to the structure, the appropriate method would be to use the maximum base moment from the elastic time history analysis for each ground motion record and then divide by the required $R_d$. However, this is more complex than is necessary and would result in different yield strengths for each structure, which creates problems when trying to compare a set of structures. Furthermore, it is not consistent with what would be done in practice, which would contradict one of the objectives of the analysis. The resulting differences in ductility are acceptable because the scaling of ground motions will mean that the results will be similar.

Lastly, it is important to note that better models exist for simulating the behaviour of tall concrete walls. For example, the EPP model has no stiffness reduction, which is reality is cause by cracking through cycles. As well, the EPP model can either over or under estimate the hysteretic damping depending on the record. These issues will be discussed further in Section 6.1.

## 3.5 Nonlinear Beam-Column Element

Once the section has been defined, it must be input into some type of element. This analysis uses one-dimensional beam-column elements to connect the nodes and define the stiffness matrix. Of these, the choice must be made to use either force-based or displacement-based elements. To represent shear wall structures, where the individual sections are primarily in single curvature with a linear profile, either method is suitable. However, it was found that when the displacement-based

element was used the shear deformations were not accounted for correctly. This can be seen by looking at the first 5 modal periods for the 30-storey structure:

*Table 3.4: Comparison of periods in the 30 storey structure using the force and displacement based elements*

| Mode Number | Force Based Period (s) | Displacement Based Period (s) |
|---|---|---|
| 1 | 3.009 | 2.972 |
| 2 | 0.513 | 0.474 |
| 3 | 0.201 | 0.169 |
| 4 | 0.115 | 0.086 |
| 5 | 0.078 | 0.052 |

Although it seems that the difference is not that large, especially in the first mode, it becomes larger at the higher modes, which are important for this work. Note that the first period from Table 3.4 matches that from Table 3.2. Because of the fact that the model does not have to be optimized to reduce computation time due to its simplicity, the choice was made to use the force-based element with 5 integration points. In order to simulate shear deformations using the displacement-based element, springs would have to be placed at the nodes, adding unnecessary complexity.

## 3.6 DAMPING

Other than the stiffness and mass characteristics of the structure, one of the most important parameters to set is the damping, which can have a large effect on the structural response. For example, see Boivin & Paultre (2010), who showed that a large part of the amplification of shear that they observed was due to choosing a damping ratio of 2% instead of the code prescribed 5%. As the central goal of this study is to examine the higher mode contribution to the amplification of shear, an average damping ratio of 5% will be used, based on the last committed stiffness. Then, because Rayleigh damping is used in the analysis, the only decision that remains is to choose which modes to set to 5%.

From the work reviewed in Chapter 2, it appears that the higher modes have a dominating effect on the shear response, so it is logical to attempt to be as close to 5% as possible over the first 3-4 modes. On the other hand, the first mode response is still very important, especially because examining the base moment and its relation to the shear is a major area of interest. So, the usual

approach of setting the first mode at 5% was used, and then the choice of setting either the second, third, or fourth mode to 5% was examined. Table 3.5 shows the effective damping ratios for these options.

*Table 3.5: Damping in the first five modes depending on modes set*

| Modes Set | Damping in Mode x | | | | |
|---|---|---|---|---|---|
| | Mode 1 | Mode 2 | Mode 3 | Mode 4 | Mode 5 |
| 1 and 2 | 5% | 5% | 11.19% | 19.30% | 28.35% |
| 1 and 3 | 5% | 2.64% | 5% | 8.41% | 12.26% |
| 1 and 4 | 5% | 1.90% | 3.07% | 5% | 7.23% |

It can be seen that to select the first and second mode results in the higher modes being heavily damped, making them irrelevant. This is not a desirable result, so it would seem that choosing one of the other two combinations is preferable. On the other hand, it is also important to examine the damping ratio in the second mode, which can contribute largely to the total shear force. If the damping in that mode is too small it could end up dominating the results, when the effect of other modes may also be important. To illustrate the large effect that changing the damping ratios has on the response, consider the following figure, showing the variation of the base shear force with time for the same earthquake record under the three different damping ratios.

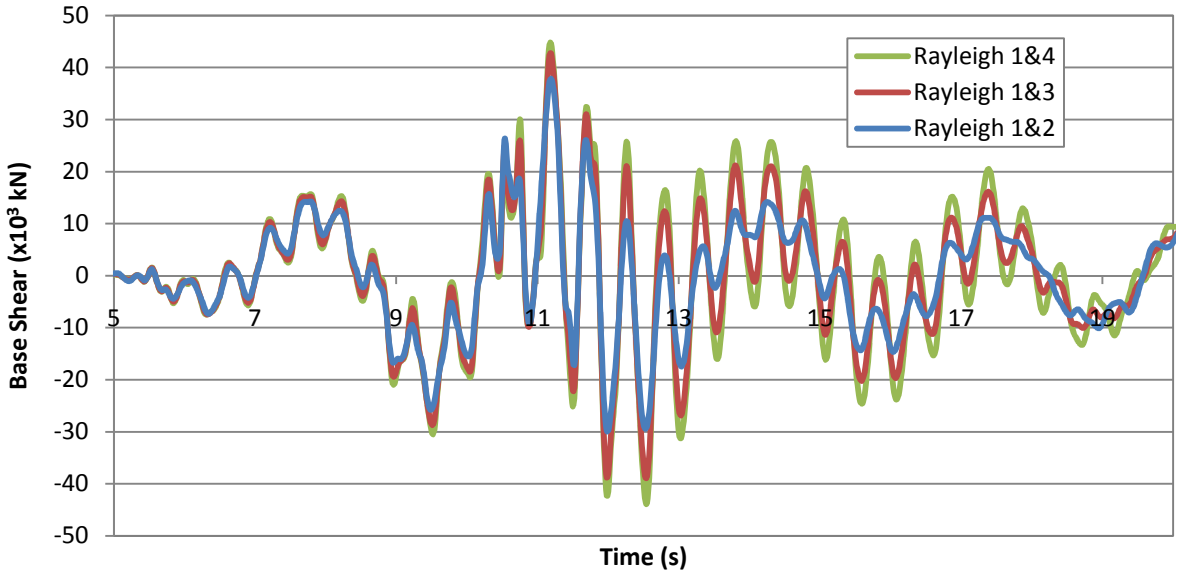


*Figure 3.3: Variation in base shear depending on selection of modes to set damping, from linear time history analysis*

Not surprisingly the effect is large, and the increasing dominance of the second mode (at a period of 0.5s) as increasingly higher modes are set to 5% damping can be seen. It was decided to fix the first and third mode at 5% damping for the remainder of the study, as that seems to give the most reasonable balance between lower and higher modes.

## 3.7 GROUND MOTIONS

The choice of ground motions and the method to scale them is very important when relying on the results of the LTHA and NLTHA to draw conclusions. It was seen in Section 2.2.2 that many of the previous works on the topic of shear amplification seem to have suffered from poor selection and scaling. Because the selection and scaling problem is so important, most of Section 5.1 is devoted to discussing issues with the process. This section will only describe the records selected and how they were scaled.

In order to get a good result, the 40 ground motion records from FEMA 440 (ATC, 2005) were selected. These records are from a large number of earthquakes, and as such have a large variance in frequency content, which is desirable. Further information about the records can be found in Appendix B. The weakness of selecting these records is that many of them were not recorded with instruments capable of representing the long period portion of the spectrum. In this case, however, this is acceptable because the method used to scale the records was fitting the earthquakes to the spectrum by modifying the frequency content.

The scaling program used was RSPMatch (Abrahamson, 1993), and the records were scaled to the spectra defined in Section 3.2 up to a period of 8 seconds, so that the modified records could be used with the entire range of structures. Figure 3.4 shows how well the records fit for the Vancouver spectrum:

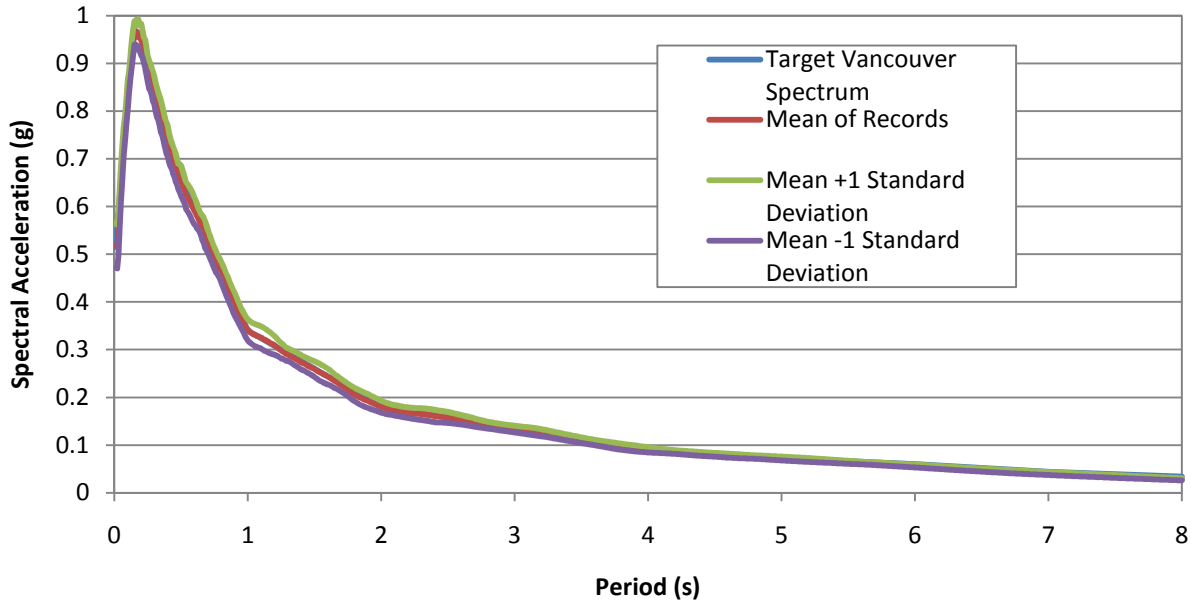


*Figure 3.4: Comparison of scaled spectra (using the fitting method) to target Vancouver spectrum*

It should be noted that for some parts of this thesis, namely Section 5.2.2 which deals with the time history results, and Section 6.2 which deals with the shear peaks, the linearly scaled response will be used. More details are available in these sections, but the reason for the change is that while fitting the records is more appropriate for analyzing the envelopes, it distorts the original earthquake record enough that the difference becomes apparent in the time history results.

# 4 LINEAR RESPONSE SPECTRUM ANALYSIS

The analysis of shear wall structures by linear response spectrum analysis (RSA) can potentially reveal many characteristics of the dynamic behavior that are either too difficult or considerably more complex to observe using non-linear time history analysis. As well, it is the primary method used by practicing engineers to determine design forces on shear wall structures in Canada, information useful in this study due to its practical goal. Finally, the simplicity of the procedure allows the engineer to run many analyses while varying input parameters, without the analysis taking an excessive amount of time.

## 4.1 GENERAL RESPONSE BEHAVIOUR

Before refinements are made or parameters are varied, it is instructive to consider the simple fixed-base model using the defined stiffnesses and masses, without attempting to account for any yielding or shear cracking. Furthermore, this simple analysis corresponds to the kind of analysis that the NBCC 2005 and CSA A23.3-04 expect designers to perform. Of particular interest is that it is possible to break down the modal contributions to each response quantity to determine how important higher modes are in each case.

For each of the sample structures an analysis was performed using the NBCC 2005 Vancouver design spectrum, with the spectral acceleration leveling off after 4.0 seconds. Then, the structures with a first period above 4.0 seconds (50, 60, and 70 storeys) were analyzed using the same spectrum, except modified as described in Section 3.2. An RSA was also performed on select structures using the NBCC 2005 Montreal design spectrum modified in the same way, in order to determine the effect that this different spectral shape had. In each case the displacement, moment, and shear profiles were plotted along with the matching profiles from each of the first four modes, the absolute value taken to assist in visually determining the contribution of the modes to the CQC envelope.

### 4.1.1 MAXIMA ENVELOPES AND MODAL CONTRIBUTIONS

Dynamic shear amplification is primarily an issue with higher mode effects in walls, and so along with finding out the maximum response envelopes, RSA can be extremely useful in allowing the user to break the envelope down based on modal contributions, unlike nonlinear time history analysis.

While this study is primarily concerned with the shear forces in walls, the displacement and moment information is also useful, particularly because many code design procedures as well as many proposed procedures for dynamic amplification assume some relationship of the moment to the shear. Although the RSA envelope and the corresponding modal contributions are dependent on the spectral shape and the structural characteristics (which determine the mode shapes and periods), it is possible to get an idea of the types of shapes one would expect to see in walls from a sample of 3 different cores under a single spectrum. Shown below are the displacement, moment, and shear envelopes for the 10, 30 and 70 storey sample walls under the modified Vancouver code spectrum.

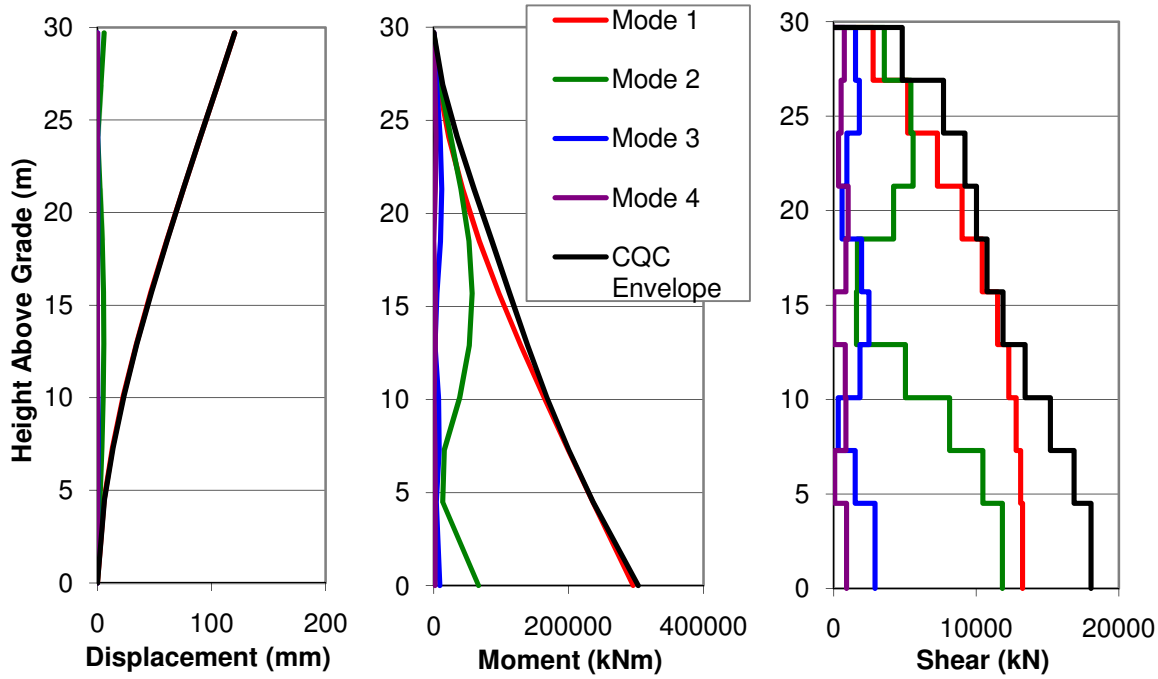


*Figure 4.1: Displacement, moment, and shear profiles for the 10 storey structure*

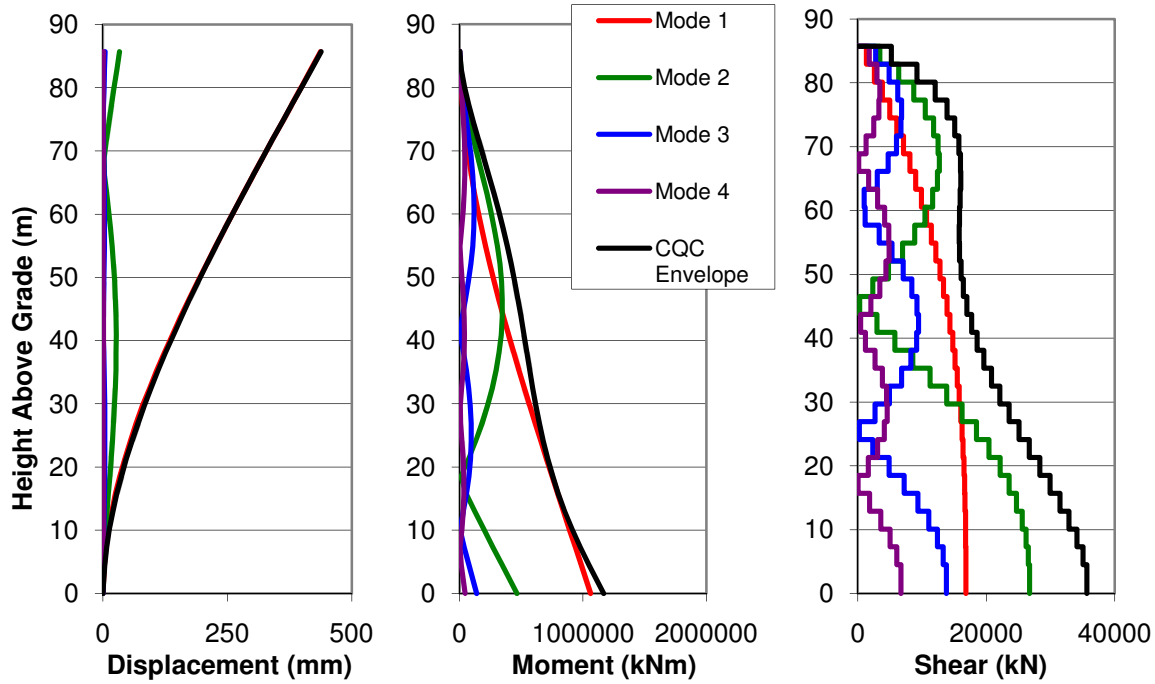


*Figure 4.2: Displacement, moment, and shear profiles for the 30 storey structure*

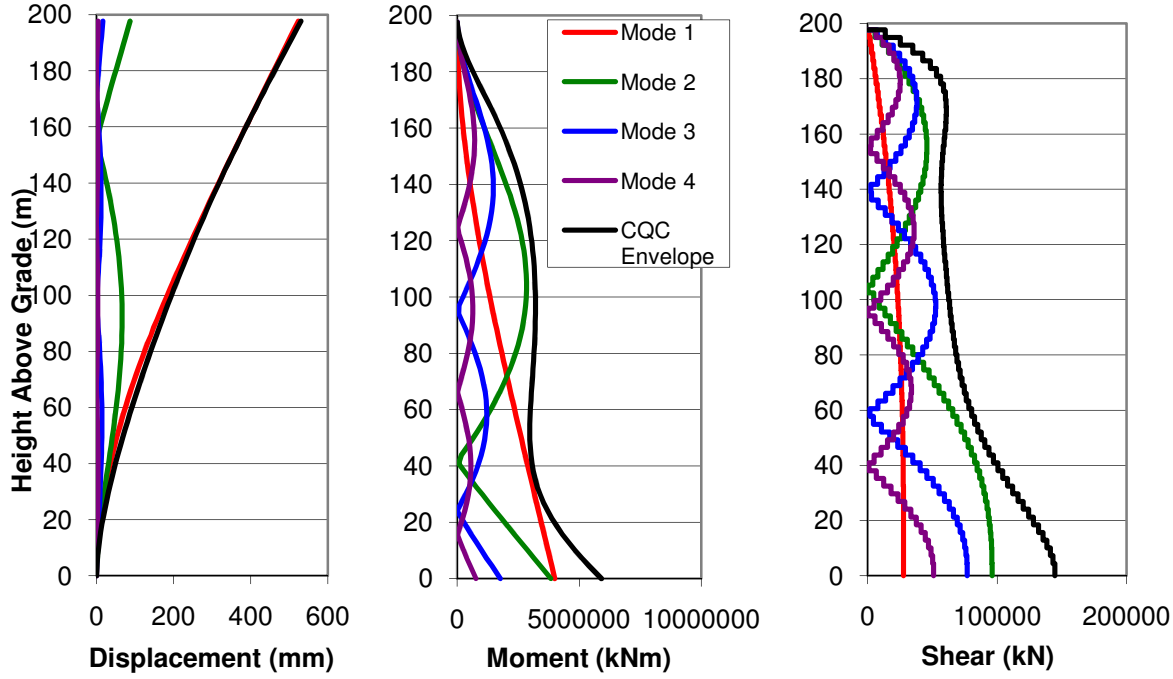


*Figure 4.3: Displacement, moment, and shear profiles for the 70 storey structure*

Note that in the above figures while the total envelope is always positive by definition, the absolute values have been taken of the modal contributions for clarity. From these figures it is possible to

draw some general conclusions about the trends. First of all, as the structural height increases, the higher modes become more dominant in all response characteristics. This makes sense considering the shape of the spectrum – as the first period becomes very long, the corresponding spectral acceleration will be small relative to those of the higher modes, even if the mass participation of the first mode is large compared to the higher modes. Furthermore, this allows predictions to be made regarding the shape of the envelopes for different spectra. If, for example, the Montreal spectrum is used (where the acceleration falls off faster than the Vancouver spectrum), it would be expected that the higher modes would be more relevant to the total response at shorter periods. Although not shown here, this is in fact what is seen, with a Montreal wall appearing to have similar envelope shapes to a taller Vancouver wall.

The next interesting observation that can be made from Figures 4.1 to 4.3 is that the modal contributions to the total response envelope are considerably different between the displacement, moment, and shear. While the displacement is almost entirely first-mode dominated, with the second mode only starting to play a role in very tall buildings, the moment and shear envelopes display considerable higher mode response. In the case of the moment, while short structures are mainly first-mode dominated, the effects of the second mode can be clearly seen as height increases, appearing as a "bulge" slightly above the mid-height of the structure. Finally the shear, which is the primary focus of this study, sees considerable contributions from the second mode even in short structures, and in higher structures it is not unreasonable to say that the response is second mode dominated. Already it is possible to ask if it is fair to then assume that the moment and shear will display the same inelastic behaviour under seismic loads (as is assumed by the NBCC 2005). From past work, it has already been seen that yielding serves primarily to limit the first mode, so the answer would have to be that it is unreasonable to apply the same factor to the shear and moment unless they have identical modal contributions, which they clearly do not.

It is important to note that even though the influence of higher modes can strongly be seen, these response profiles make it clear that using a response spectrum analysis still assumes yielding and maximum shear at the base of the wall. However, consider Figure 4.2 – if the yield strength of the wall were designed using an $R_d$ of 3.5, it is conceivable that the forces developed by the second mode alone could initiate yielding at the base of the wall. More importantly, if the rest of the wall were designed to the shape of the envelope, it is further possible that it would not in fact be the

base of the wall that would yield first, but rather the wall may yield somewhere above the base. Furthermore, the shear from a second mode distribution of forces may have its resultant below that which is expected from the envelopes, causing higher shear at yielding than expected. While not directly connected to the problem of dynamic amplification of base shear, the phenomenon of mid-height yielding is rooted in the same physical explanation – the influence of higher modes.

## 4.2 RSA WITH A BASE PIN

Already it has been shown that using RSA to determine elastic response characteristics of a cantilever shear wall is useful in understanding the phenomenon of shear amplification, but it is worthwhile considering modifications that can be made to the analysis in order to gain even more information. One such modification is to release the rotational degree of freedom at the base of the structure (i.e. replace the rigid condition with a pin). The goal of such an analysis is to attempt to recreate to some extent what happens to the structure after yielding.

### 4.2.1 EFFICACY OF THE MODEL

Considering the goal of this model is to attempt to simulate the post-yield response of a shear wall yielding at its base only, it is important to define what the characteristics of this response are. In this case, a bilinear moment-curvature relation is assumed with the post-yield slope being zero. While this is inaccurate and better models are available for more complex analysis, it conforms with the models used in much of the previous research. As such, when modeling this structure the objective should be to have the stiffness of the bottom element be as close to zero as possible, representing the zero tangent slope of the post-yield curve. It should be made clear that this pin-ended structure does not include any geometric nonlinearity – if P-Delta effects were included, the structure would fall over under its own weight as soon as any horizontal displacements were imposed.

Now that the requirements for the model have been established, it is straightforward to add a rotational spring element at the bottom of the structure with low stiffness compared to the stiffness of the structure as a whole. This soft spring model still results in a complete set of results when running RSA, but it essentially removes the contribution of the first mode by making it so long that it has no significant acceleration. Note that this type of model is similar to that mentioned in Keintzel

(1992) and Sullivan et al. (2006), the former using it purely to qualitatively explain the phenomenon and the latter using the numerical results.

This work also uses this method extensively, but it must be kept in mind at all times that this is a very simple model and, unlike the fixed base model, is not actually a complete model of the system in question. Furthermore, it is important to note that it is a complete model of a different structure, so care must be taken when trying to combine it with other models. Other limitations of the model include that fact that yielding may not simply occur at the base, but at other heights as well. In addition to this, the model assumes that the hinging will remain while the higher modes cycle back and forth, perhaps causing moment in the direction opposite of yielding. Lastly, while this model is appropriate for simple research applications, it is unclear how a designer would model these soft springs in a real structure with multiple walls and coupling action.

### 4.2.2 Qualitative Results of the Pin Model

One of the chief advantages of the pinned model is its explanatory power. Chapter 2 of this thesis discussed previous work, and while different papers may have reached different conclusions on how to account for shear amplification, almost all agreed that the source of the problem was modal contributions in the nonlinear range. Because the idea of the pinned model is to simulate the post-yield condition, studying the results of the RSA should give some insight into the reason for dynamic shear amplification.

The following figures show a comparison of the moment and shear envelopes for the fixed base and pinned base structures:

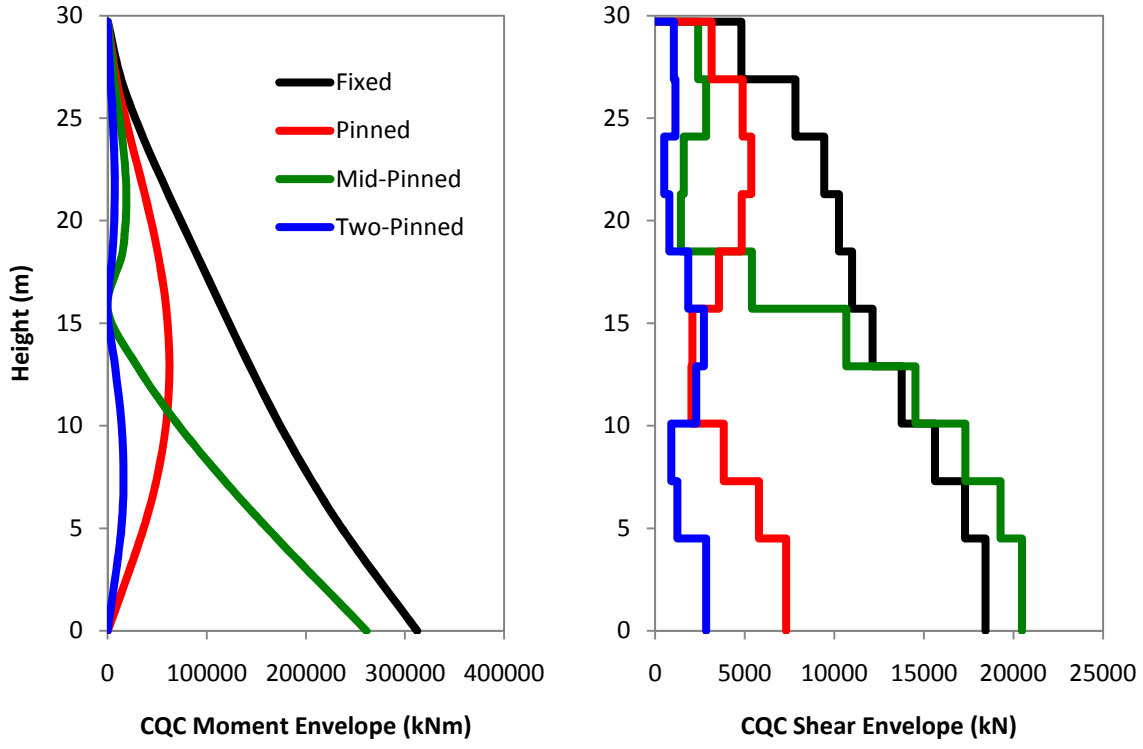


*Figure 4.4: 10 storey CQC moment and shear envelopes for various pin conditions*

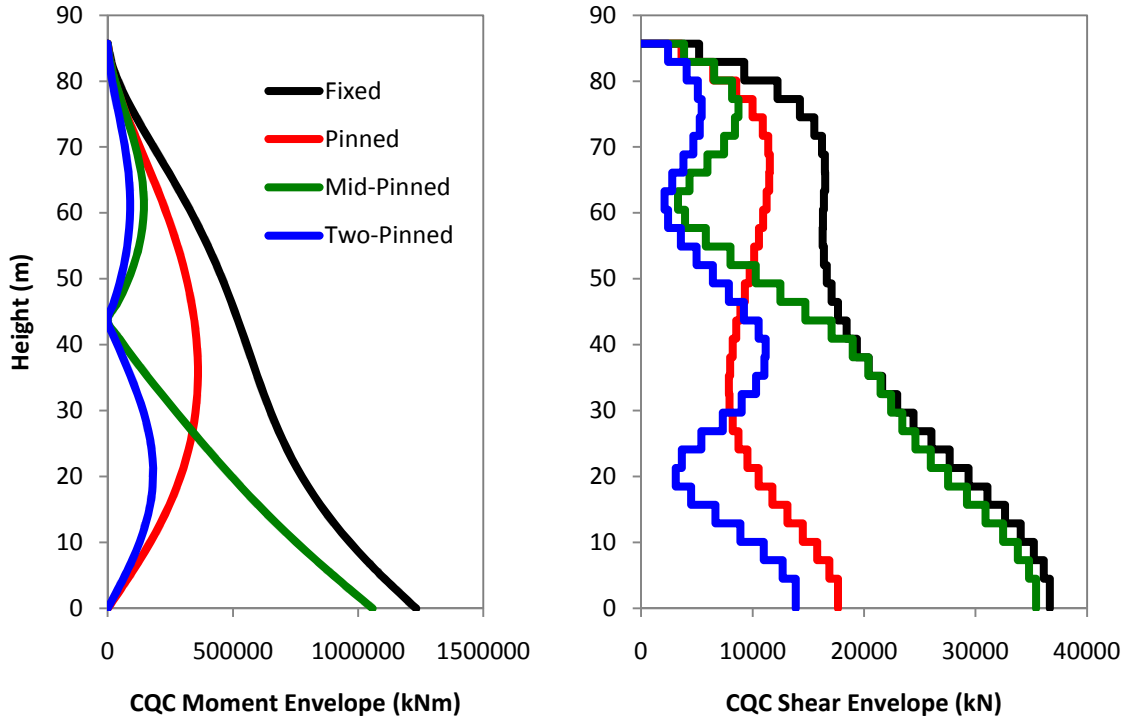


*Figure 4.5: 30 storey CQC moment and shear envelopes for various pin conditions*

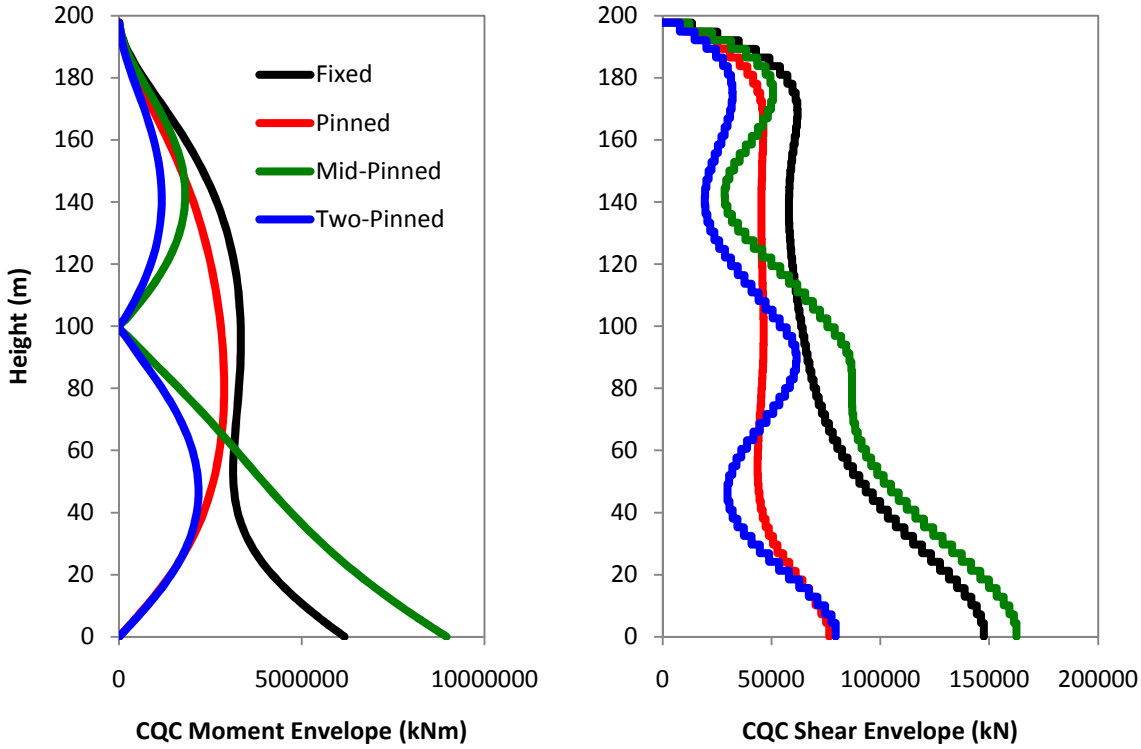


*Figure 4.6: 70 storey CQC moment and shear envelopes for various pin conditions*

Upon analyzing the structure a couple of things become clear. The first is that while the moment at the base of the structure cannot increase (because it is a pin), the shear is not limited in any such fashion and in fact a significant amount of shear force does develop at the base of the wall. This is precisely the inelastic effect of higher modes mentioned previously, and the RSA of this model shows that it is possible for modes to combine in such a way as to add shear without increasing moment. Furthermore, it can be seen that while the moment at the base of the structure is constrained, moments in the rest of the elastic structure can increase. Using these results it is easy to see why mid-height yielding is so often observed in addition to shear amplification – the two phenomena have the same cause.

Having confirmed that these inelastic higher modes are the source of shear amplification, the next step is to investigate the nature of the modes. Are they the same higher modes as are seen in the elastic structure? It turns out that they are surprisingly similar, although not identical, as seen in the following figure:

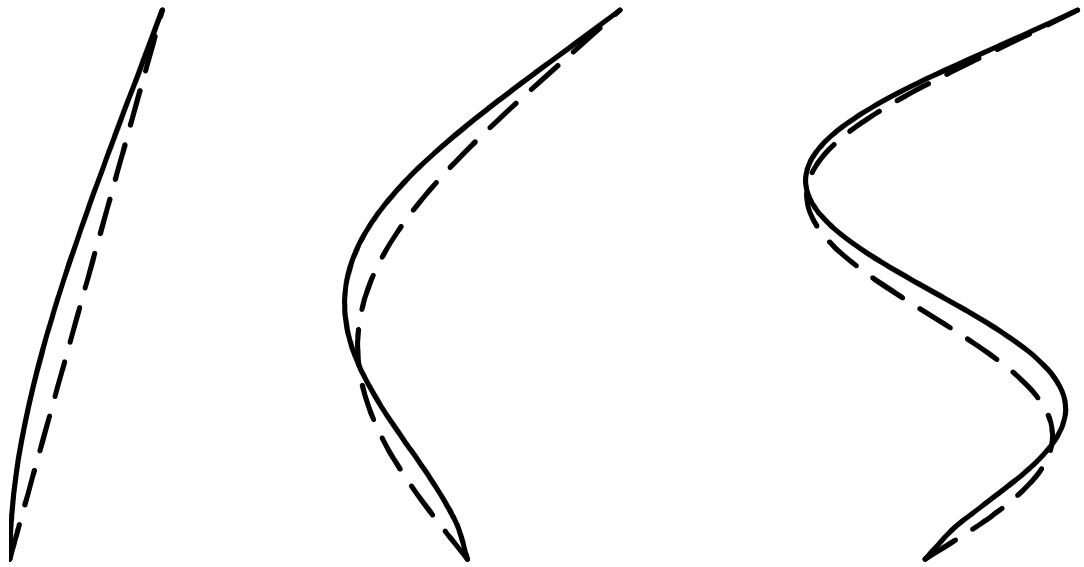

*Figure 4.7: Comparisons of the first three mode shapes for the fixed base (solid line), and pinned base (dashed line) structure, normalized to unity at the top of the structure*

The first mode essentially just becomes a sway mechanism as expected – the period becomes infinite as the stiffness of the rotational spring at the base of the structure is decreased. Because the spectrum continues to drop off at a rate of $1/T^2$, this means that there will be no forces developed in this mode. Due to this effect, it can be deemed an "unreal" mode, so that the second mode would be the first "real" mode, or in other words the first one in which forces are actually developed. This gives some credibility to the common idea that base yielding is primarily related to the first mode. However it can also be seen that the higher modes do change somewhat, which is expected because equilibrium demands that they cause zero moment at the base of the structure. It is impossible to tell from the figure, but the periods of the higher modes also lengthen somewhat, generally resulting in somewhat lower forces. This partly explains why attempts to directly use the elastic modes (i.e. Priestly, 2003) tend to overestimate forces.

The sample analysis shown above was performed using only one spectrum, but it should be possible to predict the influence of changing the spectrum. The primary piece of information is that yielding at the base of the structure causes the first mode to become unreal, as discussed above, while the other modes remain relatively similar to their equivalents in the fixed-base system. Therefore, it would be expected that the less of an effect the first mode had to start with (for example in a

spectrum where the acceleration of the longer periods drops off more rapidly), the higher the amplification would be.

### 4.2.3 Quantitative Results of the Pin Model

As briefly discussed earlier, the RSA of the pinned base structure produces a full set of information about the moments and shears. It is worthwhile analyzing this data even though the model is by no means perfect. There are two main issues addressed in this section – the first is simply analyzing the data and seeing how it compares to the fixed base structure, and the second is trying to generate simple equations to describe any trends. The latter part is of particular importance if any method using the data is to be codified, because it is unreasonable to expect designers to perform the pinned-base analysis.

Each of the sample structures was analyzed under both the Vancouver and Montreal spectra, and also analyzed under a range of shear stiffnesses expressed in terms of percentage of gross stiffness (100%-1%). Masses were not adjusted to keep periods constant when shear stiffness was varied, as the goal was to try to capture some of the softening in shear that a real building may experience.

There are several different ways to plot this data, but because the base shear is the main concern, one convenient way is to consider the normalized base shear versus one of the periods of the structure. Several different periods were tried, and it was found that the trends were strongest with the second period. Figure 4.8 shows the fixed base shear versus the second period:

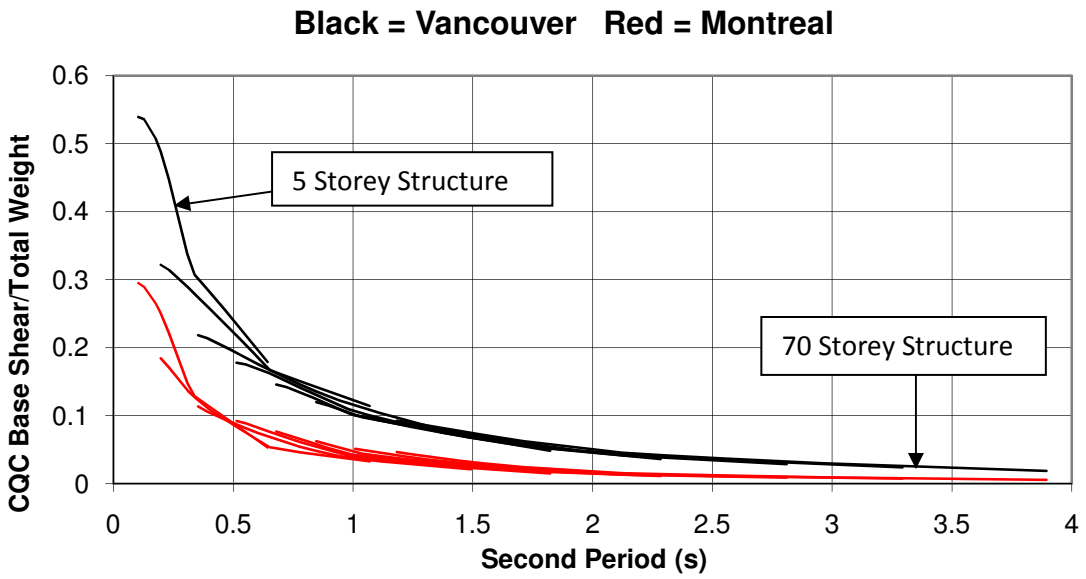


*Figure 4.8: CQC fixed base shear vs. second period of fixed-base structure, for all example structures, and shear rigidities from 100%-1% of gross*

By comparison, Figure 4.9 shows the same data plotted against the first period of the structure. It can be seen that unlike in Figure 4.8 where all of the curves (representing each structure) seem to fall on top of each other, the curves in Figure 4.9 have some separation.

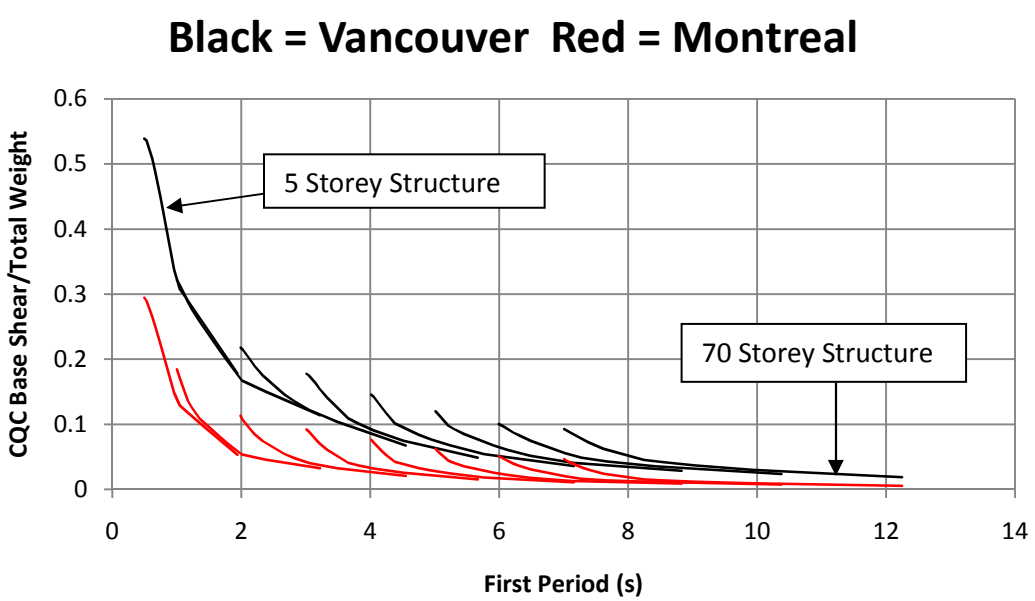


*Figure 4.9: CQC fixed base shear vs. first period of fixed-base structure, for all example structures, and shear rigidities from 100%-1% of gross*

Likewise, for the pinned-base structure, it was found that using the third period (the second "real" period) produced the strongest trend. Figure 4.10 below shows this data.

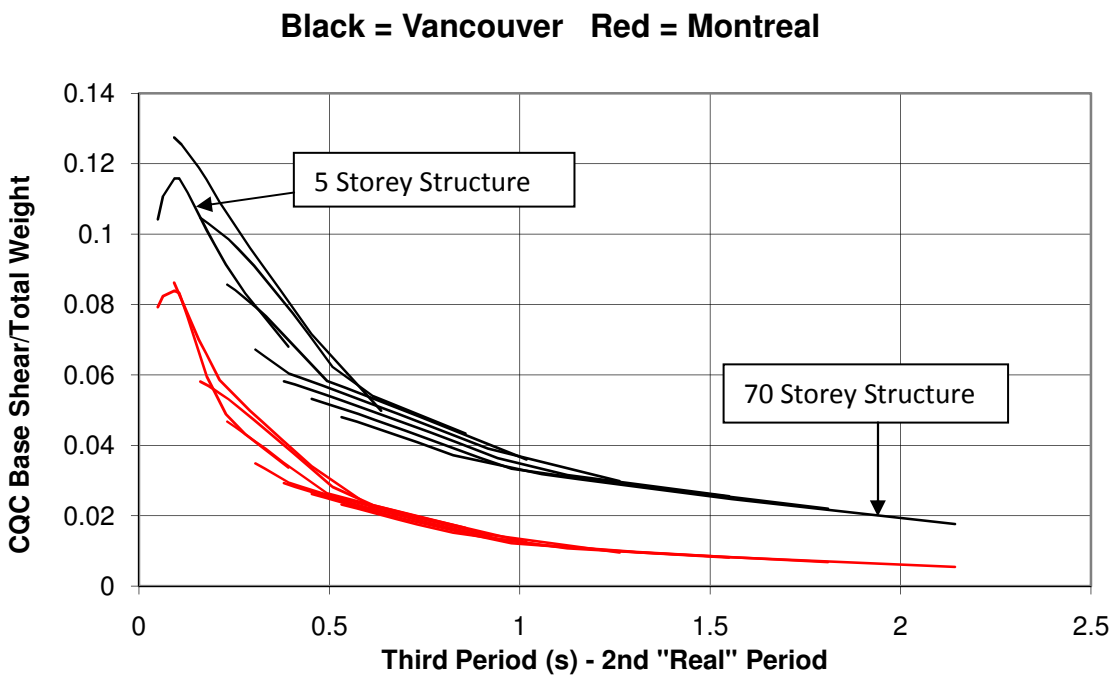


*Figure 4.10: CQC base shear of pin-based structure vs. third period of pin-based structure, for all example structures, and shear rigidities from 100%-1% of gross*

Figures 4.8 and 4.10 contain information from all of the sample structures, and represent a range of shear rigidities (see Section 4.3 for more information). It can be seen that the trend between the CQC base shear and the second period (or technically third period in Figure 4.10) is quite strong, suggesting that the shear force at the base of the structure is primarily a second mode phenomenon, something that has already been observed in Section 4.1.1.

As stated previously it is not especially useful to plot the pinned shear versus the pinned period, because it is difficult for the designer to determine the pinned period. However, it was found that plotting the pinned shear versus the fixed period gave a very similar graph, but with the advantage of the determinability of the fixed periods.

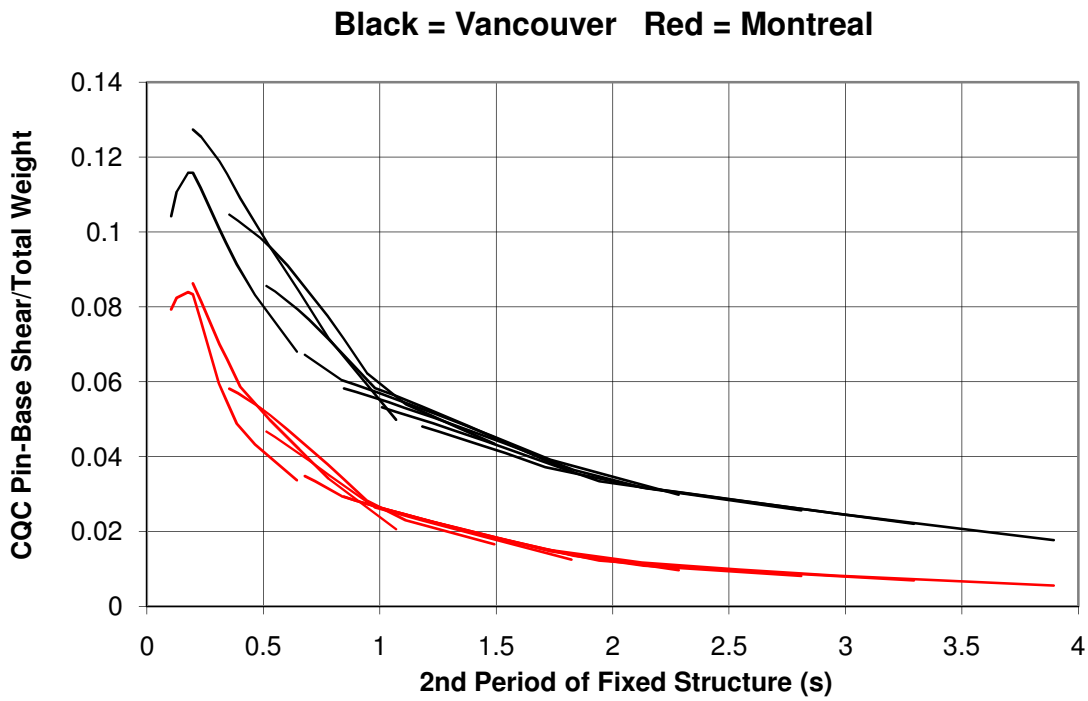


*Figure 4.11: CQC pinned base shear vs. second period of fixed structure, for all example structures, and shear rigidities from 100%-1% of gross*

This is potentially a very useful plot if at some point it becomes important to determine the pinned shear. However, fitting a curve to Figure 4.11 proves somewhat difficult – not because it is hard to fit curves to the data, but because it is hard to relate to account for the differences in spectrum. So an alternative method is suggested – plot the ratio of the pinned shear to the fixed shear versus the second fixed period. That plot is shown below:

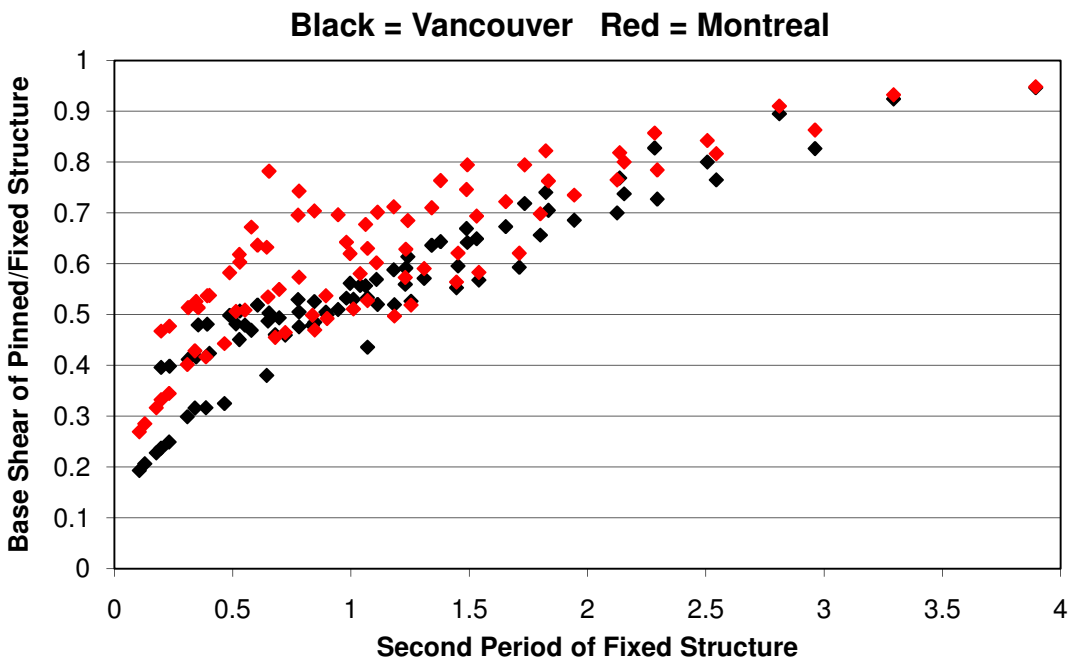


*Figure 4.12: Pinned base shear/fixed base shear (both from RSA) vs. second period of fixed structure, for all example structures, and shear rigidities from 100%-1% of gross*

Part of the reason to plot the data like this is not only to make it simpler to fit a curve to the data but also to permit a more logical interpretation. If the pin model is taken as completely representative of the whole of the behaviour of the structure after yielding, then Figure 4.12 gives the amount of shear in addition to that already calculated – or in other words the shear amplification. Admittedly it is not the case that the model is perfect, but even so it can be taken as something of a guideline to the amount of shear generated during the inelastic action of the structure.

Unfortunately the figure is not nearly as simple as it first seems, due to the fact that such a wide range of shear stiffnesses have been plotted. It appears at first that the graph starts at zero as expected (there is no amplification for a single degree of freedom system) and gradually heads towards one, representing the maximum shear amplification (it would be equal to $R_d$). This trend appears to be only dependent on the shape of the spectrum, and not on the stiffnesses, so it seems very appealing. However further analysis revealed that while the ratio of stiffness does not significantly affect the trends in Figures 4.8 or 4.10, this assumption does not hold for Figure 4.12. In other words, a structure that has the same second period but a significant difference in stiffness

ratios may not have the same ratio of pinned to fixed shear. Therefore it becomes very important what the relative stiffnesses are, adding to the complexity of the task. Figure 4.13 below shows only the Vancouver data for the 100%GA and the 1%GA cases from Figure 4.12 to highlight the issue:

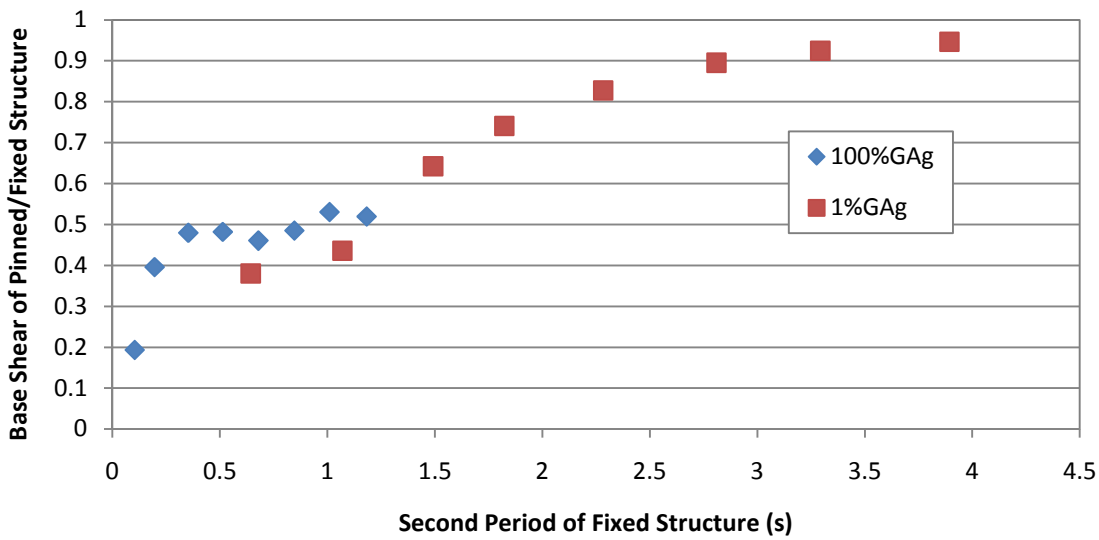


*Figure 4.13: Pinned shear/fixed shear vs. second period of fixed structure for 2 shear rigidities*

It can be seen that the two plots have somewhat varying shapes – the 100%$GA_g$ case rises rapidly and then seems to level off at about 0.5, while the 1%$GA_g$ case continues to rise and slowly levels off around 1.

Without getting into too much detail, it turns out that when the shear stiffness is reduced, the shear drops off by a considerable amount due to lengthening of the periods (see Section 4.3.3 for more information). This means that there are two options – either require designers to calculate the expected shear stiffness given the forces, or just ignore possible reductions in stiffness. The first option is untenable, because it is difficult to determine what the effective shear stiffness should be to account for cracking, and no guidance is given in the design codes. The other option may seem poor as well, but it is acceptable to use this method. Even if cracking does occur, because it will reduce the shear force demand it is not something to be concerned about, and may even help the problem. Therefore, similar analyses were done using shear stiffnesses ranging from 20%-500% of the gross, representing most possible configurations of the walls in an elastic state (i.e. walls with

thin webs and large flanges to rectangular walls). Figure 4.14 shows the same ratio as Figure 4.12, but now the data looks quite different:

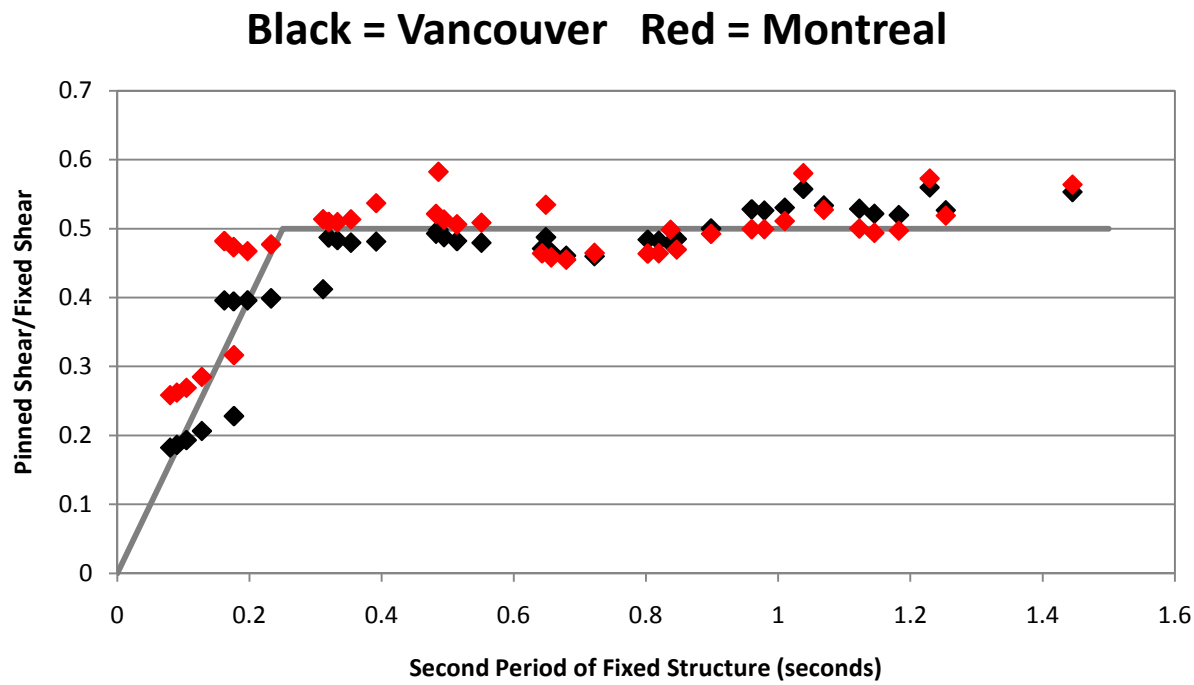


*Figure 4.14: Pinned shear/fixed shear for a range of "uncracked" stiffnesses, for all example structures*

It can be seen that instead of continuing to increase, the ratio levels off at about 0.5. Presumably this is because for the taller structures the modal ratios end up being very similar, so removing the first mode has the same effect in all cases. The grey line in Figure 4.14 is a simple estimation of the ratio of the pinned shear to the fixed shear, and could potentially be used in a model for the total shear demand. Equation 4-1 describes the line:

$$R_{pf} = \begin{cases} 2T_2 & T_2 < 0.25s \\ 0.5 & T_2 \geq 0.25s \end{cases} \tag{4-1}$$

Where $R_{pf}$ is the ratio of pinned to fixed shear, and $T_2$ is the second period of the fixed structure. Note that for both the Montreal and Vancouver spectra this relationship is valid.

### 4.2.4 Pins at Locations Other than the Base

It has been observed several times in previous sections that it is possible, and even likely, that a shear wall could yield not only at the base, but also higher up. Because of this possibility, and because higher mode yielding is so closely related to shear amplification, it is worth attempting to determine at least qualitatively the effect that such yielding would have.

One way to do this is to use the same methodology as before, and simply add very soft springs representing pins at locations where it is suspected that yielding might occur. In the analysis that follows it is assumed that yielding occurs either at the base of the wall, at the mid-height of the wall, or both. While it may not be the case that yielding would occur exactly at the middle of the wall, it will be seen that it is a good enough approximation to gain an understanding of the behaviour of the wall under such circumstances.

Although only the results with the pin at the base of the structure have been discussed so far, Figures 4.4 to 4.6 also show the shear and moment response when a pin is placed only at mid-height of the structure while the base remains fixed, and the case where a pin is placed at both the base and the mid-height. One central conclusion that can be drawn is that when a pin is placed at mid-height, the effect it has on the shear below it is relatively small. It appears that it is only the shear above the location of the pin that is mainly affected by this addition. This has been observed previously by Babak (2009).

Having a pin at mid-height and at the base of the wall is an attempt to model higher mode yielding after the structure has already yielded at the base. Before more discussion, it is important to note that there may not in fact be two distinct yielding zones, but instead some papers such as Seneviratna & Krawinkler (1994) show a continuous yielding zone up to approximately mid-height. Considering this result, it is perhaps most appropriate to consider the two pin model as a guideline, rather than an accurate representation of what might happen.

Again it is found that adding a pin at the mid-height of the structure affects primarily the shear above that point. It can be seen that for the 10 and 30 storey structures the mid-height pin does reduce the shear at the base of the structure somewhat, but for the 60 storey structure it does not at all. The apparent modal contributions are also interesting – theoretically the first two modes

should both be extremely large, and therefore non-existent, and this is what is seen, with the shear force diagram showing mainly higher mode action.

## 4.3 Reduction of Shear Stiffness

Section 4.2.3 discussed briefly the effect of reductions in the shear stiffness, but it is worthwhile to take a closer look at the subject, because it has not been looked at explicitly in previous work, appearing only briefly in Keintzel (1992). In particular, the goal is to determine what kind of reductions in shear stiffness are likely due to shear cracking or even possibly shear yielding, and then to try to understand what kind of effect this would have on the shear demand of the wall in general.

### 4.3.1 Appropriate Shear Stiffnesses

One major factor that can contribute to reductions in shear stiffness is shear cracking, which can drop the shear stiffness by a factor of up to 10. Shear yielding is also possible, further reducing the shear stiffness. This reasoning was the driving factor in the choice to analyze the structure from 100%-1% of the gross shear rigidity.

These are not the only two sources of variations in the shear stiffness, and perhaps the most common reason for a change in the shear rigidity relative to the flexural rigidity is simply the dimensions of the wall. The eight sample walls chosen for analysis were all designed assuming some kind of flanged core wall section, whereas in reality walls can range from having no flanges at all to having even greater flanges, increasing or decreasing the relative effect of shear stiffness respectively. As such, gross shear stiffnesses can probably vary from 500% to 20% of the gross rigidities of the sample walls.

What ends up mattering in the end is the proportion of shear stiffness to flexural stiffness. This ratio controls not only what the mode shapes will look like (shear type versus flexural type) but also the ratio between the periods, which is critical when dealing with shear amplification. All of this can be summarized neatly in Figure 4.15 for a cantilever system with uniformly distributed mass (i.e. shear walls).

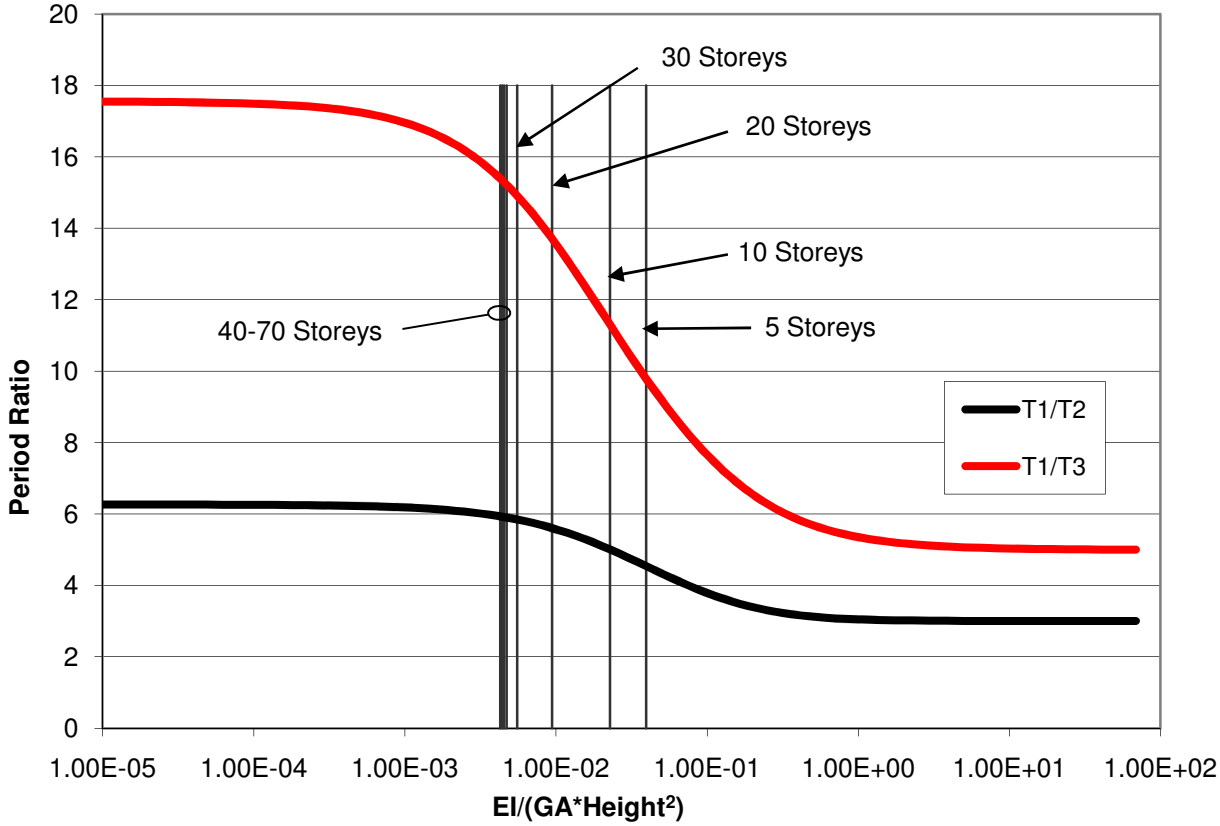


*Figure 4.15: Ratios of periods ($T_1/T_2$ and $T_1/T_3$) for shear wall structures depending on the shear and flexural stiffnesses, with example structures shown for reference*

Plotted on the figure are also the ratios for the uncracked sample structures in this study. It can be seen that they fall somewhere in the middle of Figure 4.15, with the very tall structures tending to be dominated by flexure as expected.

Because the x-axis of Figure 4.15 is logarithmic, it is very easy to see what kind of effect increasing (moving left) or decreasing (moving right) the shear stiffness would have on the ratio of periods. The effect of dimensional changes can be seen to be relatively minor – increasing or decreasing the shear stiffness by a factor of 5 does not dramatically change any of the period ratios. Furthermore it does not take the structure very far outside the range of sample structures, meaning that any behaviour should already be captured by the other structures. On the other hand, attempting to represent the shear cracking or yielding of the structure by reducing the shear stiffness by a factor of 10 or 100 respectively has a fairly dramatic effect on the period ratios, taking them into the range where shear behaviour dominates.

Another major issue when trying to model variations in shear stiffness is determining where to apply the changes. This is an easy enough issue to address when it comes to variations in the gross shear stiffness because it is solved simply by modeling each story accurately, but is more of a challenge when it comes to shear cracking and/or yielding. It is clear that a uniform wall will start cracking first where the shear force is highest and potentially where flexural cracks have also formed, but the previous RSA has shown that the shear force is significant over most of the height of the wall, so it is not unreasonable to expect shear cracking over a greater height after some cycles of loading. Shear yielding is a more difficult issue to examine, because it requires a larger force level. For this analysis it was assumed in all cases that the variation in shear stiffness is uniform over the height for simplicity.

### 4.3.2 Full Height Stiffness Reduction

For all of the sample structures RSA were performed with shear rigidities ranging from 100% to 1% of the gross. The base shear normalized by the weight versus the percent shear rigidity reduction is plotted in Figure 4.16 for the 10, 30, and 50 storey structures.

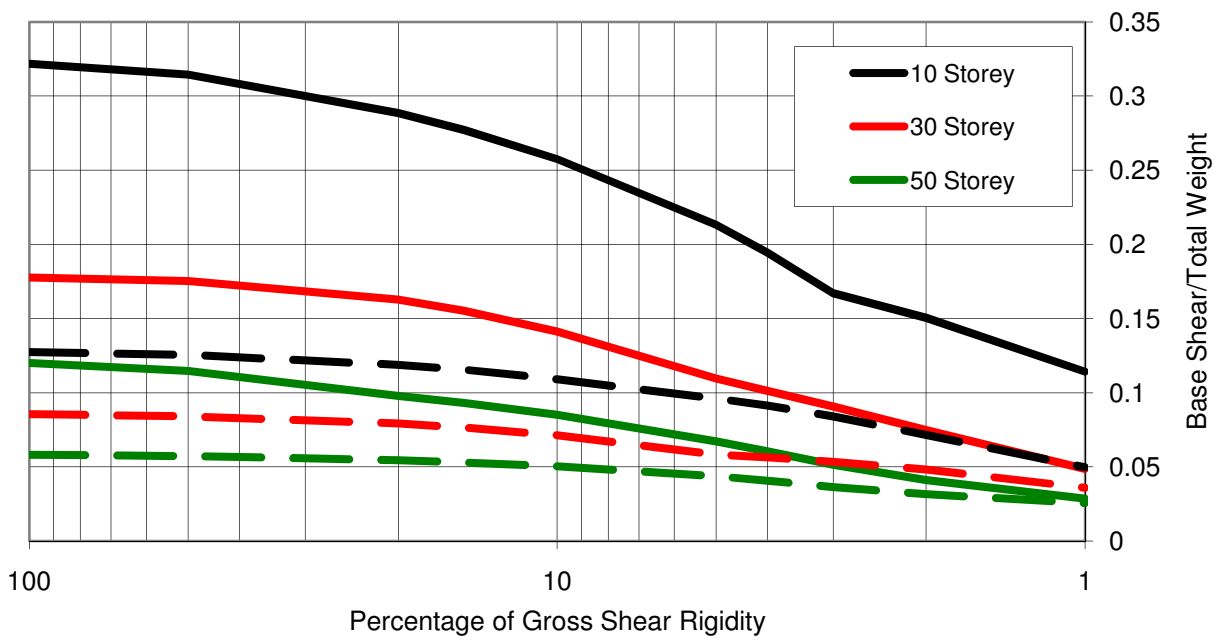


*Figure 4.16: Normalized base shear vs. percentage of gross shear rigidity, solid = fixed base, dashed = pinned base*

For all structural heights the base shear reduces along with the shear rigidity. The most immediate and easy to understand reason for this is simply that the periods are lengthening as the shear rigidity drops, moving the structure farther down the spectrum and therefore reducing the forces. However, there are two other causes for this reduction which are not so obvious. The first relates back to the period ratios figure – as the shear rigidity decreases (moving rightwards), the higher periods shift more than the first period, causing all the periods to grow closer together. Because the higher modes contribute significantly to the base shear, this effect causes a further reduction.

Finally, the mass participation ratios shift from the higher modes to the first mode, on the order of 15 percent. This phenomenon can be explained by considering the mode shapes of a structure with 100% and 1% of the gross shear rigidity.

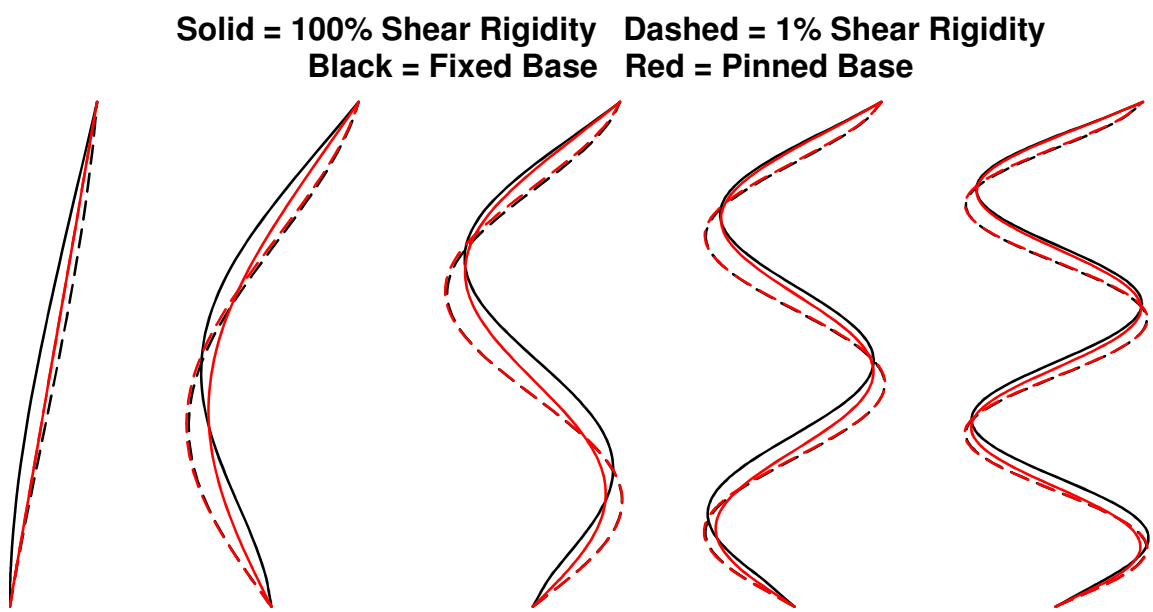


*Figure 4.17: First 5 mode shapes for pinned and fixed structures with different shear rigidities*

The first mode becomes closer to the imposed load shape (uniform over the height), which is the reason for the shift in mass that decreases the base shear. All together, these three effects – period lengthening, periods getting closer together, and mass participation ratios shifting – cause reduced base shear.

Thus far only shear demand has been discussed, but what about the effect on shear amplification? To answer this question further analyses with a pin at the base were performed. Figure 4.16 above also contains data from these analyses, and reveals interesting information. It shows that as the shear reduction becomes large, the fixed base shear and the pinned base shear draw close together, leading to the conclusion that shear amplification would in fact increase. This follows from the previous work where the percentage of base shear remaining after the pin formed at the base was considered to be an indication of the shear amplification present (see Section 4.2.2 and 4.2.3). An explanation can be found in Figure 4.17, where it can be seen that as the shear reduction becomes dramatic, the mode shapes for the fixed and pinned structures become very similar. Mechanically, the reason for this is because a pure shear mode does not cause any base rotation demand, so whether there is a pin at the base or not does not matter.

Together with the first period lengthening considerably (and therefore taking with it less base shear when it is eliminated by yielding), the constant mode shapes and periods of the higher modes results in higher amplifications. However, it is important to note that the drop in total base shear demand is considerably more than the increase in shear amplification, resulting in a net decrease in the base shear. Because of this, it is possible that a solution to the shear amplification problem could effectively ignore reductions in shear stiffness, knowing that if anything it will be a conservative result. In addition to this, for a designer to accurately predict the reductions in shear stiffness that a wall would undergo would likely require complex enough analyses that the shear amplification would be a result of the analyses and would not require a simplified method.

## 4.4 Potential Models

Due to the large amount of data that the RSA has provided, it is possible to already start considering potential models for shear amplification. In Chapter 2 of this thesis, solutions presented have come in two main varieties – strictly empirical solutions based off time history analysis results, and more theoretical solutions based off modal analysis results which are then compared to time history results. Clearly it is not yet possible to come up with a strictly empirical result, so what models or components of models can be generated using the data from RSA?

Partly because of previous work, and partly because it has been seen that the pinned model can produce interesting data, this section will focus on a two part solution. The first part will attempt to

address the shear force developed before yielding (sometimes called the capacity component), and the second part will attempt to account for the inelastic higher mode shear.

### 4.4.1 Capacity Component

Typically the so-called capacity component is assumed to be first-mode based. That is, it is the shear corresponding to the development of the yield moment due to a first mode distribution of forces only. Based on what has been observed so far, this seems reasonable – if the higher modes continue to oscillate even while yielding, it is questionable how much they would contribute to the base moment.

Taking the capacity component as first mode also corresponds well with tall structures with low shear stiffness, where the bulk of the shear comes after yielding. In this case, the maximum shear levels off at $R_d$, which is what one would expect. Another possibility is that the capacity shear is simply the shear from the RSA divided by the reduction factor, in the same way as the moment. At this stage it is difficult to tell because the modal relations become complex when yielding occurs.

Lastly an issue arises if attempts are made to extend the same principle to the two-pinned case. In that situation it becomes very hard to tell what kind of shapes should be assumed. However, if the goal is to accurately determine the base shear, it has already been shown that yielding higher up in the structure has minimal effect.

### 4.4.2 Higher Mode Component

In Section 4.2.3, the quantitative results from the pinned RSA were discussed, and it seems that this is the most promising possibility when trying to come up with the effect of the higher modes. However, the issue of attempting to come up with a simple relation based on the second fixed period is still problematic. If an attempt is made to use Figure 4.11 the lower end of the spectrum becomes very sensitive to slight aberrations from the exact line. On the other hand, if attempts are made to use Figure 4.12 there are issues regarding how to fit the curve when there is a large variation between different shear stiffnesses. Figure 4.14 shows that it is possible to create a simple model based on the uncracked shear stiffnesses, but whether this model is precise enough or not is impossible to determine at this point.

Despite these issues, it does appear to be possible to extract a value for the shear force after yielding from the pinned model, given the spectrum and the second period of the fixed wall. In this case, the question of how to combine the capacity component and the higher mode component becomes important. The two simplest ways are to either just combine them linearly or to use a square root sum of the squares (SRSS) approach. Here it is interesting to note that the SRSS approach is what Sullivan, et al. (2006) used, and their results seemed to underestimate the shear. Therefore, it may make sense to combine the two components by simply adding them together. This makes physical sense particularly if the capacity component is assumed to be entirely first mode and the higher mode component is taken from the pinned structure. This can be thought of as two structures acting together at the same time, and the reason they are not combined by SRSS is because the capacity component is not fluctuating but it a fixed amount.

### 4.4.3 Shear up the Height

A final important component of any model is to give information about the shear up the height of the structure. Here there are two possible ways to go – the first is to determine the base shear, and then create a separate model to find the total shear from the base shear, and the second is to incorporate the total shear in the model for the base shear. If in fact it turns out that using the two components described above does create a good model, it would seem most likely that the first option would be used. To try and predict the shear at all points could end up being unreasonably difficult, especially if it were to be based on the pinned model, which designers would not have access to under normal circumstances.

## 4.5 The Effect of the NBCC 2005 Spectrum – A Case Study

In order to illustrate the complex relationship between the response of a structure, the spectral shape, and the structural characteristics, this section deals with a matter relevant to Canadian practice – the leveling off of the design spectrum after T = 4.0 seconds in the NBCC 2005.

As the goal is to compare the NBCC 2005 design spectrum to a more “realistic” example, a similar spectrum to that detailed in Section 4.2 can be used. Specifically, instead of the acceleration leveling off after a certain spectral period it would instead be expected that at some point the response would transition into the constant displacement zone, and the acceleration would fall off proportional to $1/T^2$. Some guidance can be found in the ASCE 7 spectra, and it is not unreasonable

to apply some elements of the Seattle spectrum to the NBCC 2005 design spectrum for Vancouver. Graphically, the spectra compare as shown in Figure 4.18.

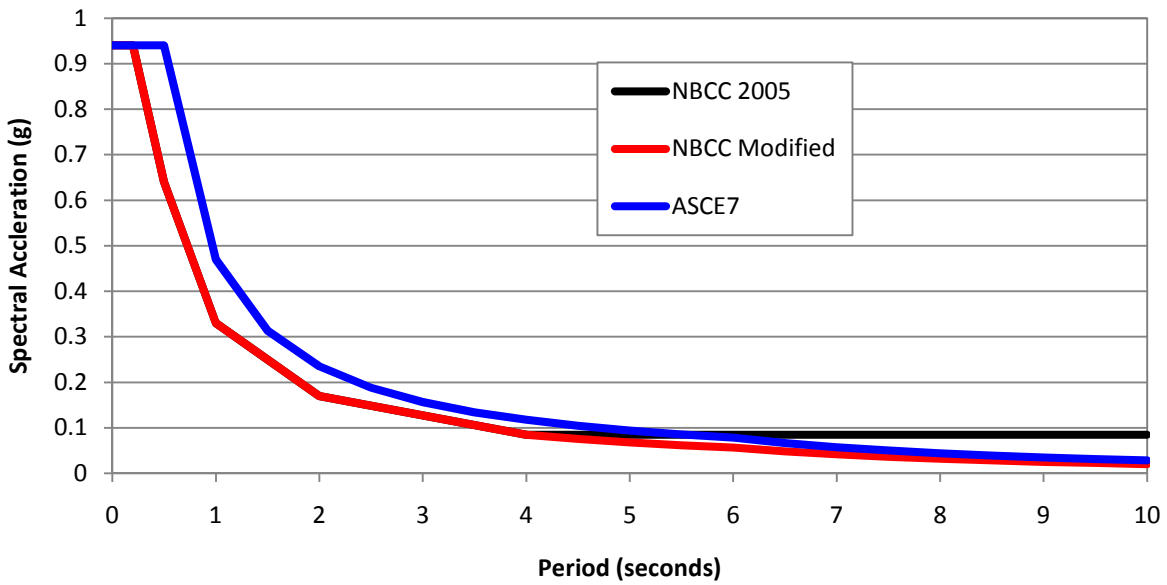


*Figure 4.18: Comparison of NBCC 2005, NBCC modified, and ASCE 7 spectra*

A couple of main differences stand out between the two spectra: first is that ASCE 7 maintains constant acceleration until 0.5 seconds, while NBCC 2005 until 0.2 seconds, and second that ASCE 7 goes at 1/T until 6.0 seconds, then moves to $1/T^2$. Because the objective is to focus on what happens after 4.0 seconds, a modified spectrum was constructed using the NBCC data up until 4.0 seconds, then after that applying the ASCE 7 method. This modified NBCC spectrum is also plotted in Figure 4.18. Note that the only difference between the spectrum used in the rest of the thesis and this spectrum is the leveling of the short periods.

### 4.5.1 Comparison of Moment and Shear Diagrams – NBCC Conservative?

In order to emphasize the importance of the differences in the spectra, the structure chosen for analysis is the 70-storey model structure ($T_1$ = 7.0s, $T_2$ = 1.2s, $T_3$ = 0.5s), whose first period falls squarely in the constant displacement portion of the modified NBCC spectrum.

One of the main assumptions of the NBCC 2005 design spectrum is that leveling off the acceleration after T = 4.0 seconds is conservative, since it will result in higher moments and shears. It can be

seen in Figures 4.19 and 4.20 that this is the case over the entire height of the structure. From the original moment and shear curves alone it seems reasonable to conclude that because the NBCC 2005 design spectrum overestimates the moments and shears, it is indeed conservative.

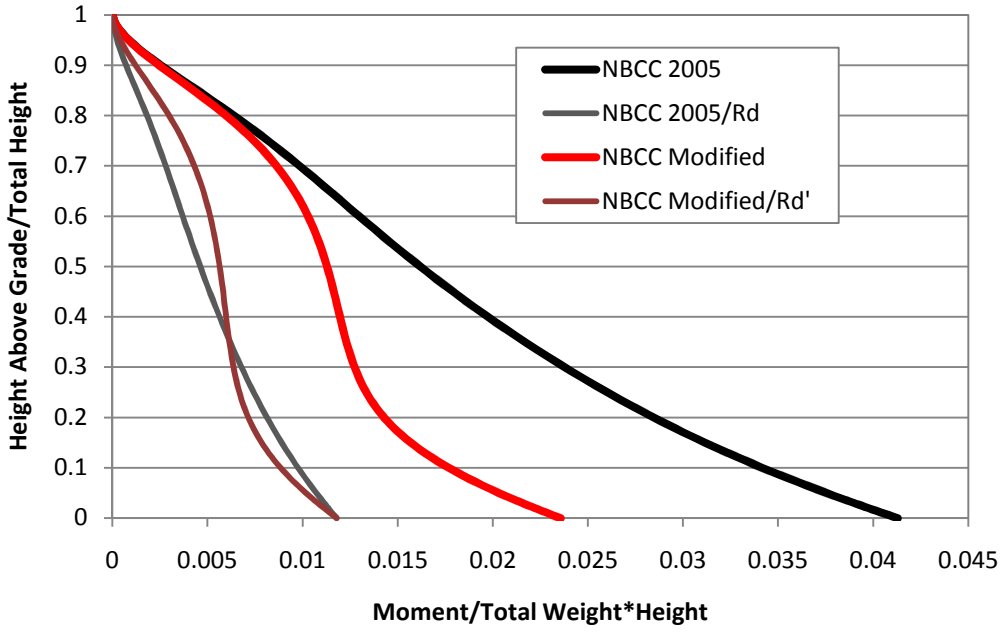


*Figure 4.19: 70 storey CQC moment envelopes*

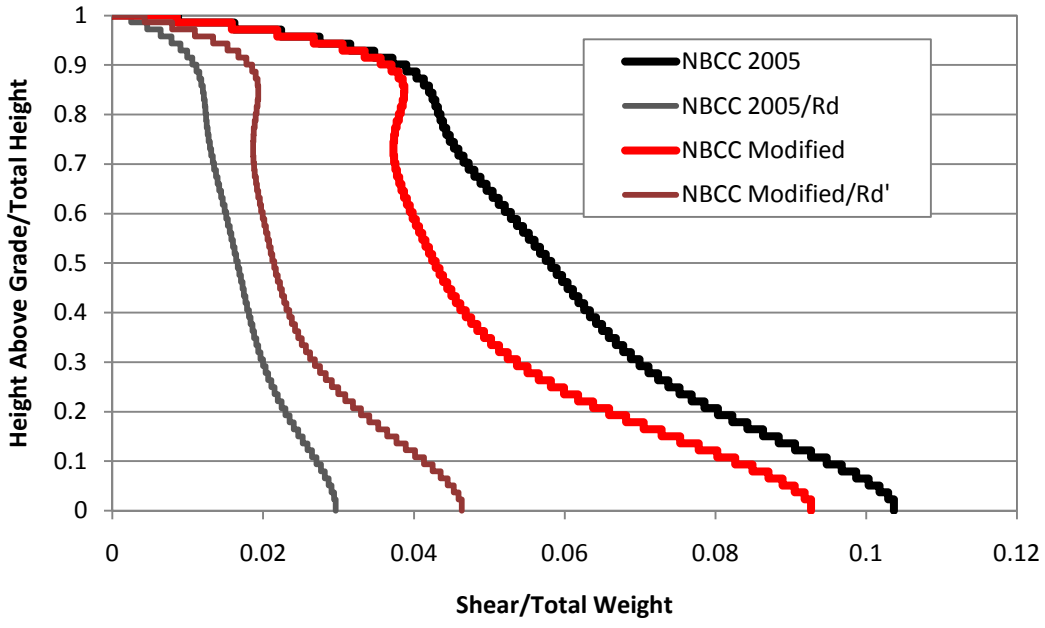


*Figure 4.20: 70 storey CQC shear envelopes*

However, what does this mean for the structure? In essence, it's equivalent to artificially decreasing the ductility demand ($R_d$), which in current design is strongly tied to the moment capacity at the base of the wall. For example, the base moment in the 70 storey structure reduces by 43%, essentially reducing $R_d$ from 3.5 to $R_d' = 2$. It's important to recognize that the structure will still yield, but that many of the remaining response quantities will be scaled up by the increase in the base moment. The CQC envelopes of the NBCC 2005 spectrum divided by $R_d$ (what is designed for), and the NBCC Modified spectrum divided by $R_d'$ (what is expected) are also plotted on Figures 4.19 and 4.20.

### 4.5.2 Scaling of Moment Diagrams and Mid-Height Yielding

Following the idea that other responses will scale to the new base moment, Figure 4.21 can be produced by normalizing the moments to the base moment, similar to the moments divided by ductility factors in Figure 4.19.

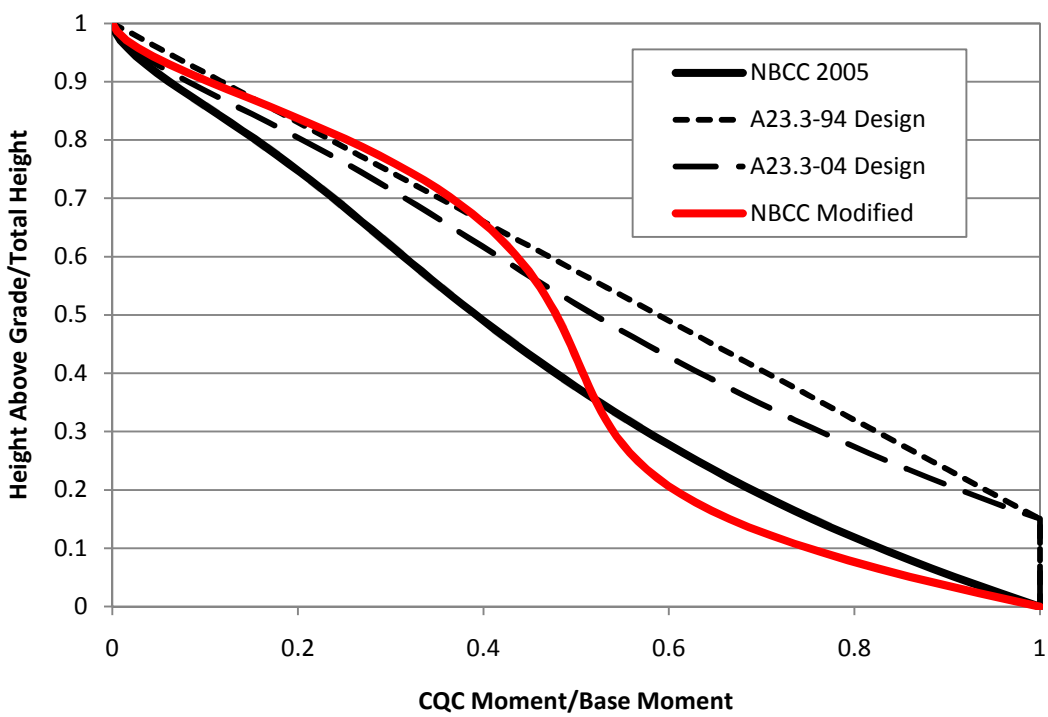


*Figure 4.21: 70 storey CQC moment envelopes, normalized so that they are unity at the base*

The theoretical bending moment envelope according to CSA A23.3-04 Clause 21.6.2.2 has also been plotted from the NBCC 2005 design spectrum for comparison. A plastic hinge height of 1.5 times the

length of the wall is used, with the $h_w/l_w$ ratio being roughly 10.8. Figure 4.21 makes it very clear that if no point on the moment envelope of the modified spectrum exceeds the design moment envelope then yielding can reasonably be expected to occur at the base. However this is not what Figure 4.21 shows, and in fact the modified NBCC envelope exceeds the design envelope from about 55% of the height of the structure up to the top.

### 4.5.3 Amplification of Shear

The other major issue occurs even if yielding does initiate at the base of the structure first. Essentially, the problem is due to the same behavior that causes mid-height yielding – under a real earthquake the structure will still behave non-linearly, but with increased forces at yielding. This particular phenomenon can be described in a number of different ways, and two are presented here.

The first is to look at the problem from the perspective of ductility factors, as has already been discussed. It can be clearly seen in Figure 4.20 that applying the same ductility factors to the shear as to the moment results in an increase of the shear over the entire height of the structure. Because higher modes contribute more to the shear than to the moment, the artificial increase in the first mode moment from leveling off the spectrum raises the base moment more than the base shear. When ductility is taken into account, this leads to an underestimation of the shear force at yielding.

Another way to consider the problem is to notice that an RSA predicts some constant relationship between base shear and base moment, related partly to the contributions of different modes and partly to the spectral shape. This can be thought of as the height up the wall at which the shear resultant acts to produce the moment. As the structural height (and therefore periods) increases, it is expected that this height (represented as a fraction of total height by M/Vh) will drop as the contributions of higher modes become increasingly more relevant. However, because the NBCC design spectrum artificially increases the contribution of the first period, the M/Vh ratio actually increases after $T_1$ = 4.0 seconds as seen in Figure 4.22.

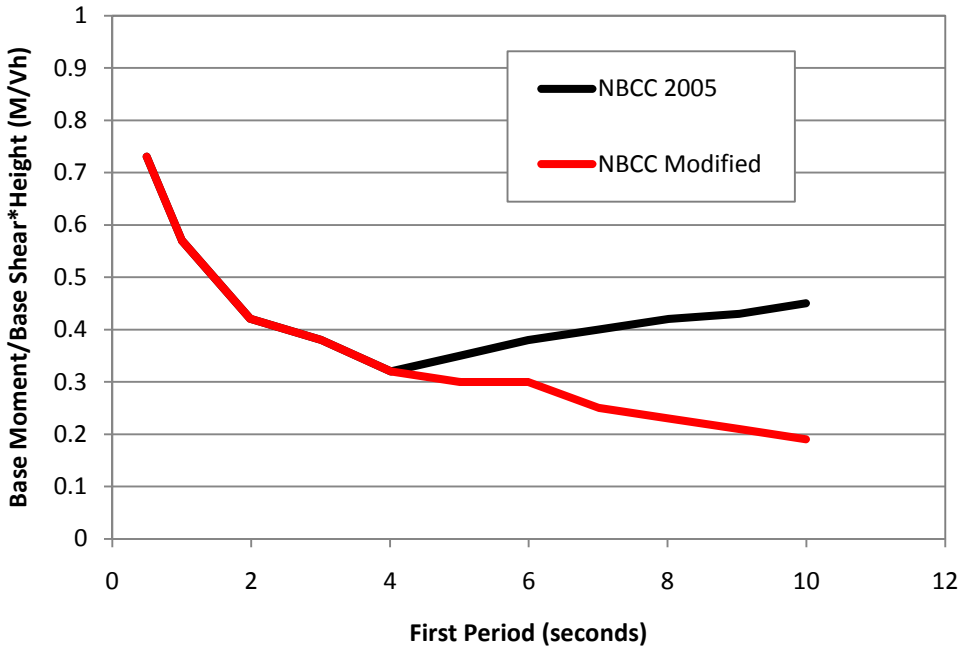


*Figure 4.22: M/Vh ratios as a function of first period*

So, for a given moment at the base of the structure the NBCC predicts a larger moment arm and therefore a lower shear than the more accurate spectrum does. This amplification of shear can be characterized by the ratio of the effective heights:

$$\omega_v = \frac{(M/Vh)_{Code}}{(M/Vh)_{Real}} \tag{4-2}$$

Where $\omega_v$ is the amplification factor. This factor is plotted versus first period in Figure 4.23. For buildings with a first period over 4 seconds the amplification factor can become quite significant.

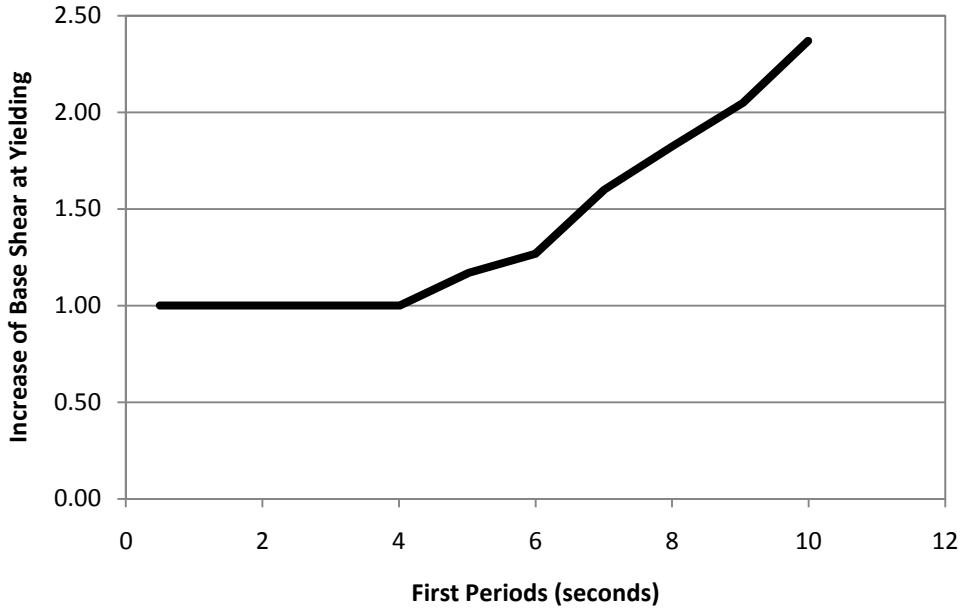


*Figure 4.23: Shear amplification due to choice of spectrum as a function of first period*

This case study reinforces the notion that in earthquake engineering it is often not possible to simply make assumptions that seem conservative. Because of the differing modal contributions between the shear and the moment, changing the spectrum will have effects that may be undesirable. As well, this case study clearly showed that the relationship between the maximum base moment and shear (M/Vh) from response spectrum analysis has a large influence on the overall design of the wall. This concept is important in the discussion of shear amplification, and will be returned to later.

# 5 TIME HISTORY ANALYSIS

This thesis has so far examined structures using linear response spectrum analysis (RSA) methods, and some tentative conclusions about the nature of the problem of shear amplification due to higher mode effects have been drawn. However, it is a principally nonlinear problem, and so the next logical step is to use nonlinear methods to both determine real levels of shear amplification and to examine the accuracy of assumptions and methods used in previous chapters.

There are several ways to approximate the nonlinear response of a structure. Some of the simpler methods have already been used, for example the code method of dividing the linear response by a strength reduction factor. Other methods include more complex ways to modify the linear results, nonlinear static methods of various complexity such as pushover analysis, and full time-history analysis using nonlinear material models. Of these, nonlinear time history analysis (NLTHA) will be used in the following sections because it is the best representation of the structural response available.

## 5.1 LINEAR TIME HISTORY ANALYSIS RESULTS

The analysis of structures by linear time history analysis is in some ways an intermediate step between using RSA and NLTHA, and can therefore be useful. Advantages of using the LTHA include being able to see the full time history of the response, and also not having to use modal combination rules to approximate the modes. In Section 5.1.1, LTHA will be compared to RSA, and in Section 5.1.2, issues from the previous section regarding the selection and scaling of records will be considered.

The LTHA results in Section 5.1.1 have all been computed using the input parameters described in Chapter 3. To summarize, the example structures were modeled using elastic beam-column elements with the same stiffness and mass used in Chapter 4. Forty records were fitted (by modifying the record in the frequency domain) to the spectrum in Figure 3.2, and these records were used for the comparisons in Section 5.1.1.

### 5.1.1 Envelope Results

Base moment and shear responses for the 10, 30, and 60 storey structures are shown below in Figures 5.1 to 5.3:

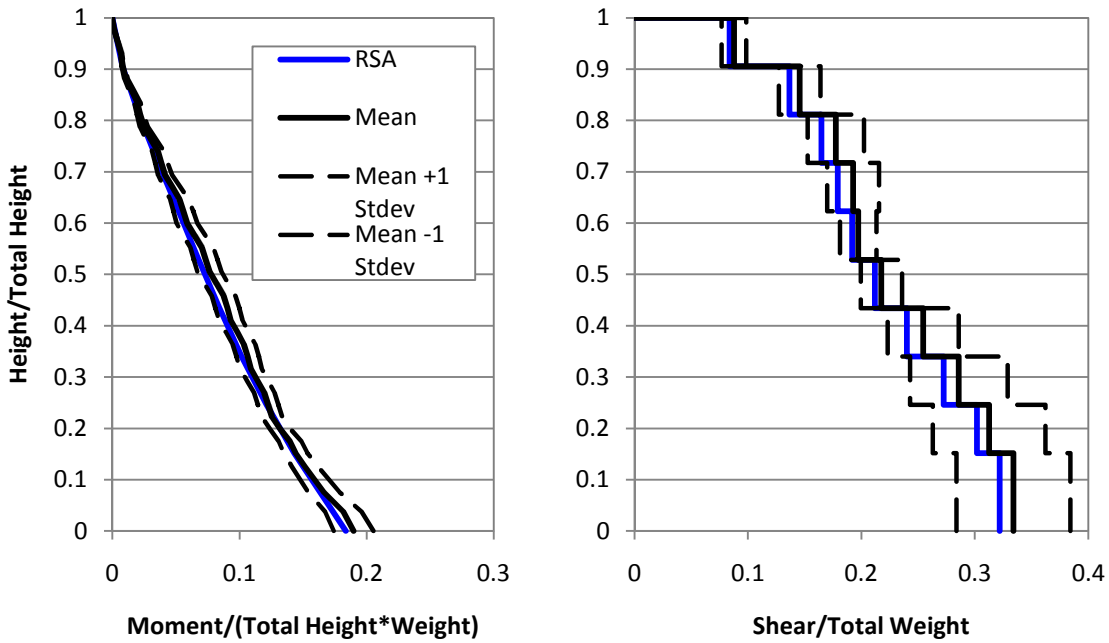


*Figure 5.1: LTHA envelope results for the 10 storey structure*

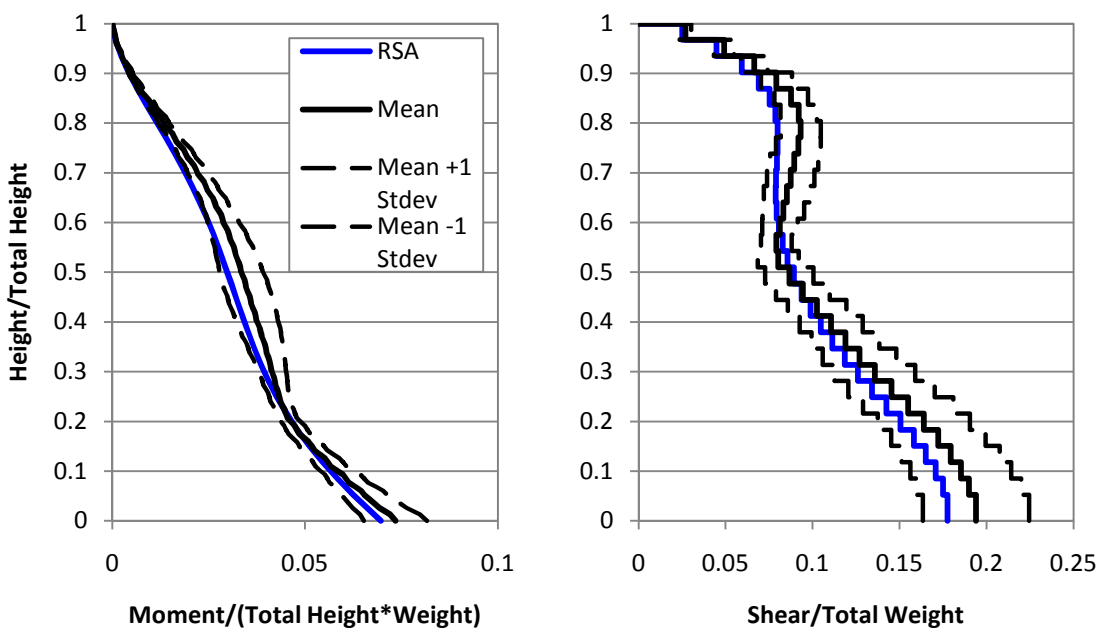


*Figure 5.2: LTHA envelope results for the 30 storey structure*

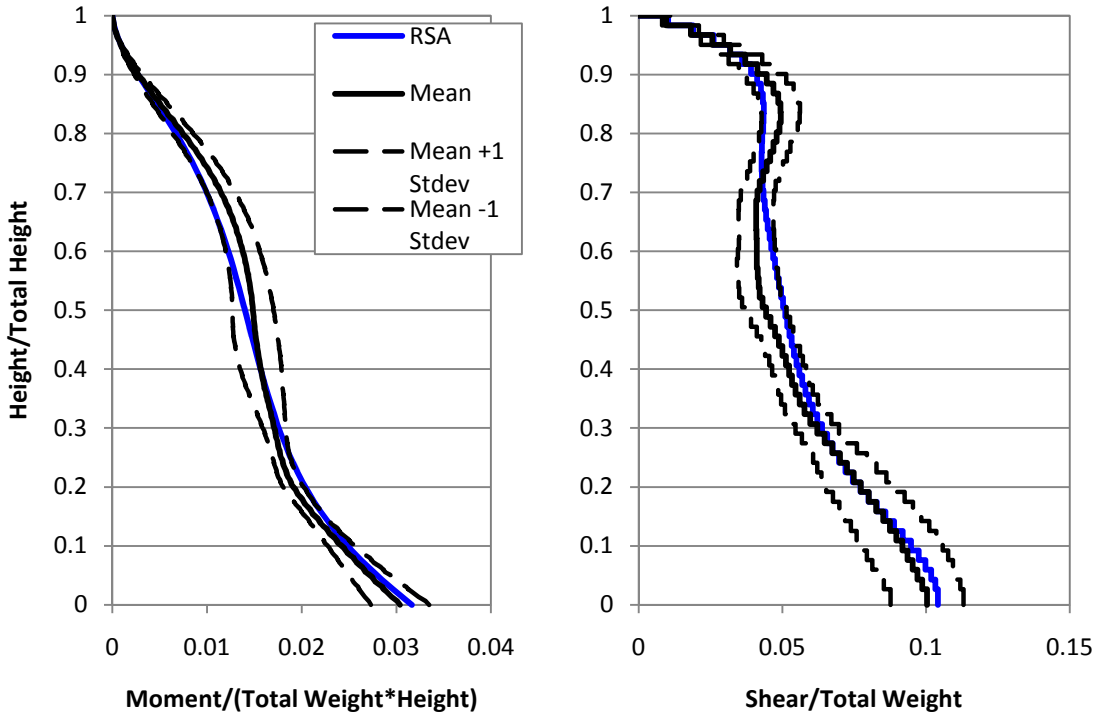


*Figure 5.3: LTHA envelope results for the 60 storey structure*

It can be seen that in most cases, the LTHA results are fairly similar to the RSA results. The base of the structure is of the most concern to this study, and although in the 10 and 30 storey cases, the shear appears to be underestimated by the RSA, the 60 storey case does not follow the trend. As there is no distinct pattern over the different heights, and considering that in all cases the RSA shear falls well within one standard deviation, it cannot be concluded that the RSA systematically over or under estimates the base shear. Figures 5.1 to 5.3 show that there is a difference higher up in the structure, where in all cases the RSA under predicts both the moment and the shear. However the discrepancy is fairly small, at a maximum of one standard deviation away from the mean.

The dashed lines on Figures 5.1 to 5.3 show the scatter in the data from the LTHA, which is quite interesting. Figure 3.4 showed that the fitting of the earthquake records resulted in a very good match to the target spectrum, so much so that the differences were nearly indistinguishable. Despite this very good match, there is a fair amount of variance in both responses, and especially the shear. While this is an issue that is somewhat interesting, it should be noted that the profile of the mean plus one standard deviation curve is very similar to the mean curve. Therefore, conclusions drawn about one curve can likely be extended to the other. Because of this, most of the

results in the following sections will focus on the mean values, with the knowledge that if someone wanted to design to a lower probability of exceedance they could do so.

### 5.1.2 Ground Motion Selection and Scaling

There is no clear consensus on either the issue of ground motion selection or ground motion scaling, and the two topics could constitute a considerable study. Selection and scaling for tall buildings poses a number of problems which are unsolved, largely due to the participation of the modes not being the same in all the structural responses. The PEER Tall Building Initiative has a subgroup devoted to attempting to solve this problem, but as recently as July 2010 have not come closer to finding an acceptable solution (Hamburger & Moehle, 2010).

Furthermore, ground motion selection and scaling is often talked about in the context of the practicing design engineer, who is concerned with a specific site. In that situation, geological information and hazard information from both historical and other sources can be used to select or generate records that are suitable for the site. Even then scaling is still an issue, but at least the focus is narrow and code procedures are available. On the other hand, for research where there is no specific site in mind, and a large number of structures needed to be analyzed, the process is less clear. Which records should be used? How should the scaling be done, and to what criteria? And how do the records relate back to the code specified hazard levels? There are clearly several issues here, and a brief discussion of each is in order.

**Ground Motion Selection**

In order to obtain an acceptable suite of ground motions, selection criteria must be identified. The first is undoubtedly that enough ground motions must be selected. If not enough motions are used in the analysis, the resulting statistics of the response quantities may not be representative of the intended hazard level. For example, choosing only 7 ground motions (the minimum required by ASCE 7 to take the average) would not likely be adequate for the purpose of trying to understand a general phenomenon. This has been raised in Section 2.2.2 as an issue with much of the previous research.

Another issue is ensuring that the recordings of the ground motions have sufficient long period information. It is common for instruments to be unable to measure long period information well,

and in a study such as this where first periods are as large as 7.0s for the tallest structure, this long period information is critical. Furthermore, if the structures are allowed to yield or crack this could potentially elongate the periods. Because it is desirable to be consistent and use the same ground motions for both linear and nonlinear analysis, it is important to select ground motions that have reliable data up to at least periods of 8 seconds.

The third requirement is that the shape of the ground motions be varied enough to represent a wide range of spectral shapes. This means getting ground motions from all the potential mechanisms, including subduction, crustal, and subcrustal events. The effect this will have is that to cause a large variation in the spectral magnitudes at different periods, helping to get a real representation of the possible scatter in the data. It is also important to get records from a wide range of different earthquake events, and ensure that not too many records are obtained from any one event.

Lastly the source and site characteristics, such as site class, magnitude, and distance, can be issues. It has been noted earlier that these are not as relevant for a research study as for the design of a new structure, and while this is true it is not possible to ignore this completely. For example, it makes sense to only choose earthquakes above a certain magnitude, since weak earthquakes will not cause any nonlinear behaviour and will therefore not display shear amplification. As well, following the previous point about different mechanisms, it makes sense to choose records that have a variation in distance.

All of these requirements add up to a long list of conditions that must be met, and to select a set of ground motions that meet these criteria can be very difficult. Considerable differences in the structural response can be observed depending on the motions selected. Furthermore, the record selection interacts with the scaling – certain types of records will give poor results when scaled in a certain way. This concept will be further illustrated in the ground motion scaling section (see Figure 5.7).

**Ground Motion Scaling**

It is not entirely clear how to scale earthquakes to a spectrum when several periods are important, nor is it even clear which spectrum they should be scaled to. Perhaps the best way to approach the problem is to define why it is necessary to scale the earthquake records in the first place.

Once again it is useful to contrast the objectives of this study to those of the practicing engineer. The goal of the practicing engineer in scaling the earthquake records is to make sure that they at least meet the code specified hazard levels, to ensure an acceptable level of performance under the design earthquake. On the other hand, the structures being subjected to ground motions in this thesis have no such need, because the analysis is only concerned with understanding a particular phenomenon, regardless of the hazard. So why then can the unscaled records not be used? It would be theoretically possible to analyze the structure both linearly and nonlinearly under all the records and compute effective $R_d$ values, and then determine levels of shear amplification. However, the problem arises when one wants to deal statistically with all of the earthquakes. The result of this procedure would be a large range of responses, and it could be very difficult to arrive at any conclusions, since it could not be assured that any two earthquakes would give similar $R_d$ values. Furthermore, to what strength should the original structure be set? And lastly, how would any comparison to RSA be possible? For these reasons it still is necessary to scale the records. Then the question becomes, to which spectrum should they be scaled?

There has been much made about the fact that the uniform hazard spectrum (UHS) does not generally represent any particular realistic earthquake scenario, and for structures with multiple important periods it overestimates the hazard considerably. This has led to the invention of the conditional mean spectrum (CMS), a useful tool that addresses these issues. So should the scaling be done to the CMS? Once again the problem of multiple periods arises – in using the CMS the user must pick a period about which to perform the modification, so when there are multiple periods, it is not clear which is the best choice. It has been suggested to use two different CMS to represent the lower and upper period ranges respectively, and this is an option. Fortunately, it turns out that this debate is largely irrelevant for this study, because the shape of the spectrum is one of the parameters. It has been shown in previous research, and strongly suggested in Chapter 4, that the shape of the spectrum has a large effect on the shear amplification. Therefore if the shape of the spectrum matters anyways, it is far less important as to which spectrum the earthquakes records should be fit, and more important to vary the spectra enough that differences reveal themselves.

Now the real problem arises, and that is what method to use to scale the ground motions. There are two main options, scaling in the time domain (linear scaling by a factor), or frequency scaling (where the spectrum is matched exactly). There is no clear consensus on which technique is better,

so both should be considered. The advantage with frequency scaling is that there is no need to worry about how well the spectrum matches over a given range, nor is there a need to pick a range at all. The disadvantage is that the frequency content of the ground motion is changed considerably, which can have large effects on the time history. In particular, while the frequency scaling does an excellent job of predicting the maximum response, it fails somewhat in capturing the cyclic peaks of the seismic motion. Furthermore, it also produces much less scatter than the linear scaling, which may be of concern assuming that the linear scaling in fact represents the true amount of scatter and is not an overestimation.

The linear scaling method has its own set of problems. The first is that a choice must be made as to which period range to scale the records over. Current codes such as ASCE 7 recommend that the spectrum be linearly scaled to match over the range of $0.2T_1$ to $1.5T_1$, the idea being that this range will capture both period lengthening due to inelastic behaviour and the effects of higher modes. This works well for structures that are both dominated by the first period and do not have a very large first period, such as short moment frames. Tall shear wall concrete structures satisfy neither condition, and when periods above the second become important it is not enough to stop at $0.2T_1$. Furthermore, when the first period is large the range that one is scaling over ends up becoming very large, often amplifying the shorter period range of the spectrum to compensate for the longer period range. Figures 5.4 to 5.6 below show the average scaled spectrum (over the range of $T_1$ to $T_2$) of the earthquakes for the 10 storey, 30 storey, and 50 storey case. Appendix C contains the associated scaling factors.

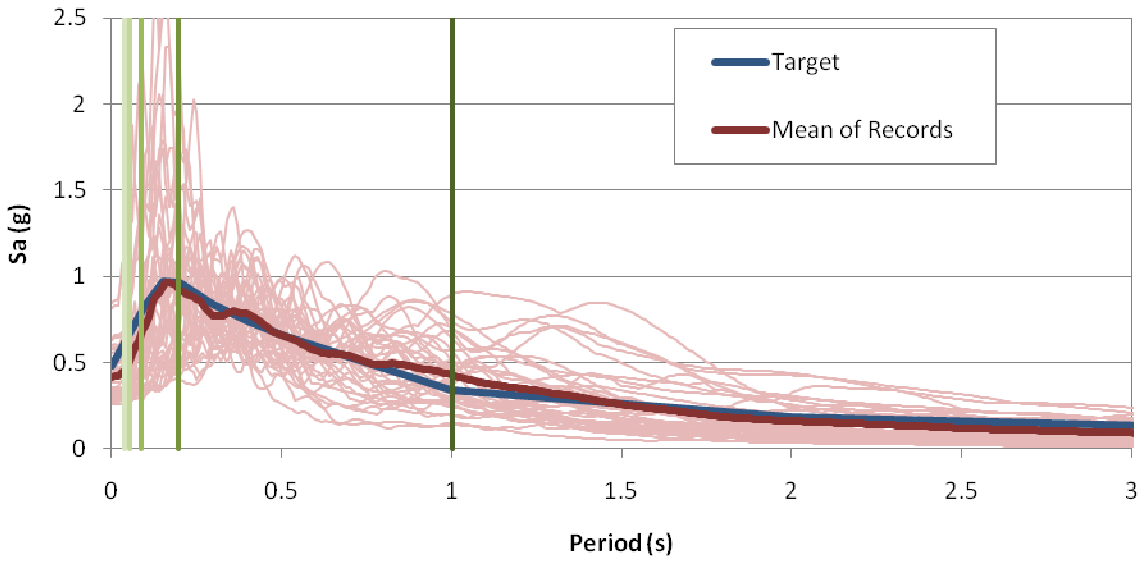


*Figure 5.4: Scaled records for the 10 storey structure (periods shown in green, 1st to 5th darker to lighter, thin lines are individual records)*

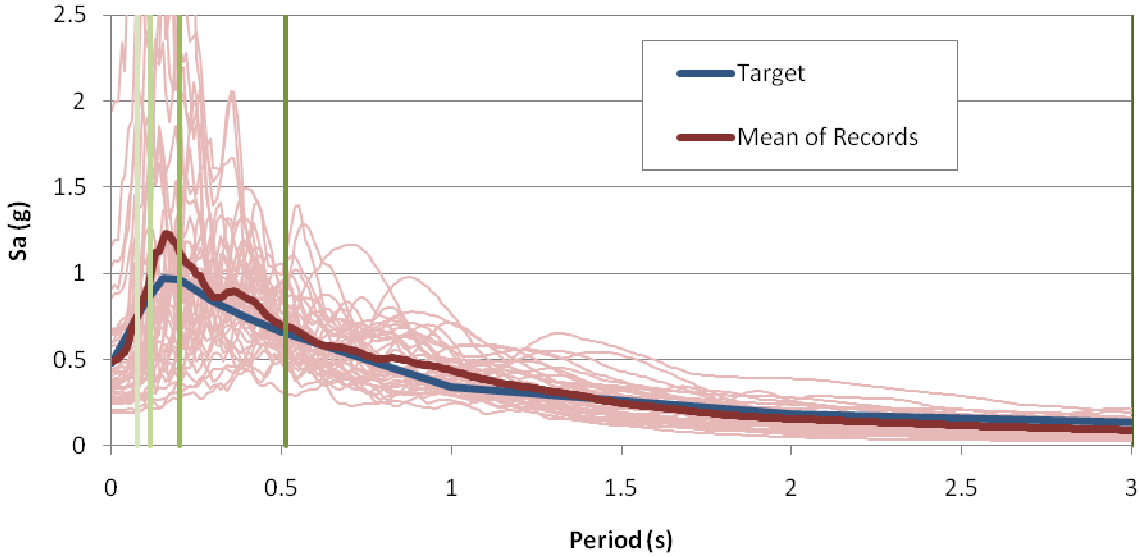


*Figure 5.5: Scaled records for the 30 storey structure (periods shown in green, 1st to 5th darker to lighter, thin lines are individual records)*

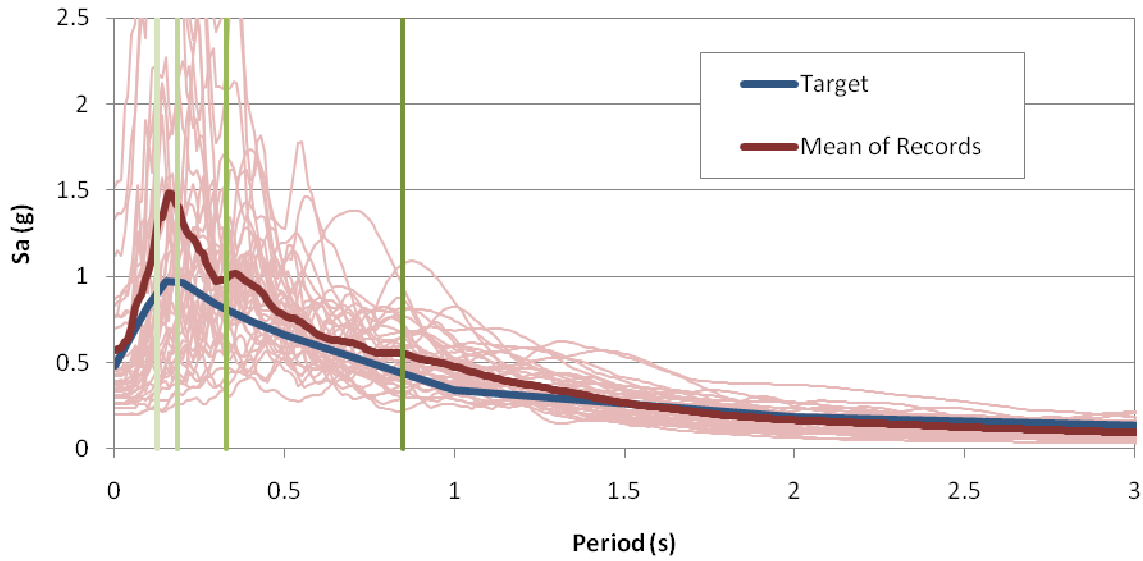


*Figure 5.6: Scaled records for the 50 storey structure (periods shown in green, 1st to 5th darker to lighter, 1st is at 5 seconds, off the figure, thin lines are individual records)*

It can be seen that the spectrum at the shorter periods is much larger than it should be as height increases, so using this method would result in shear forces that are much larger than expected. The secondary result of this type of scaling is also to increase the scatter of the data, because the shorter period range of the spectrum is controlled by the long period scaling. Note that the problem could be even worse is the code method of scaling from $0.2T_1$ to $1.5T_1$ was used.

The upshot is that there are issues with both methods – the frequency scaling may be simpler to deal with and it predicts the maxima well, but at the cost of some of the other important parameters like the scatter and peaks other than the maximum. On the other hand the linear scaling retains the original characteristics of the ground motion, but is plagued by problems with scaling over a wide period range. The advantage of looking at the LTHA is that running the analysis is very fast and the output is simple. Figure 5.7 below shows the moment and shear envelopes for the 30 storey structure with the ground motion scaled linearly.

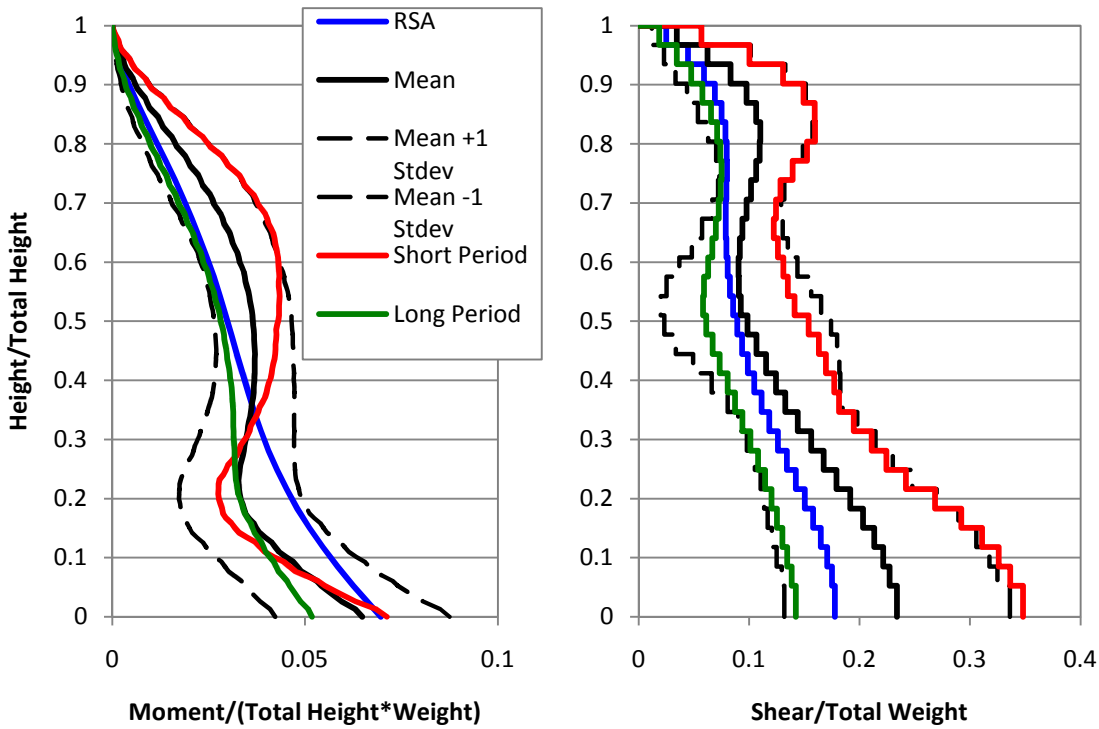


*Figure 5.7: LTHA envelopes for the 30 storey structures with linear scaling, short period and long period curves from records shown in Figure 5.8*

Figure 5.7 is very different than Figure 5.2. Not only does the RSA appear to underestimate the shear forces over the entire height and the moment over the upper part of the structure, but the scatter in the data is large. The shear and mid-height moment are controlled by this short period part of the spectrum, and so a large amount of variance occurs.

The red and green lines in Figure 5.7 demonstrate this principle even more clearly. The red line is composed of 9 out of the 40 records that have most of their energy in the short periods, while the green line is 9 of the 40 records with significant energy in the long periods. It can be seen that due to the problems with the scaling, the responses of these two sets of records are quite different. This also relates back to the issues raised in Section 2.2.2 – if only a small set of records are selected, how can one be sure that they are representative of ground motions as a whole? Figure 5.8 compares the average spectra of the short and long period records:

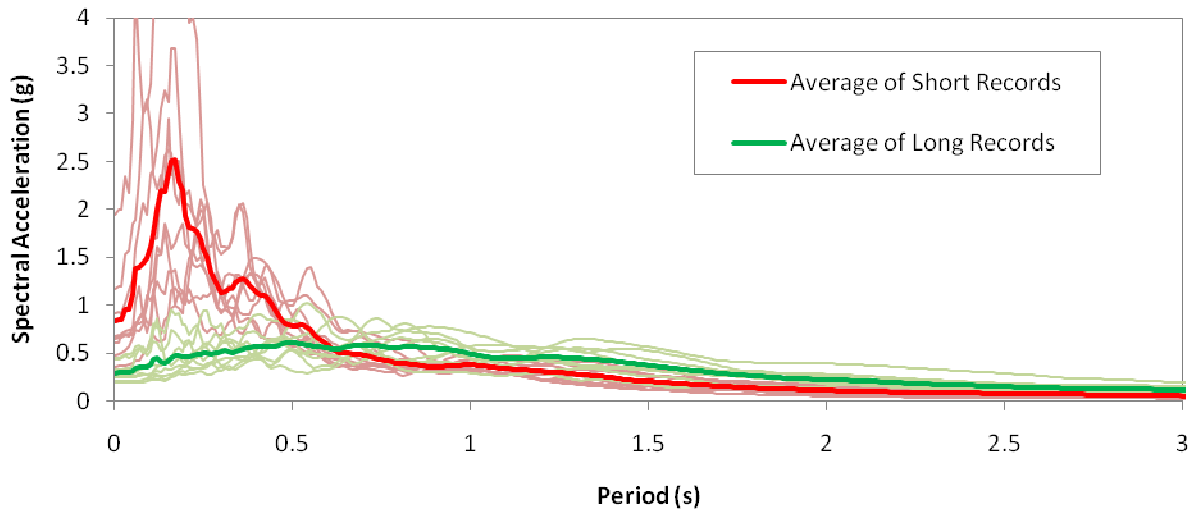


*Figure 5.8: Spectral comparison of the short period (red), and long period (green) records, thick lines are averages, thin lines are individual records*

To compare, consider the fitted results. Figure 5.9 is the same as Figure 5.2 except that the short and long period ground motions have been separated out in the same way as in Figure 5.7:

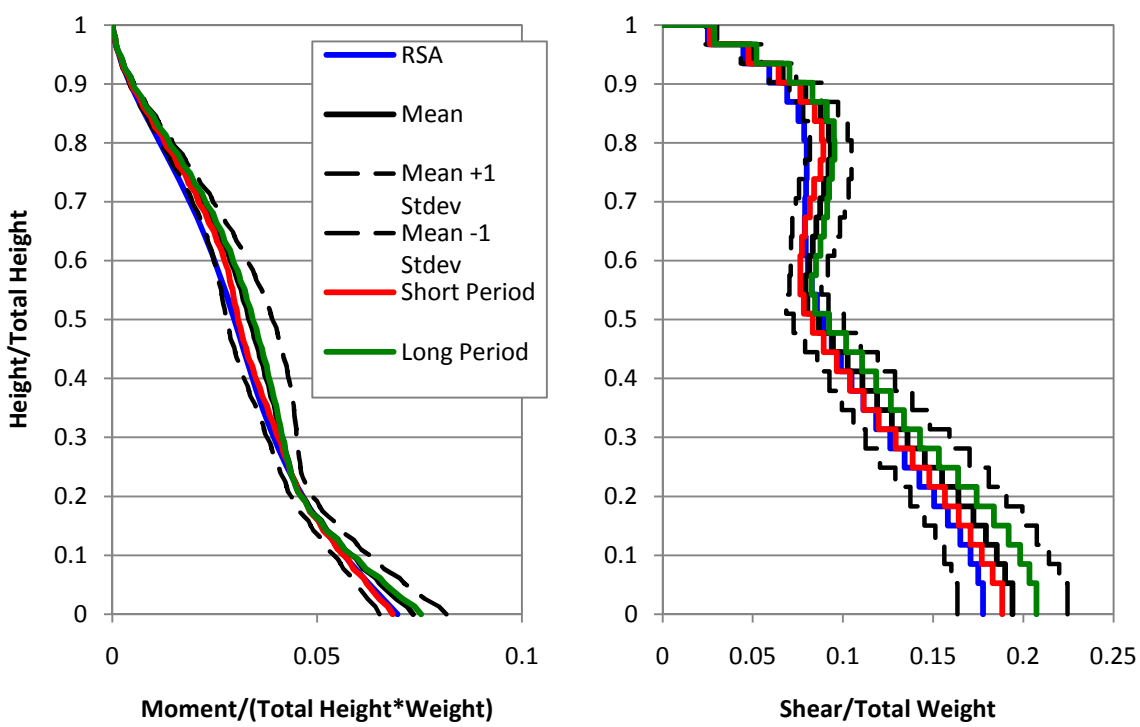


*Figure 5.9: LTHA envelopes for the 30 storey structure with short and long period records*

With the fitted records, the effects of the frequency distribution in the records have been eliminated, and all the records give very similar results. This is why fitted records are the most suitable for looking at the averages of many records.

## 5.2 General NLTHA Results

A full set of outputs from a NLTHA can be quite extensive, ranging from member forces to reactions to displacements. For the purposes of this study it was decided to look at mainly the time history moment and shear response of the base of the structure, and the shear and moment envelope over the height of the structure. The time history at the base of the structure allows one to easily visualize the dominant modes as well as providing valuable information about the relationship between the moment and the shear. The response envelopes complement the time histories by providing a concise summary of the information needed for the design of the wall, and are easy to compare to the results from the RSA. Lastly, the displacement time history at the top of the structure was also recorded – not only because it is easy to compare to the RSA results, but also because the top displacement (and hence the global drift ratio) is an important parameter for the design of high rise core walls and it is interesting to see how it varies with time.

### 5.2.1 Envelope Results

The first set of nonlinear analyses were performed assuming only the base element yields. This is consistent with the concept of a plastic hinge forming at the base of the structure while the rest of the structure remains elastic. Realistically the plastic hinge would extend over more than just the length of one element, but this type of model is adequate to understand the general behaviour of such a structure.

Nonlinear analyses were performed on all 8 of the sample structures under all 40 ground motion records for values of $R_d$ varying from 1.0 to 5.0. Note that it is necessary to plot the results from the $R_d$ = 1.0 case because the strength has been assumed to be equal to that from the RSA, something that is not necessarily true, but is an adequate assumption, as seen in Section 5.1. As well, the elastic results have been incorporated for the purposes of comparison.

For the sake of clarity, it was decided to plot only the linear, $R_d$ = 2.0, 3.5, and 5.0 cases. Figures 5.10 and 5.11 below show the mean shear and moment envelopes from the 40 records.

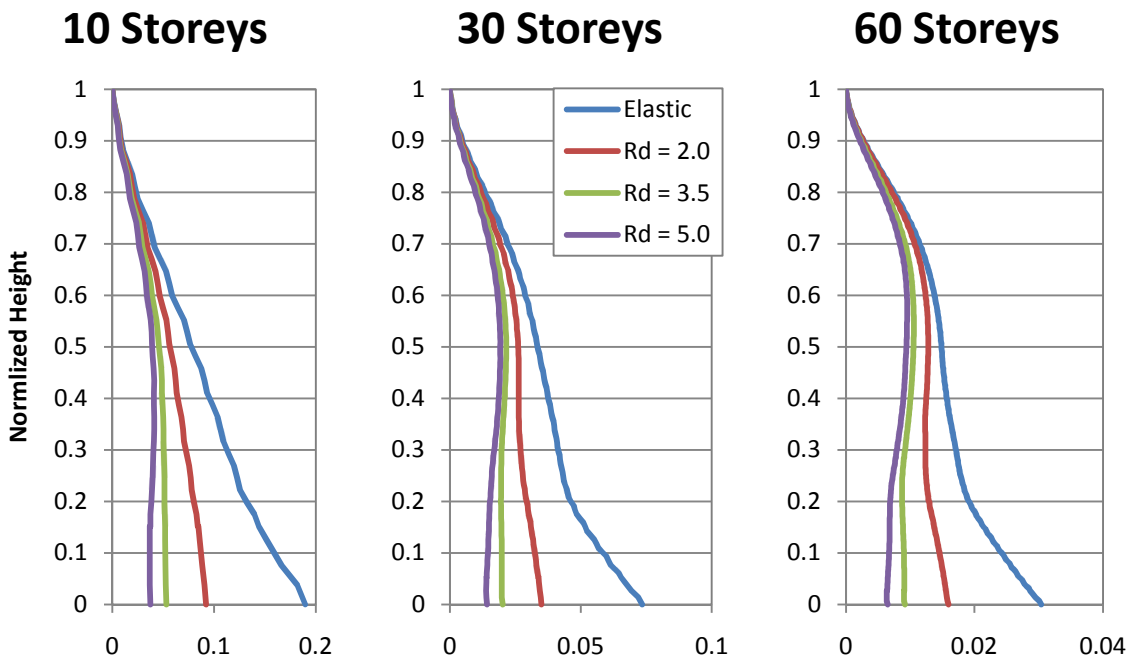


*Figure 5.10: Normalized height vs. normalized base moment (moment/total weight time height) for the 10, 30, and 60 storey structures*

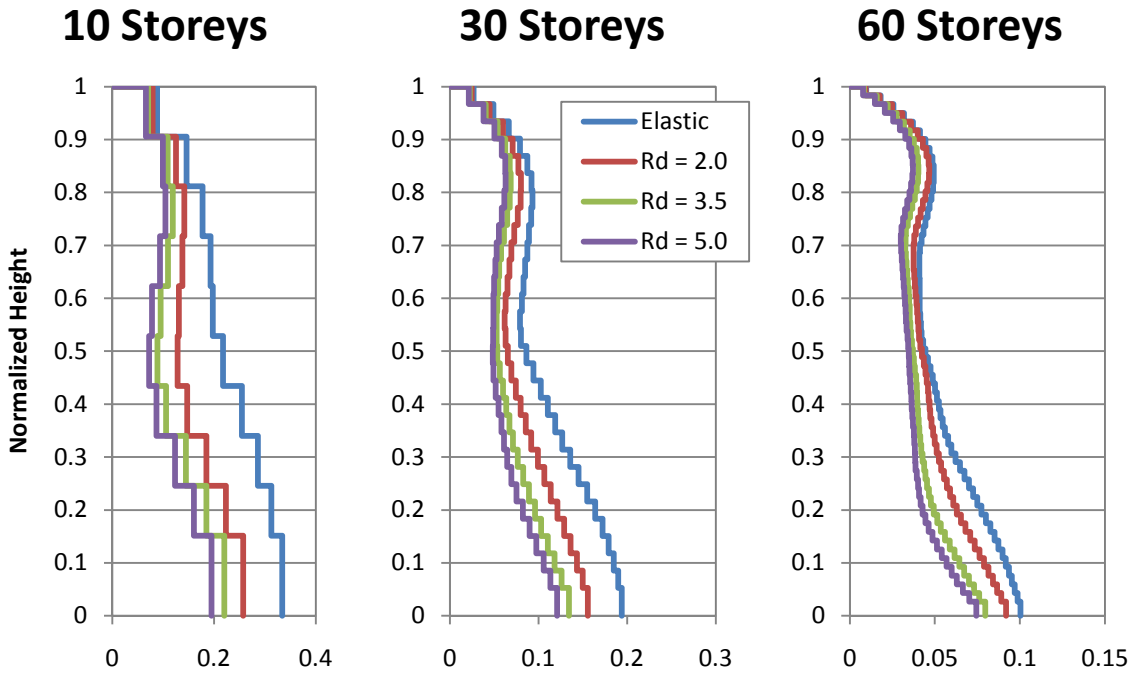


*Figure 5.11: Normalized height vs. normalized shear force (shear/total weight) for the 10, 30, and 60 storey structures*

One conclusion that can be drawn from these results is that the effects of higher modes are much more important than the results from even the linear time history analysis suggest. Even in the 10 storey case, where it would be expected that the result would be dominated by the first mode, it is clear from Figure 5.10 that the reductions due to yielding seen in the base moment do not translate into reductions higher up the height of the structure. As the structural height and the periods increase, the effect becomes even more pronounced, until it can be seen that in the $R_d$ = 5.0 case the moment at 60% of the height of the structure is not reduced by even a factor of 2.

The shear forces tell a similar story, except that they are not limited at the base of the structure, but continue to increase over the height. This behaviour is not only prevalent in longer period structures, but can be observed in the 10 storey example. However, despite the fact that the yield strength of the base of the structure controls neither the shear nor the moment perfectly, it can be observed that yielding reduces both. Furthermore, it is promising to see that the shape of the shear force diagram predicted by the elastic RSA analysis is somewhat similar to that from the nonlinear analysis, suggesting that there may be still some kind of relationship between them.

The next step is to allow the structure to yield over the entire height, representing a more realistic model. However, the choice has to be made as to what yielding strength should be assigned to all floors. One way would be to follow the code procedure, where a plastic hinge length is calculated, and the moment demand is scaled over the rest of the height to the RSA (CSA, 2004). However, this is unnecessarily complex if the only goal is to try and get a feeling for what the structure will do when it is allowed to yield in multiple locations. For this reason, it was chosen to examine two different yield profiles. The first assumes the structure has a constant yielding moment over the entire height of the structure equal to the base yielding moment. This profile was chosen because some previous work has been done using this method, so it would be useful to be able to compare the results. This kind of profile is not realistic however – even if identical reinforcing is provided over the height of the structure, the yield moment will still vary due to the effect of the axial load. Therefore it was chosen to use a yielding profile that varied linearly from the base of the structure up to half of the base yield moment at the top of the structure. Note that some previous work (Babak, 2009) had used a yielding moment profile that varied linearly from maximum at the base of the structure up to zero at the top of the structure. This is too extreme, because requirements for minimum reinforcing will always guarantee a certain strength. Plots of the structures under the

same yielding strengths are shown in Figures 5.12 and 5.13, with all three yielding cases compared (only base yielding, uniform yielding, and linear yielding). Note that only the $R_d$ = 3.5 case is shown, because the others follow similar trends.

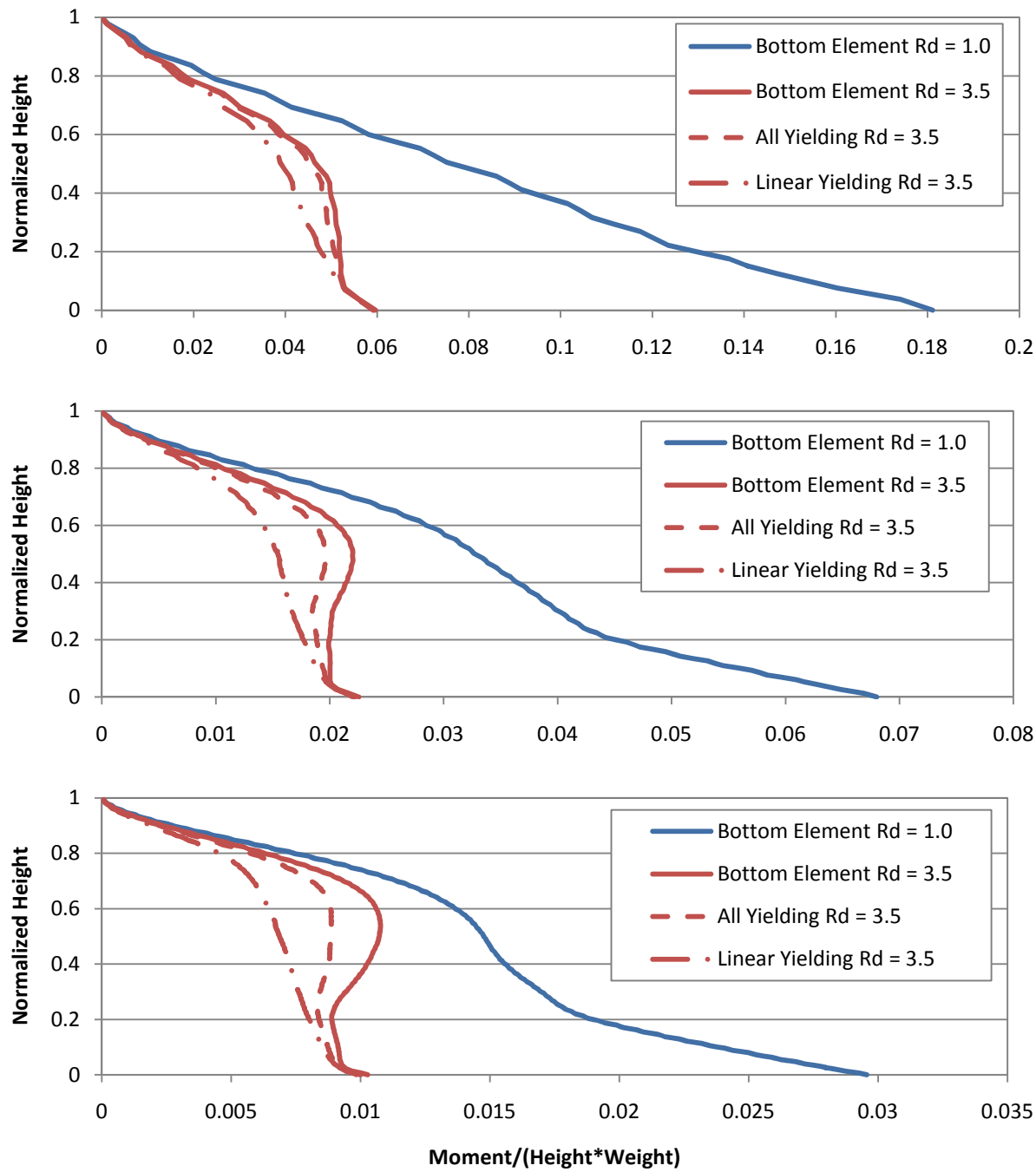


*Figure 5.12: Normalized height vs. normalized moment for various yielding conditions for the 10, 30, and 60 storey structures*

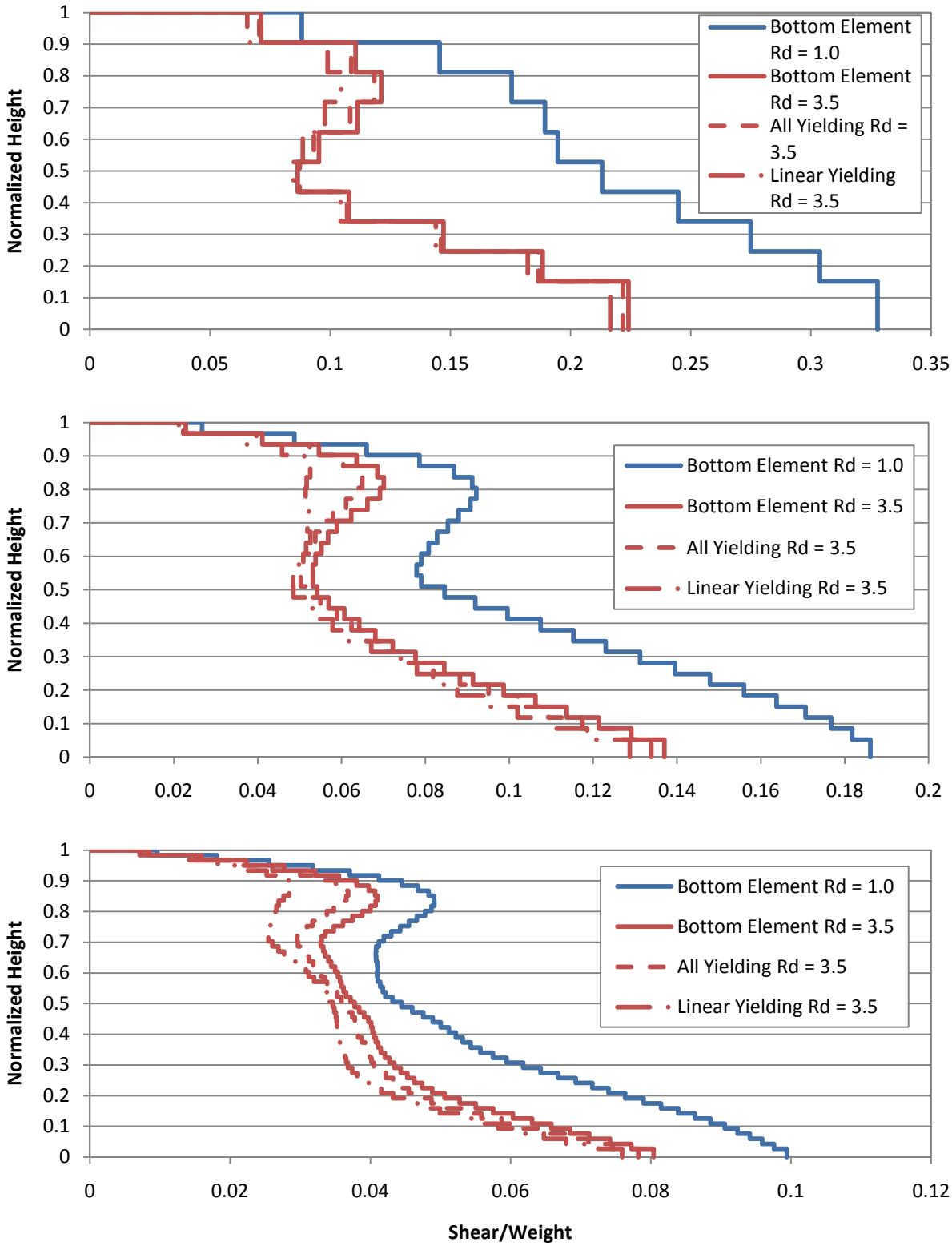


*Figure 5.13: Normalized height vs. normalized shear for various yielding conditions for the 10, 30, and 60 storey structures*

Note that the small increase in the moment observed at the base of the structure is due to an increased post-yield slope, necessary to achieve convergence in the nonlinear analysis when all components are allowed to yield. In order to facilitate comparisons the analysis performed for the structure which is allowed to yielding at the base only was done with the same post-yield slope.

What is interesting, although not unexpected, is the difference in the bending moment diagrams even in the shorter structures. It can be clearly seen that a significant amount of nonlinearity is expected, especially when a linear yielding profile is assumed. This observation becomes clearer when the structural height increases, and in the 60 storey structure the amount of nonlinearity at the higher floors is quite substantial. Furthermore, the $R_d$ = 1.0 case has also been plotted along with the $R_d$ = 3.5 structures, with the purpose of showing that even though in this case the structure could potentially yield, it does not in any of the cases actually yield. This shows that the results from the linear analyses give no indication whatsoever of the potential for yielding higher up in the structure.

More relevant to the problem of shear amplification is to examine the effect of the sometimes large amount of mid-height yielding on the shear envelope of the structure. It seems that if the mid-height moment decreases significantly, then the associated higher-mode shear phenomena would also decrease. This occurs higher up in the structure – for example in all the structures the bulge in the shear at the top of the structure is greatly reduced and nearly eliminated. However the base shear – another effect associated with higher modes – does not decrease substantially, a somewhat unexpected result. The explanation for this can be found in the RSA models performed with a pin at the mid-height of the structure. As seen in Section 4.2.2, when a pin is placed at the mid-height of the structure (symbolizing yielding), it is mainly the shear above the pin that is affected. The results from the NLTHA in this case support this observation.

As well as helping to understand the response behaviour of shear walls, the NLTHA envelope results can also be compared to the RSA results. In particular, the amplification of base shear can be plotted in a number of different ways, comparing both the $R_d$ and the structural height. Figure 5.14 shows the amplification plotted as it has been typically defined – the shear from the NLTHA divided by the design shear from the RSA (elastic shear/$R_d$). Note that the results from identical analyses

performed using the Montreal spectrum have been included to highlight the importance of spectral shape in discussing shear amplification.

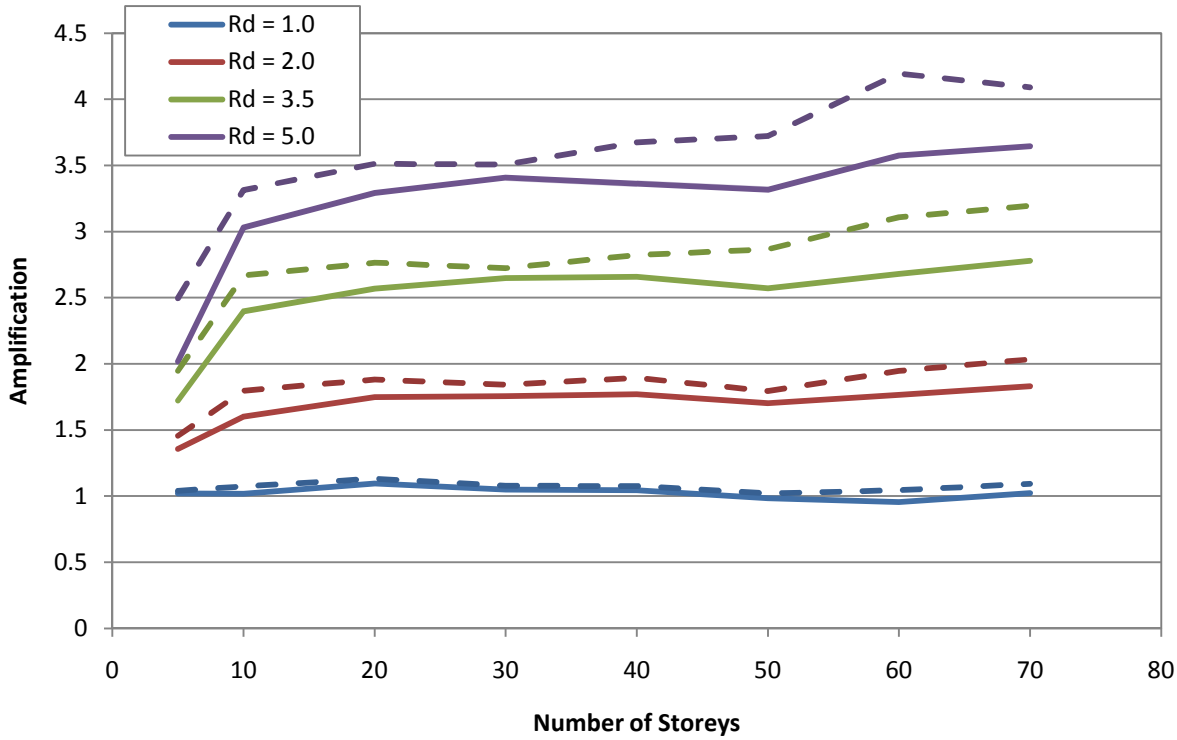


*Figure 5.14: Amplification of shear from NLTHA relative to RSA/$R_d$ vs. number of storeys, solid = Vancouver, dashed = Montreal*

Firstly, note that the $R_d$ = 1.0 case should theoretically be a straight line at an amplification of 1.0, but because of the way the yield strength was defined it deviates slightly. However, even though a difference exists, the relative insignificance is a validation of the method.

The second important thing to notice is that with the exception of the 5 storey case, most of the points tend to be fairly independent of height. This is an important finding, but some caution must be taken when trying to draw conclusions – there are a number of valid explanations for this phenomenon. The first is that in the 5 storey structure the first mode is relatively more important, so when the base of the structure yields and higher mode effects take over, they don't cause as much amplification. This would suggest that the other structures have relatively similar modal contributions, which is not true. However, relative to the 5 storey structure this may be the case. Another more convincing explanation is that because the results are being normalized to the RSA,

this is more of an indication of the inability of the RSA to be able to capture the behaviour during yielding. For example, consider Figure 5.15:

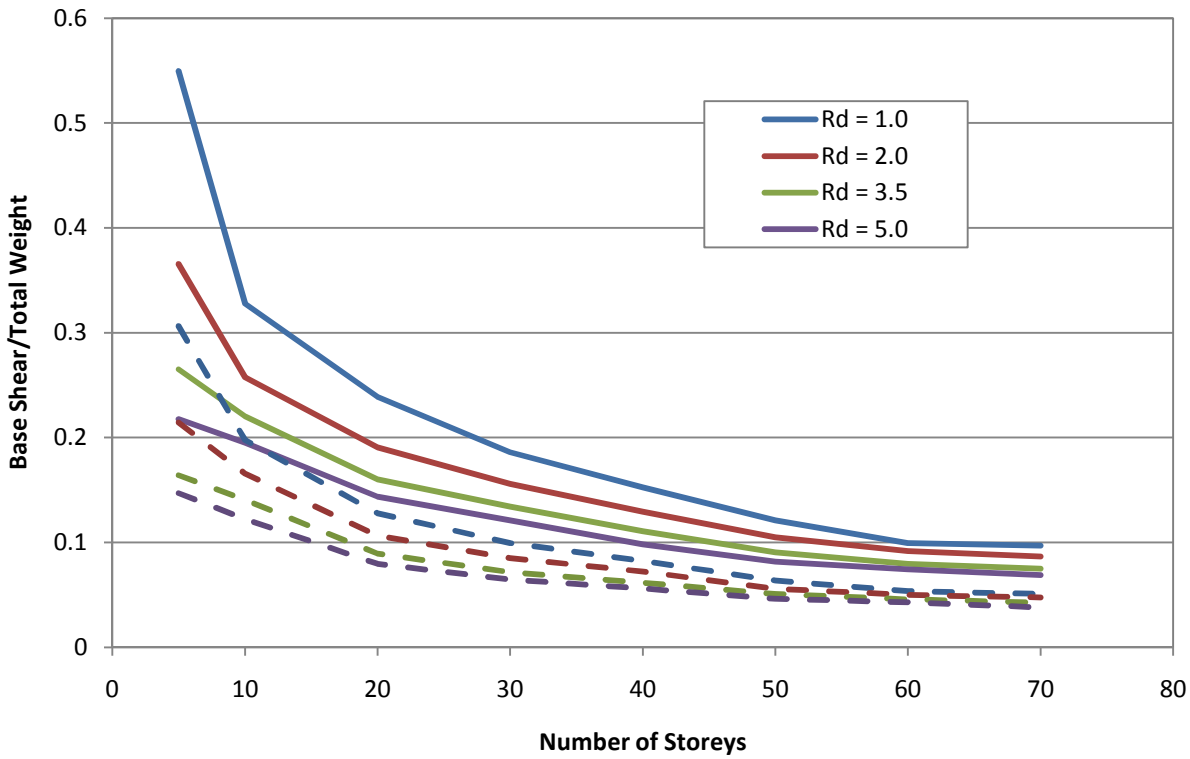


*Figure 5.15: Normalized base shear vs. number of storeys for various $R_d$, solid = Vancouver, dashed = Montreal*

Here it can be seen that the variation in base shear is less when more yielding occurs (from $R_d$ = 1.0 to $R_d$ = 5.0). However, Figure 5.14 suggests that in fact it is the higher yielding structures that vary the most. This is because the RSA results figure into the picture, which are unable to accurately capture the fact that when the structure yields, the modes are affected in different ways.

Another point to note in the amplification results is that even though the lack of dependence on height is somewhat unexpected, other trends are confirmed. For example, it is clear that the amplification increases as $R_d$ increases, as expected. As well, the shape of the spectrum plays an important role, and furthermore the tendency that is observed for the Montreal spectrum to increase the amplification is consistent with what has been predicted.

However, there are some limitations to Figure 5.14, the central one being that it is difficult to compare the results from different $R_d$ values, in particular because each set of data is being normalized to a different value (the corresponding RSA/$R_d$). This problem, although showing that clearly the "amplification" increases with $R_d$, says very little about whether increasing the ductility of the structure actually affects the base shear. Is there actually any effect at all? This can be answered by considering Figure 5.16:

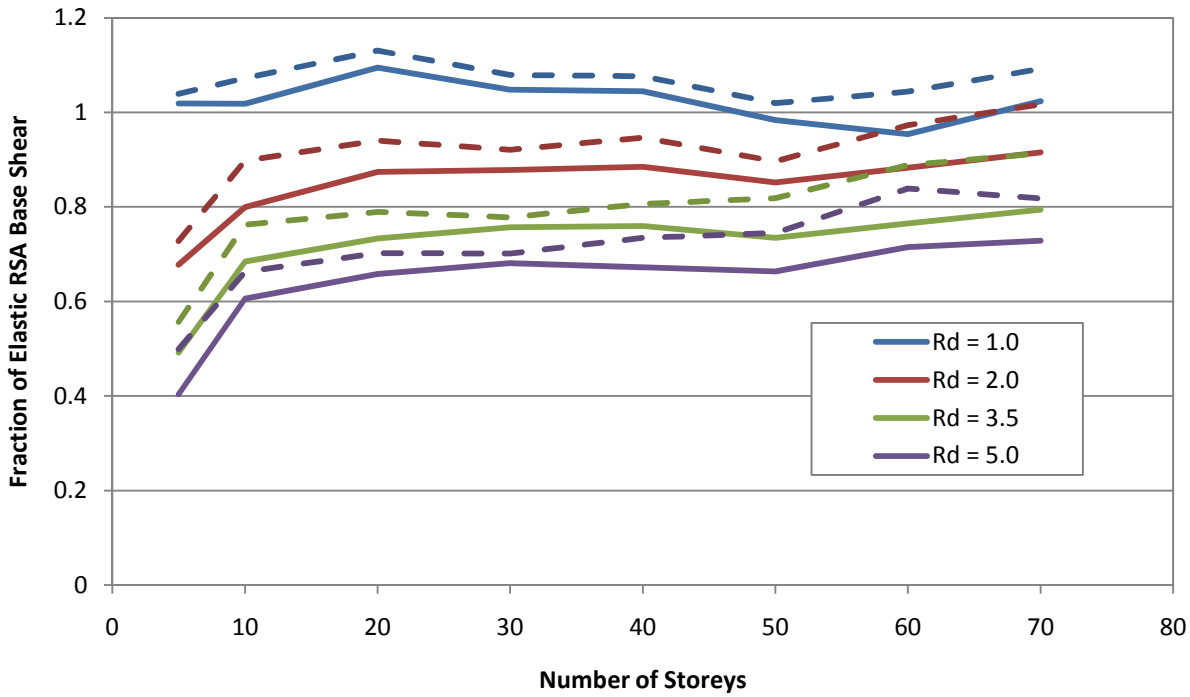


*Figure 5.16: Fraction of elastic RSA base shear vs. number of storeys for various $R_d$, solid = Vancouver, dashed = Montreal*

In Figure 5.16, all of the data has been normalized to the RSA elastic base shear (i.e. not divided by $R_d$). It can be seen that even though increasing the ductility increases the "amplification", it still reduces the total base shear expected as a fraction of the elastic shear, although this portion is still much more than the $1/R_d$ expected. One of the results of plotting the figure like this, however, is that it shows that the variation between the RSA predicted elastic shear and the THA predicted elastic shear is quite different, as seen by the $R_d$ = 1.0 case. So, the next interesting figure is to stop using the RSA results to normalize the structure at all, and simply compare the results to the elastic THA results:

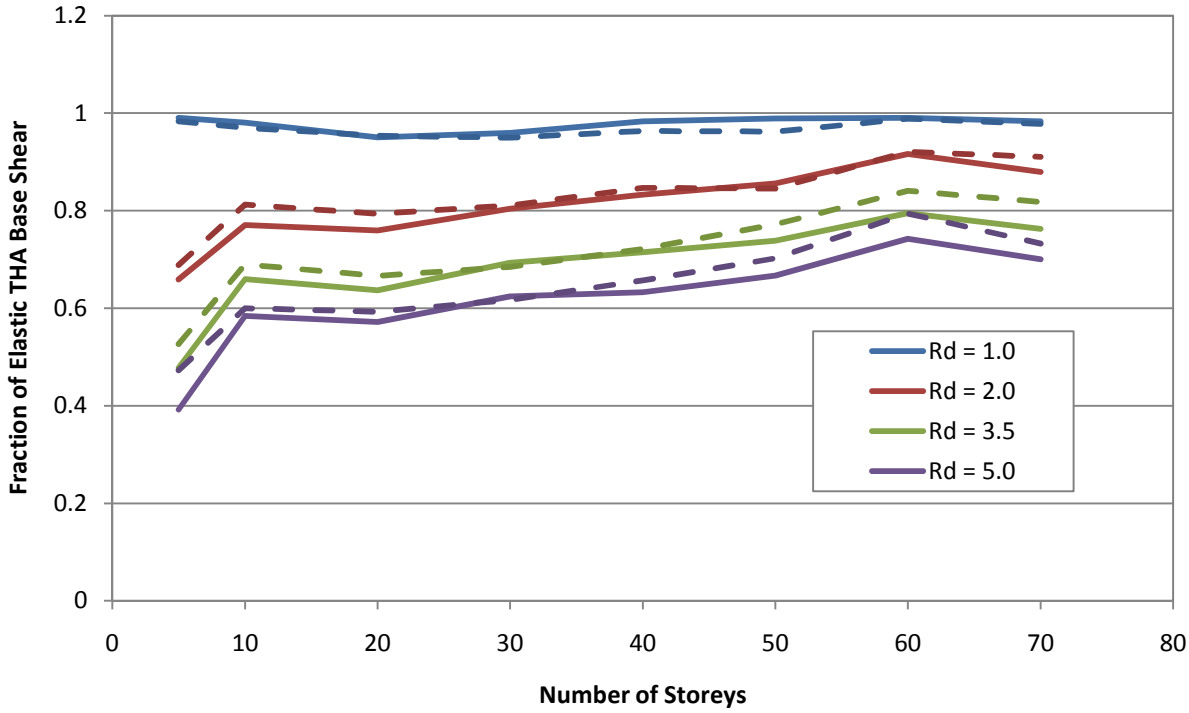


*Figure 5.17: Percentage of elastic THA base shear vs. number of storeys for various $R_d$, solid = Vancouver, dashed = Montreal*

Note that the $R_d$ = 1.0 case is still not exactly equal to one, because the yield strength is still based on the RSA moments. However, because the extra step of normalizing the NLTHA results to the RSA results has not been taken, the $R_d$ = 1.0 shear represents more accurately what is actually happening – a very small reduction in the shear force due to a small amount of yielding. Furthermore, there are two other intriguing results that present themselves when the plot is normalized in this way. First of all, there now does seem to be a definite dependence with structural height, presumably because the LTHA captures some of the higher mode effects better than the RSA does. Secondly, much of the difference between the Vancouver and Montreal spectra has disappeared, although some does still exist. This suggests that the LTHA initially captures much more of the variation than the RSA. So are the conclusions drawn from the previous figures not relevant? Fortunately this is not the case. Because one of the goals is to develop a method for practicing engineers to use when designing walls, comparing to the RSA results is the most useful technique.

### 5.2.2 Time History Results

Looking at the full time history outputs is also a useful way of interpreting the data, although it is sometimes difficult to extract useful conclusions because there is so much information. For this reason, only 3 records were selected to examine in detail, and only on the 10, 30, and 50 storey structures. Even with this narrowing of the possibilities, there are still a total of 45 shear, moment, and displacement time histories to compare (3 structures, 3 records, 5 $R_d$ values). Unfortunately it is very difficult to compare different records, because they have very different characteristics, such as the periods that they excite. It is even difficult to overlay the same record acting on different structural heights, because the differences in the dominant periods create a very confusing image. However, it is possible to plot different $R_d$ values on the same plot. This is the approach taken in the following set of figures:

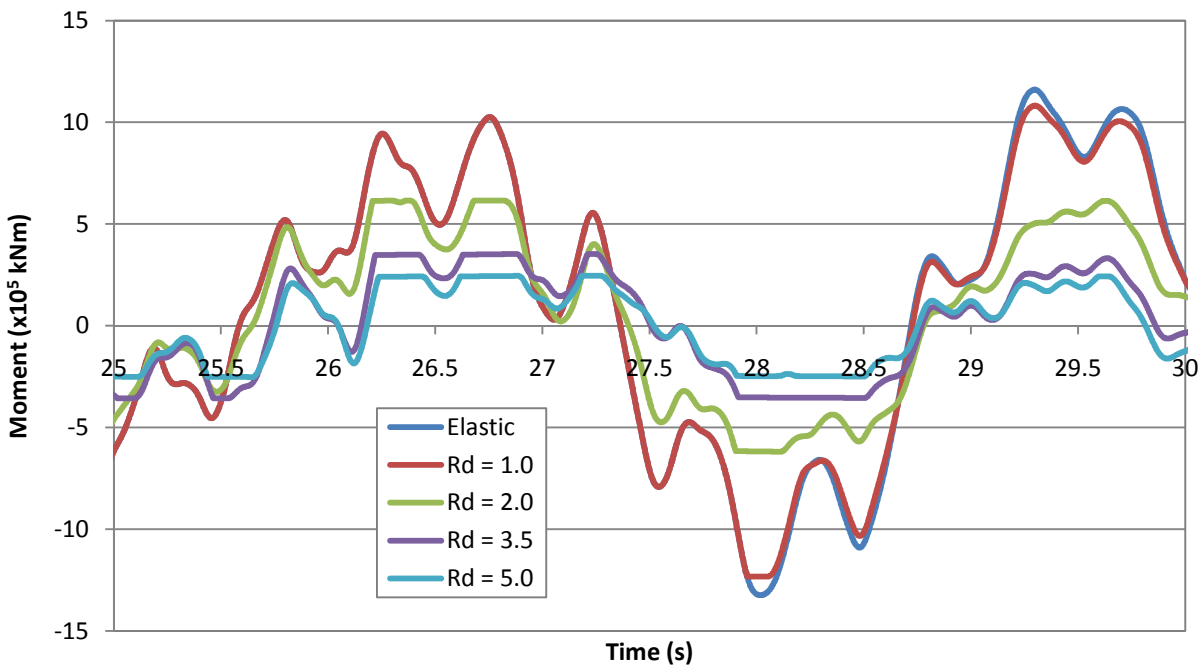


*Figure 5.18: Base moment vs. time for the 30 storey scaled B05 record, from 25 seconds to 30 seconds*

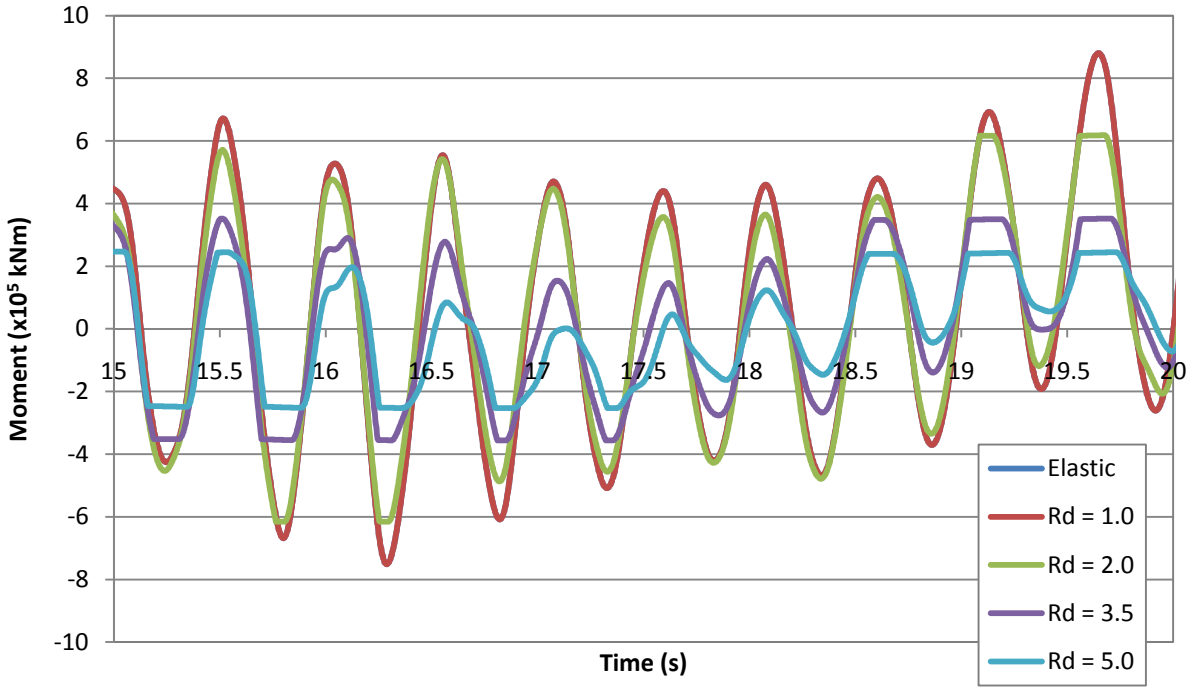


*Figure 5.19: Base moment vs. time for the 30 storey scaled C10 record, from 15 seconds to 20 seconds*

These figures are typical of the moment response in the walls, although they differ in their overall shape somewhat. What is important is to realize that they both show that no matter the ductility demand, the curves tend to have the same general peaks and valleys. The effect of the inelastic behaviour is to simply limit the moments. It is also interesting to see how much of an effect the second mode ($T_2$ = 0.5s) has on the moment response, particularly in Figure 5.19. RSA analysis would typically assume much less response in the second mode. The 10 storey and 50 storey moment responses are not shown here, but they are similar, with the main differences being that the taller structures have more higher mode action.

So will the shear force have the same type of behaviour (i.e. controlled by $R_d$)? The shear force for the same structures over the same time period is shown below:

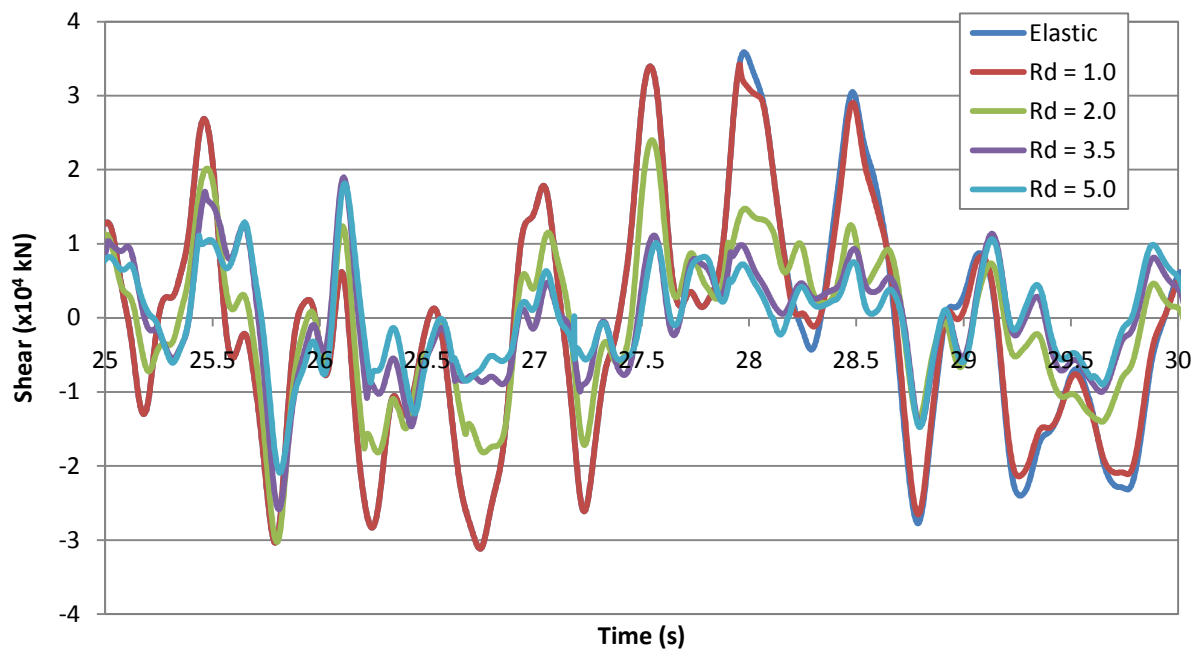


*Figure 5.20: Base shear vs. time for the 30 storey scaled B05 record, from 25 seconds to 30 seconds*

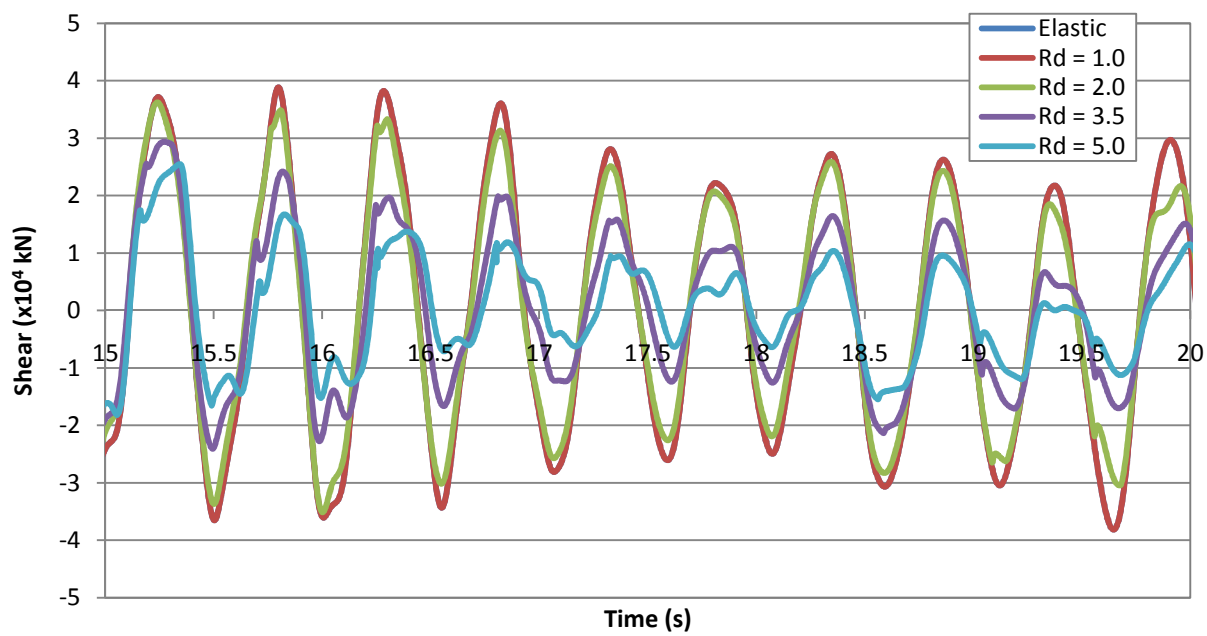


*Figure 5.21: Base shear vs. time for the 30 storey scaled C10 record, from 15 seconds to 20 seconds*

As expected, in both cases the shear force responds considerably more in the higher modes. What is interesting to note is how the changes in $R_d$ affect the response, and in this situation the two plots

illustrate variations on the same main point – that it does not have nearly as much of an effect as with the moment. In Figure 5.20 it can be seen that in some cases increasing the ductility demand actually does cause reduction of the shears, such as at approximately 26.75s. On the other hand, the peak just after 26s shows the opposite trend – increasing $R_d$ actually increases shear. Figure 5.21 is a situation where it is clear that increasing $R_d$ does have an effect on the shear, but it is not nearly as much as with the moment. For example the peak right after 15s only reduces the shear by 20% or so when going from the elastic to the $R_d$ = 5.0 case. It would be unfair to say that reducing the ductility has no effect on the shear – it clearly reduces it by a decent amount – but it would be reasonable to conclude that one cannot expect the shears to behave like the moments. This matches with what was seen in Section 5.2.1.

So far only the behaviour of the shear and the moment separately have been examined. But how do they relate to each other? Does the shear follow the moment at all, or are they independent? In order to compare the responses directly, the shear, moment, and top displacement have all been normalized to their respective maxima, and have then been plotted on the same figure. The results for the same cases are shown below for $R_d$ = 3.5:

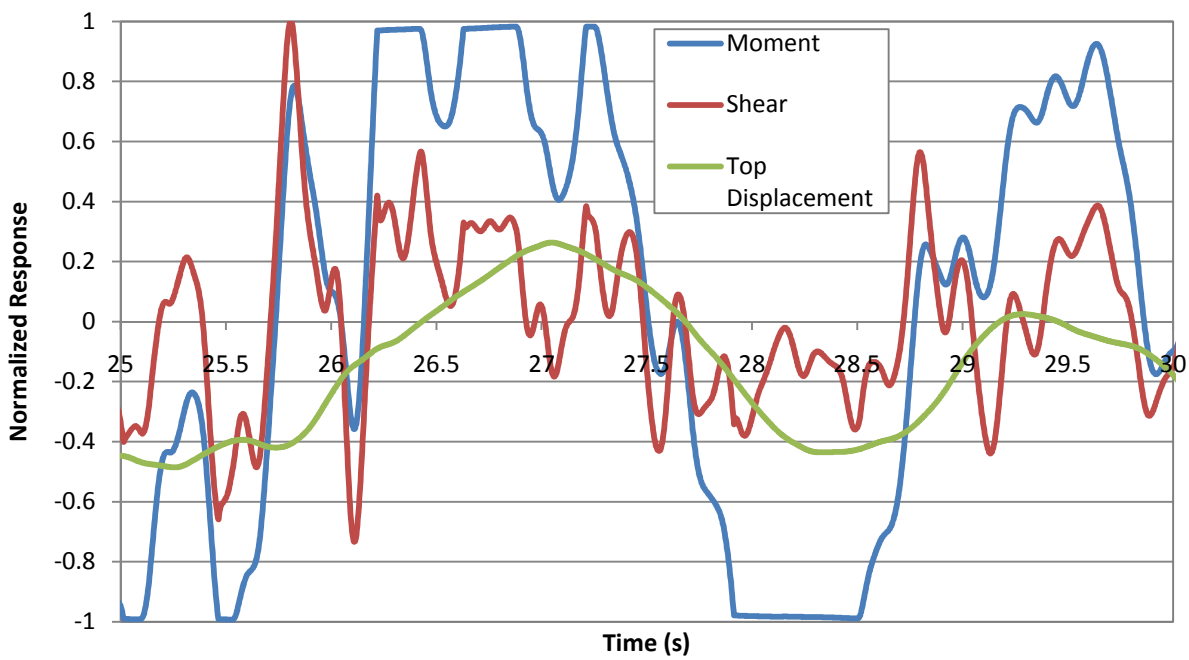


*Figure 5.22: Moment, shear, and top displacement (normalized by their respective maxima over the entire record) vs. time for the 30 storey scaled B05 record, from 25 seconds to 30 seconds*

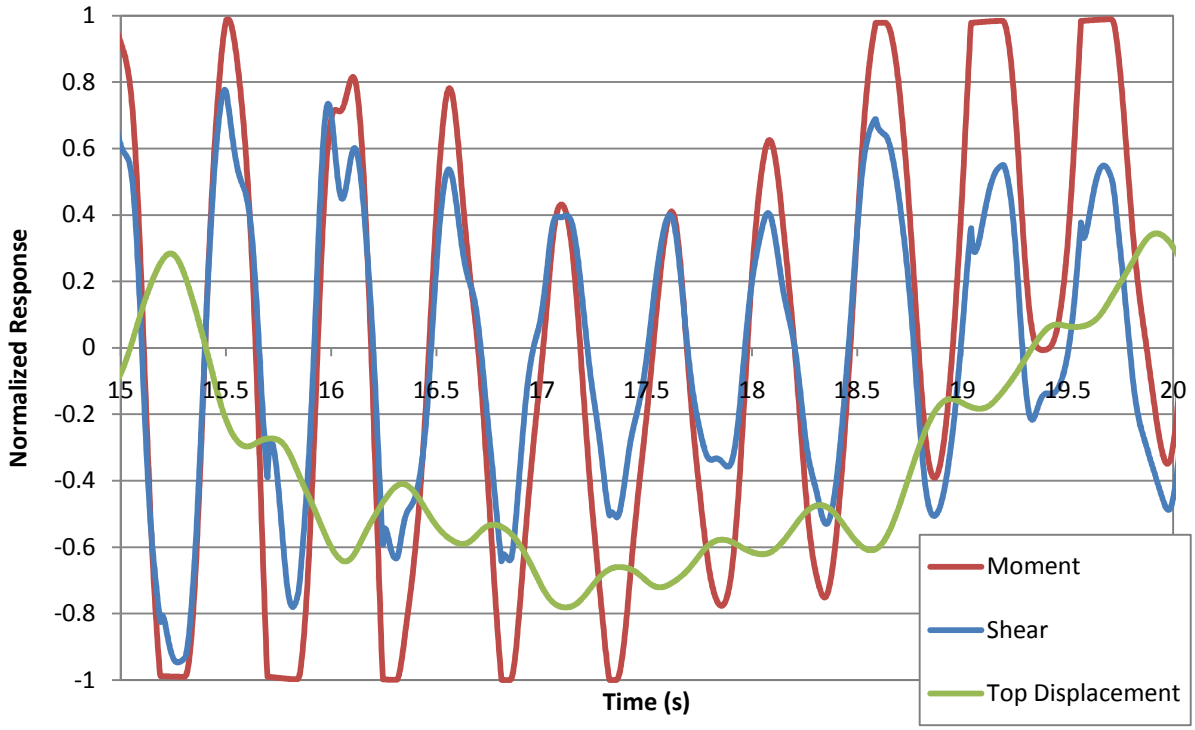


*Figure 5.23: Moment, shear, and top displacement (normalized by their respective maxima over the entire record) vs. time for the 30 storey scaled C10 record, from 15 seconds to 20 seconds*

Here the large difference in modal contributions is even more obvious. The displacement has an almost purely first mode response, while the moment and shear have significant contributions from the higher modes. It is somewhat difficult to generalize the trends seen here considering that the responses are actually fairly different, but perhaps the most important thing to note is that while the shear does not always follow the moment exactly, the two do vary in phase with each other for the most part. This suggests that at least part of the shear force may be able to be represented using the RSA results. Lastly, it is also interesting to see that in Figure 5.22, the peak shear force actually occurs when the base of the structure is not yielding. This will be discussed more in Section 6.2.

## 5.3 Development of a Model

At this point in the study it is now possible to start evaluating how useful the results from the RSA will be in constructing a model for the shear demand by comparing those results to the NLTHA. In particular, several different RSA analyses were performed with different base and mid-height conditions, and steps were taken to ensure that the pinned base shear could be modeled using a

simple relationship. It was unclear at that point in time how the results could be used, or if they were even useful at all. In the following sections the rest of the model will be developed in detail, and then compared with the methods reviewed in Chapter 2 of this report.

### 5.3.1 Proportion of Pinned Shear at Base

As was seen in Chapter 2, there are a wide range of possibilities for the type of model that can be used. Some are strictly parametric, while some relate to the higher modes. From the work that has been done so far, it would seem like the best way to go about creating a model would be to deal with the modes directly, instead of trying to empirically match the NLTHA results. This is due to the results in Chapter 4, where it has been seen that there is a rational explanation for the shear amplification phenomenon solely based on looking at the modes. A good model would then try to extend this explanation into an actual workable equation.

So the central question becomes what modes should be used, and how should they be combined? Because of the bilinear nature of the model, it would seem that the best approach to take would be to use two sets of results, representing the non-yielding and yielding ranges of the structure respectively. Fortunately the work done in Chapter 4 provides some numbers that can be used in creating this model.

The next step is to figure out how to combine these results in a way that both accurately predicts the shear force when compared to the NLTHA and also makes rational sense. For this type of model, this boils down to trying to figure out a way to represent the structure at yielding, take some proportion of the shear from the pinned structure, and combine the two. The issue is that for any given way of representing the structure at yielding (e.g. first mode capacity), and any way of combining the two pieces (e.g. SRSS), a factor can be applied to the pinned shear from the RSA to force the total result to match the base shear from the NLTHA. However, it would seem that the best model (i.e. the one that most represents reality) would be one where the proportion of pinned shear required is very near to one. Any other result would be questionable as to the meaning – what would two times the pinned shear actually mean? How would the structure develop this shear? Thus the process can be broken down into two steps: determining the behaviour at yield, and determining how the two pieces should be combined.

When looking at the behaviour at yielding, it is generally assumed that the RSA/$R_d$ results are reasonably accurate (which seems to be the case judging from the NLTHA). Then after yield, does the part of the shear that is related to the yielding at the base of the structure remain in a distribution represented by the RSA/$R_d$, or is it better represented by a first mode capacity component? This has been discussed in some detail in Section 4.4.1, and for now both options will be considered.

Another issue, no less complex, is the problem of how to combine the capacity component and the higher mode component. The approach taken by Sullivan, et al. (2006) was to combine the forces using a SRSS methodology, but it is not clear why they felt that this was the best approach. On one hand it is typical when combining modes to use some kind of approach other than absolute sum, because the peaks of the modes are happening at different times. Here it is not clear that this is the case. It is generally acknowledged, and has been seen in Section 5.2.2 that there is some shear associated with the yielding at the base of the structure, so why would this shear not be present while the higher modes from the pinned based structure are acting? If this argument is accepted, it would made sense to instead simply add the two components together, the physical interpretation being that it is the superposition of two systems that are acting simultaneously. Unfortunately it can be very difficult to conceptualize what is really going on while the base of the structure is yielding, and so it may just be the case that using a SRSS method predicts the response better. Table 5.1 summarizes the four models:

*Table 5.1: Potential models classified by capacity component (from RSA) and combination method (how the capacity component and the pinned base component are combined)*

| | | Combination Method | |
|---|---|---|---|
| | | **SRSS** | **Sum** |
| Capacity Component | **1st Mode** | Model 1 | Model 3 |
| | **All Modes** | Model 2 | Model 4 |

Without the NLTHA results, these questions would be difficult if not impossible to answer. However, because these results are available, four distinct models can be separated out, and the fraction of pinned shear required to match the NLTHA can be determined for each of them. Not only will the best model be the one with the fraction of pinned shear closest to one, but possible deficiencies in the other models will come to light. Figures 5.24 to 5.27 below show the proportion

of pinned shear required for each of the four models for $R_d$ = 2.0 and 3.5 with the Vancouver and Montreal spectra:

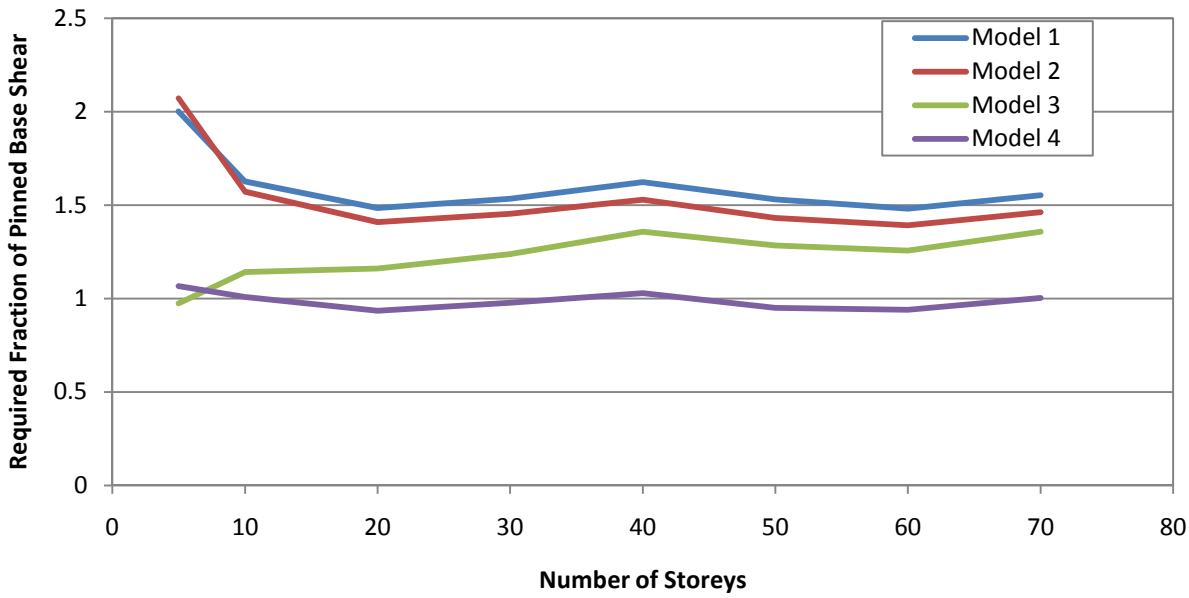


*Figure 5.24: Required fraction of pinned base shear vs. number of storeys for various models – $R_d$ = 3.5, Vancouver spectrum*

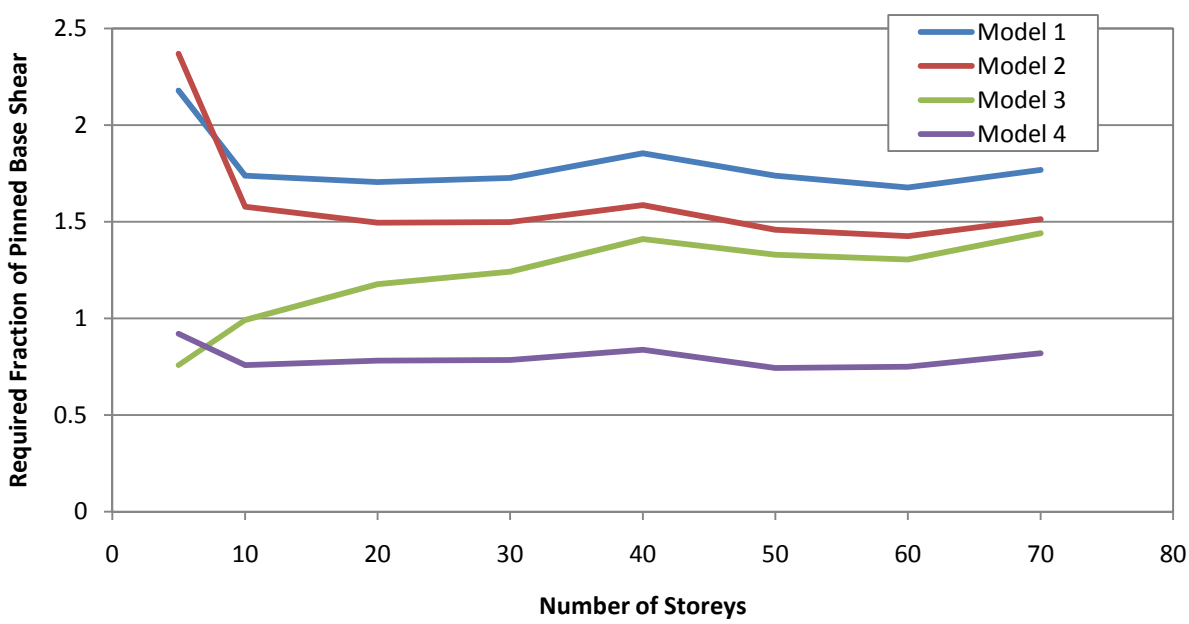


*Figure 5.25: Required fraction of pinned base shear vs. number of storeys for various models – $R_d$ = 2.0, Vancouver spectrum*

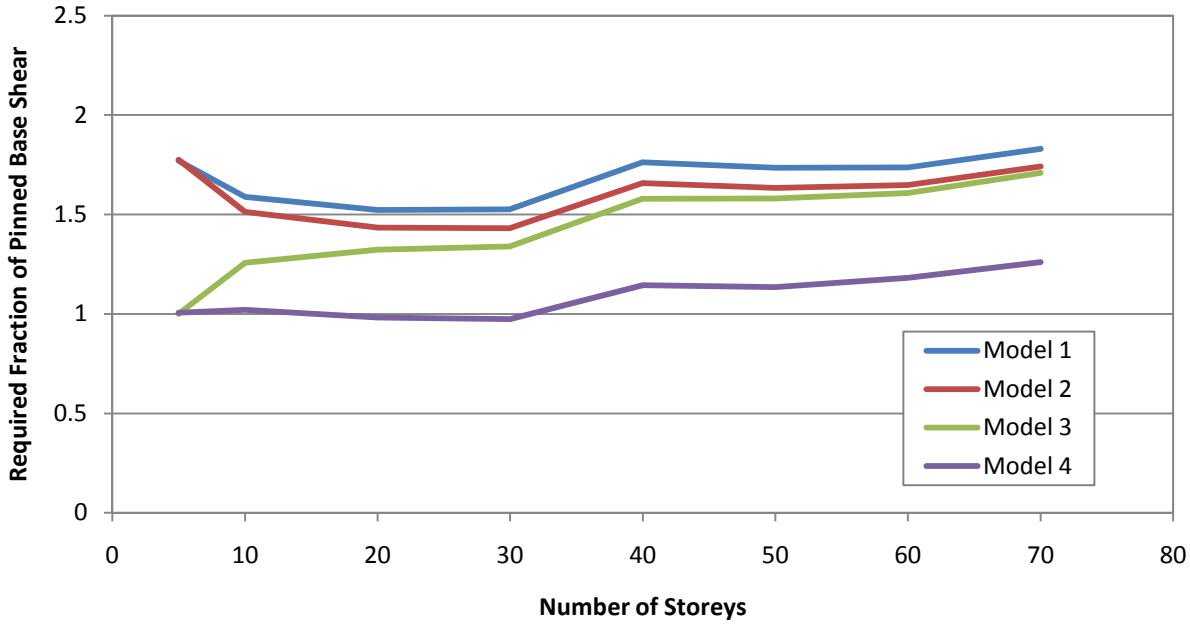


*Figure 5.26: Required fraction of pinned base shear vs. number of storeys for various models – $R_d$ = 3.5, Montreal spectrum*

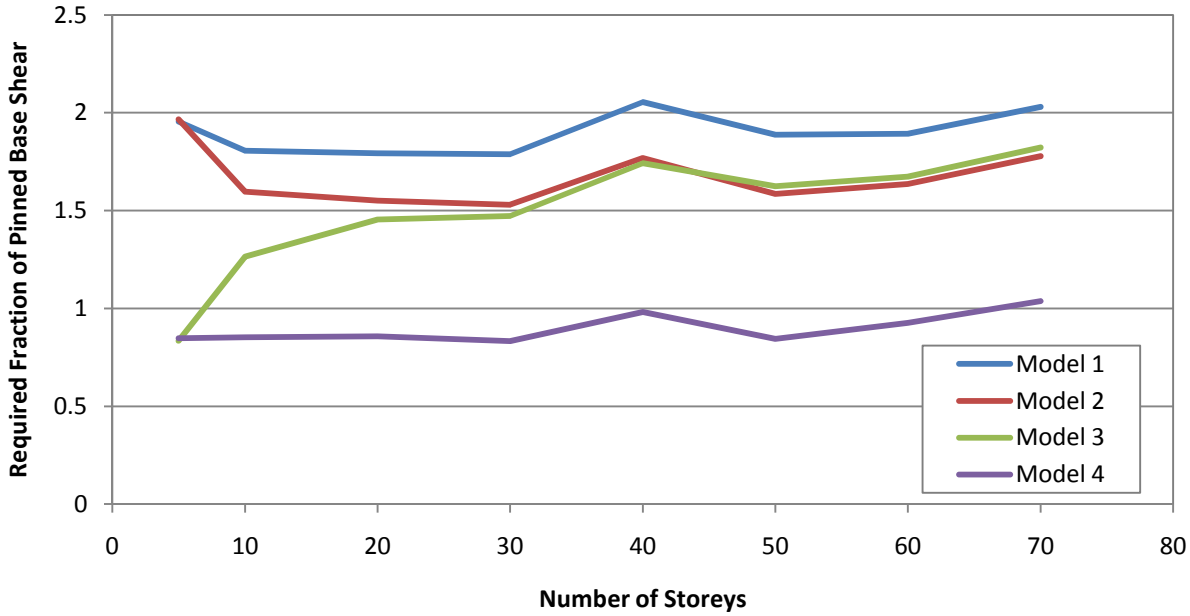


*Figure 5.27: Required fraction of pinned base shear vs. number of storeys for various models – $R_d$ = 2.0, Montreal spectrum*

Figures 5.24 to 5.27 show that the best model is to use a capacity component based on the RSA/$R_d$ results, and to combine the higher mode component by simply adding the two parts together. This not only gives fractions of the pinned shear nearest to 1, but perhaps more importantly gives results that are the most consistent across different structural heights. In particular, the choice of using the SRSS to add together the components requires a large fraction of the pinned shear, and the worst option is to use the first mode capacity with the SRSS, as Sullivan et al. (2006) did. Furthermore, using the first mode capacity at all seems to be a poor choice.

Having established which model is the best, the next step is to continue investigations into the proportion of pinned shear required to match the NLTHA. It has been shown in Figure 5.24 that it is near unity for an $R_d$ = 3.5 structure using the Vancouver spectrum, but further work needs to be done to extend the utility of the model to the other situations shown in Figures 5.25 to 5.27. Figure 5.28 shows the required proportion of pinned shear to meet the NLTHA for a range of structural heights, $R_d$ values, and looks at the Montreal spectrum in addition to the Vancouver spectrum.

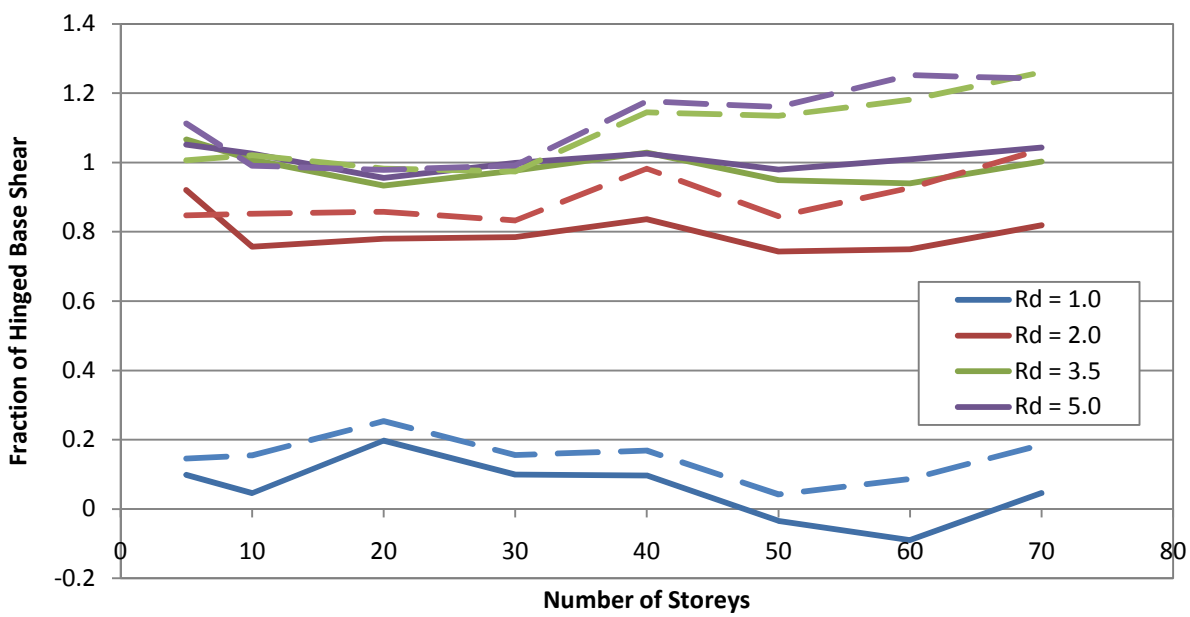


*Figure 5.28: Required fraction of hinged base shear vs. number of storeys – Vancouver = solid, Montreal = dashed*

It can be seen that unfortunately things aren't quite as simple as using a fraction of 1 at all times. It is clear that the proportion of pinned shear does change somewhat with $R_d$, and also differs slightly

based on spectrum. Although this presents some problems, Figure 5.28 still shows that the proportion of pinned shear remains relatively independent of the structural height. It would be remiss to neglect to mention that this appears to not be the case for the taller buildings under the Montreal spectrum, but even this variation is relatively small, and for the purposes of a simple model could potentially be ignored. As far as the issue of the variation based on $R_d$ goes, this too could be ignored – the $R_d$ = 2.0 proportion is around 0.8 for the Vancouver spectrum, not too far from one. However if the case of $R_d$ = 1.0 is considered, the proportion of pinned shear should theoretically be zero, or in other words no yielding at all should occur. If a very small amount of yielding were allowed, it seems that it would be unrealistic to expect that the small amount – and more importantly duration – of yielding would allow the full pinned shear to develop. This explanation can be extended to higher $R_d$ values – with less yielding comes less time to develop the full pinned shear, and therefore the variation should be accounted for.

An easy way to simplify this data is to assume that the shear is constant across structural heights. Then the proportion of pinned shear can be averaged and plotted versus $R_d$ for each spectrum used. Figures 5.29 and 5.30 below shows the results of this analysis:

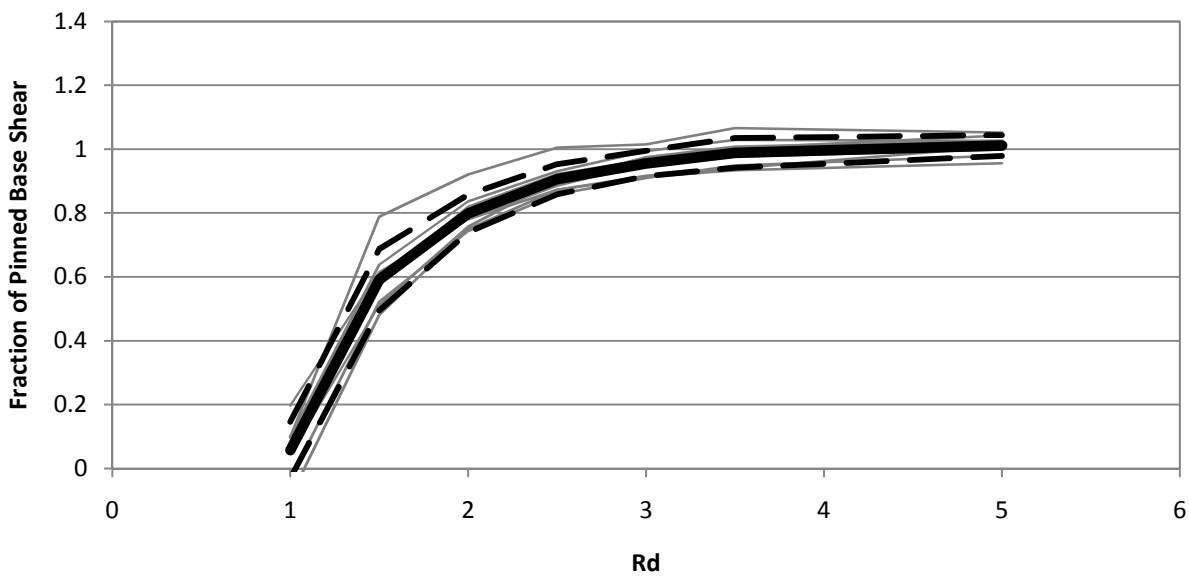


*Figure 5.29: Required fraction of pinned base shear vs. $R_d$ for Vancouver (solid line = average, dashed lines = +- 1 standard deviation, thin lines = different heights)*

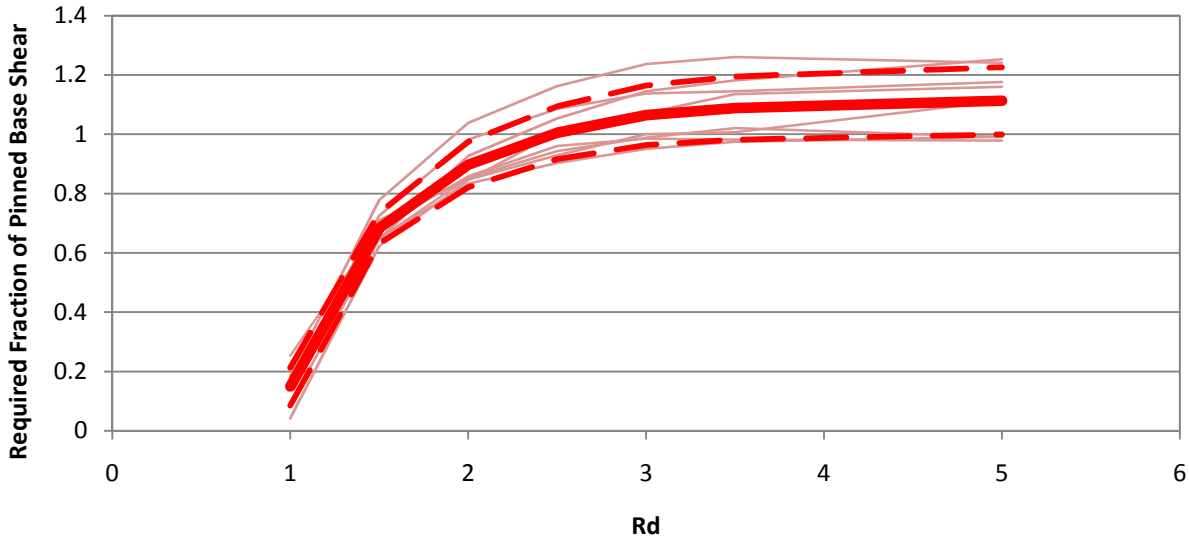


*Figure 5.30: Required fraction of pinned base shear vs. $R_d$ for Montreal (solid line = average, dashed lines = +- 1 standard deviation, thin lines = different heights)*

It can still be seen that using a proportion of 1 would not give completely unreasonable results, but considering there seems to be a relationship between $R_d$ and proportion of pinned shear, a simplified equation can be developed to model this behaviour. There are two main requirements for the equation – that it goes through 0 at approximately 1, and that it levels off at either 1 (for the Vancouver spectrum), or 1.1 (for the Montreal spectrum). This suggests that an exponential equation would be most suitable, of the form:

$$H_f = P - e^{x(1-Rd)} \tag{5-1}$$

Where $H_f$ is the fraction of pinned base shear, P is the plateau where it levels off, and x is a variable that can be tweaked to create a better fit. Experimenting with different values of x, it was found that the best fit was obtained with x = 1.6. This is shown in Figure 5.31 below:

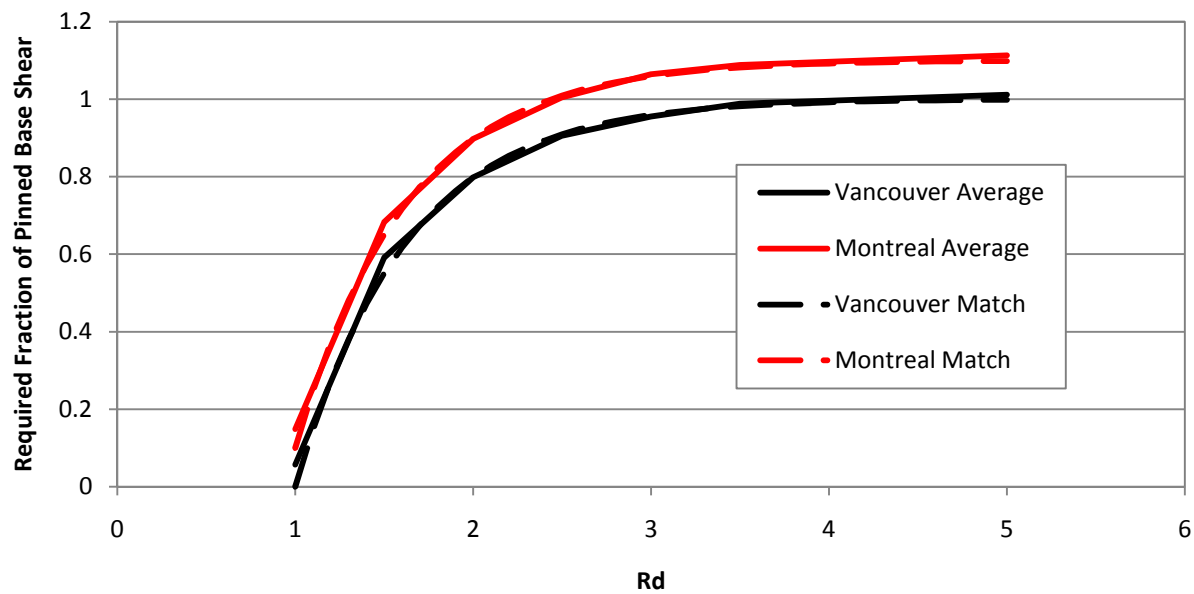


*Figure 5.31: Matching the required fraction of base pinned shear using an exponential equation*

The match is quite good, with both the Vancouver and Montreal curves being represented extremely well. It can be observed, however, that the Montreal curve does not go through 0 at $R_d$ = 1.0. Theoretically this should be the case if the RSA matches the LTHA results perfectly, but it has been observed in Section 5.1 that this is not always the case. The difference in the results at $R_d$ = 1.0 in Figure 5.14 also demonstrates this, and furthermore shows that when the Montreal spectrum is used the difference is greater. Therefore, it is not an issue that the approximate curve does not go through 0 at $R_d$ = 1.0, and in fact may better represent reality. In summary, the equation to predict the proportion of pinned shear based on $R_d$ is as follows:

$$H_f = P - e^{1.6(1-Rd)} \qquad P = \begin{cases} 1.0 & S_a(0.2)/S_a(2.0) < 8.0 \\ 1.1 & S_a(0.2)/S_a(2.0) \geq 8.0 \end{cases} \tag{5-2}$$

### 5.3.2 Model Summary and Comparison

At this point a full model is now available to predict the shear demand on a cantilever wall, accounting for dynamic amplification of shear. In a broad sense, the model uses the results from a pinned and fixed base RSA analysis to predict the results of a NLTHA. However two very important simplifications have been made. The first is to represent the pinned base shear by using the fixed base shear, allowing the practicing engineer to bypass the problem of having to analyze the

structure with a pinned base. The second is using a simple relationship to increase the accuracy of the model by accounting for the variation in required pinned base shear with $R_d$ and spectral shape. In the form of an equation, it is as follows:

$$V_a = \left(\frac{1}{R_d}\right) V_e + H_f \cdot R_{pf} \cdot V_e \tag{5-3}$$

Where $V_a$ is the amplified shear force, $V_e$ is the elastic shear from a RSA, and $H_f$ and $R_{pf}$ have been previously defined in Equation 4-1 and 5-2, repeated here:

$$R_{pf} = \begin{cases} 2T_2 & T_2 < 0.25s \\ 0.5 & T_2 \geq 0.25s \end{cases} \tag{4-1}$$

$$H_f = P - e^{1.6(1-Rd)} \qquad P = \begin{cases} 1.0 & S_a(0.2)/S_a(2.0) < 8.0 \\ 1.1 & S_a(0.2)/S_a(2.0) \geq 8.0 \end{cases} \tag{5-2}$$

Where $T_2$ is the second period of the structure. Note that $V_a$ is not the design force $V_d$, and therefore overstrength must still be accounted for separately.

Having finalized the model, it is instructive to go back and apply it to the 8 sample structures in order to compare it to both the results from the NLTHA and the methods that previous work has proposed. A sample calculation is shown for the 30 storey structure at an $R_d$ of 3.5 using the Vancouver spectrum, to further gain an appreciation of the way it works:

**Sample Calculation for 30 Storey Example Structure**

Design information for the 30 storey structure: $V_e$ = 36650kN, $T_2$ = 0.51s

Spectral Accelerations for Vancouver: $S_a(0.2)$ = 0.94, $S_a(2.0)$ = 0.17, $S_a(0.2)/S_a(2.0)$ = 5.5,

therefore P = 0.5, and then: $H_f = 1.0 - e^{1.6(1-3.5)} = 0.98$.

Because $T_2$ = 0.51s > 0.25s, $R_{pf}$ = 0.5.

Then, $V_a = \left(\frac{1}{3.5}\right)(36650kN) + (0.98)(0.5)(36650kN) = 28430kN$

In terms of an amplification, this is 28430kN/(36650kN/3.5) = 2.7.

Using Equation 5-3 is a very simple process, and is easy to perform as long as the RSA results are known. But how does it compare to other methods, and most importantly to the NLTHA results? To start, comparisons to the NLTHA for both the Vancouver and Montreal spectra are shown:

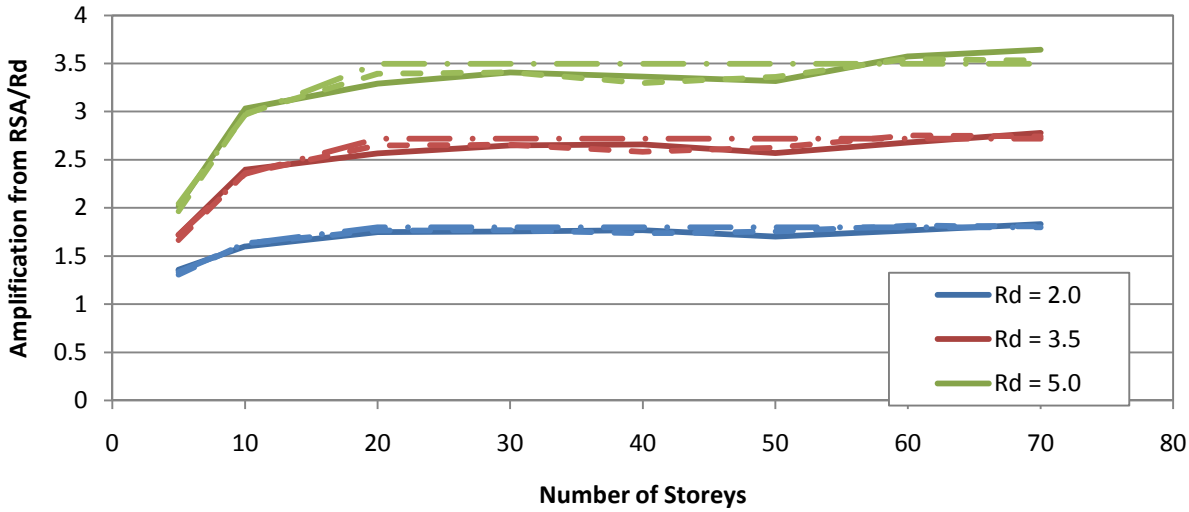


*Figure 5.32: Amplification from RSA/$R_d$ vs. number of storeys for Vancouver (solid = NLTHA, dashed = exact pin, dash-dot = Equation 5-3)*

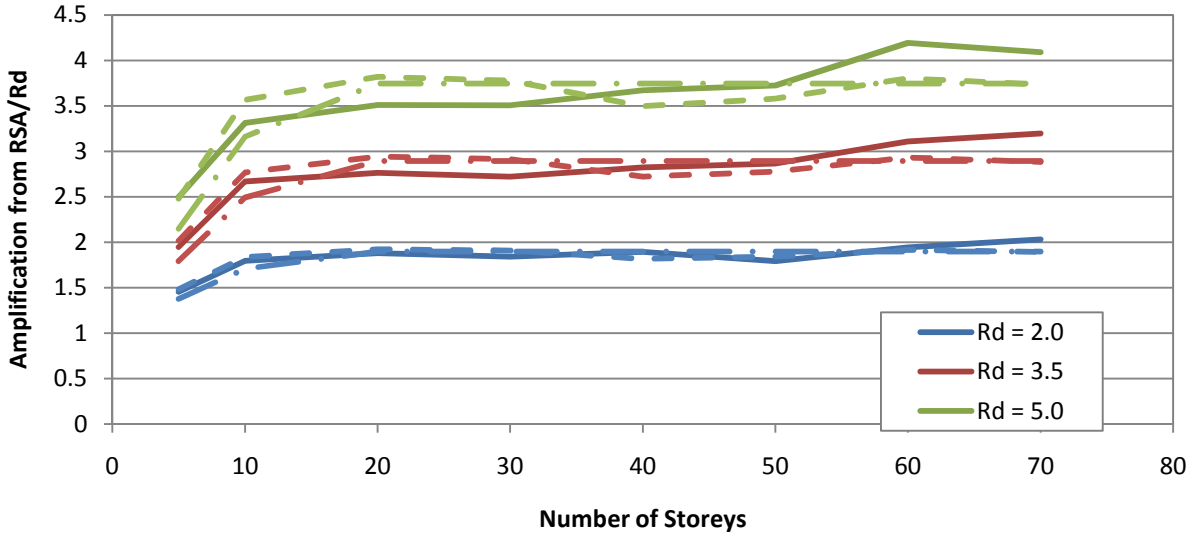


*Figure 5.33: Amplification from RSA/$R_d$ vs. number of storeys for Montreal (solid = NLTHA, dashed = exact pin, dash-dot = Equation 5-3)*

In these figures the "exact pin" curve shows Equation 5-3 if the pinned base results from the RSA are known exactly – or in other words if the $R_{pf}$ factor is not needed and instead the base shear can be input directly. It can be seen that the match is quite good for both spectra although it is better for the Vancouver spectrum than the Montreal spectrum. Furthermore, even if the exact results from the pinned analysis are used the match does not get significantly better, suggesting that most of the error comes from the averaging of all the structural heights in Figure 5.31. This can be seen most clearly at the larger $R_d$ values from the Montreal spectrum, where the scatter in the data is not insignificant. However, the model is still within about 10-15% of the NLTHA results, which is fairly accurate.

The next comparison that can be made is to incorporate the results of previous models. For the sake of clarity, only the $R_d$ = 3.5 results have been plotted in the following figures. For guidance as to the methods referred to, see Chapter 2.

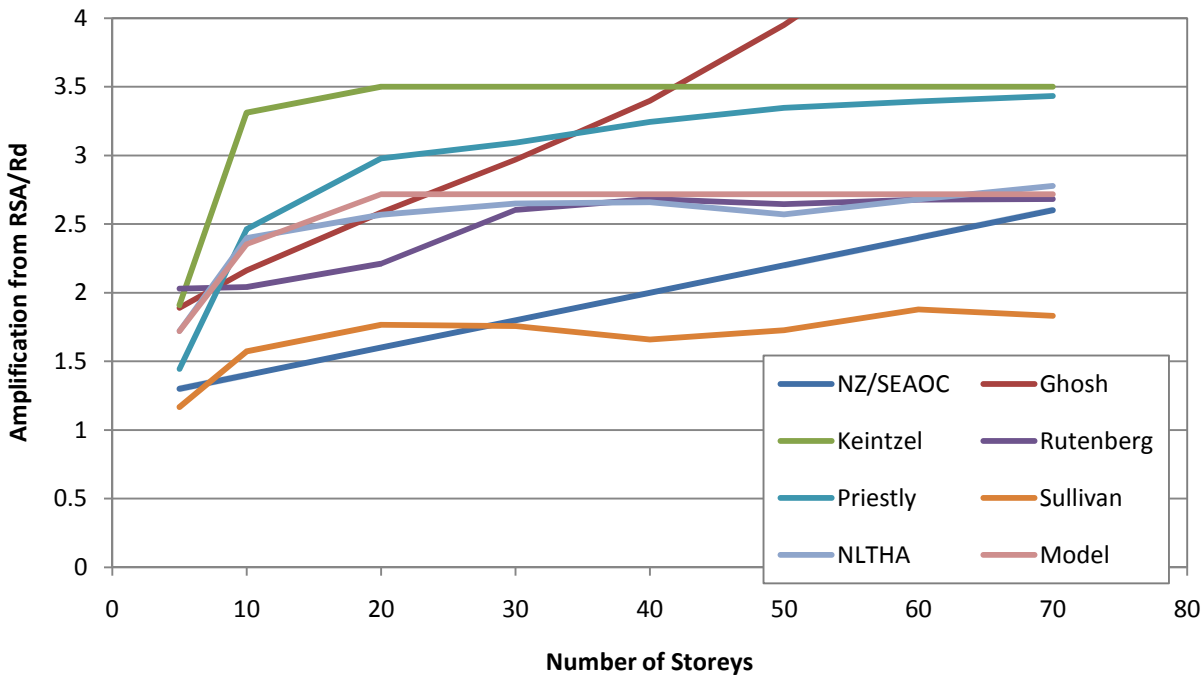


*Figure 5.34: Proposed amplifications compared at $R_d$ = 3.5 for the Vancouver spectrum*

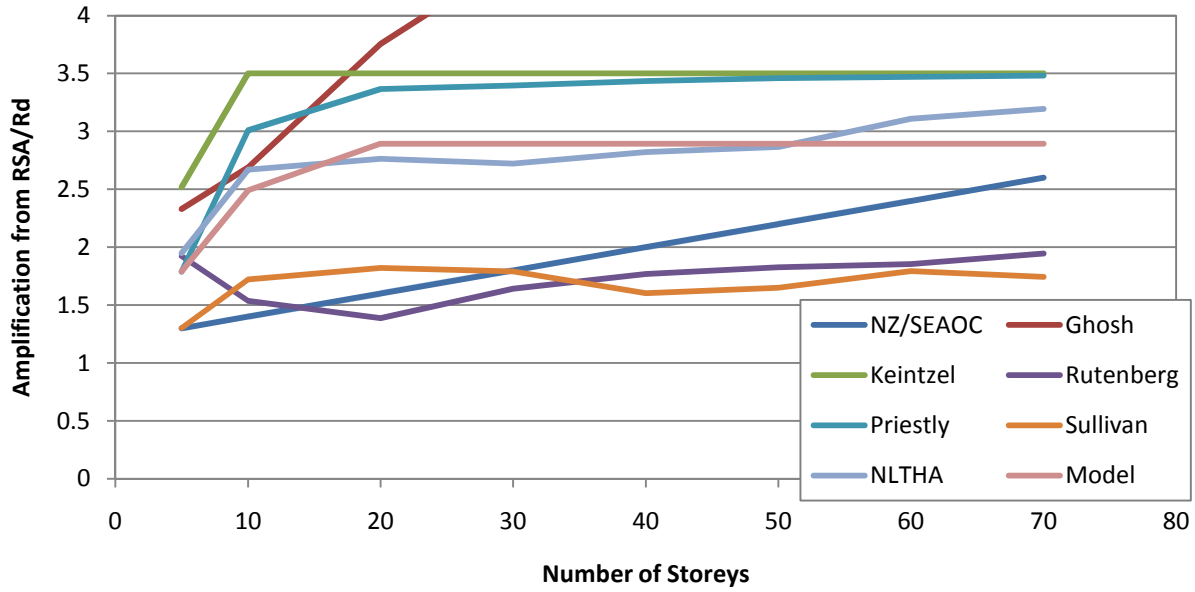


*Figure 5.35: Proposed amplifications compared to $R_d$ = 3.5 for the Montreal spectrum*

It is clear that the model proposed by Equation 5-3 is the best match to the NLTHA results. In Figure 5.34 the Rutenberg & Nsieri (2006) proposal seems to match fairly well, but then they under predict the amplification in the Montreal spectrum by a significant amount. Of the other methods, both Priestly & Amaris (2003) and Sullivan et al. (2006) seem to match the shape of the spectrum, but they over and under estimate the actual amplification respectively. The other methods match poorly if at all.

It is also important to discuss how the model has answered some of the questions posed in Chapter 2. The way the equation is structured is instructive – for example if one wanted to know how the ductility affects the shear, it can be easily seen that increasing $R_d$ will both increase the capacity shear, but also will affect how much inelastic shear the structure sees. Compare this to the height (and therefore the periods), which only affects the ratio of pinned shear to fixed shear, or in other words how much shear could potentially develop when the structure becomes inelastic. In addition to the ductility and the periods of the structure, the other important parameter identified was the spectral shape. It can be seen from Equation 5-2 that the spectrum has the effect of increasing the portion of the inelastic shear in the structure.

### 5.3.3 Forces up the Height of the Structure

Although the model developed in the previous section deals exclusively with the prediction of the base shear demand, it was seen in Section 5.2.1 that both the moment and the shear differ considerably from the RSA predictions. Therefore, a full model would account for both the shear profile up the height of the structure and the increase in the mid-height moments observed.

The simplest way to attempt to model the shear force is to see how accurate the RSA profile is if scaled by the proportion of base shear predicted by the model to that predicted from the RSA. This simple approach actually turns out working quite well in the majority of circumstances:

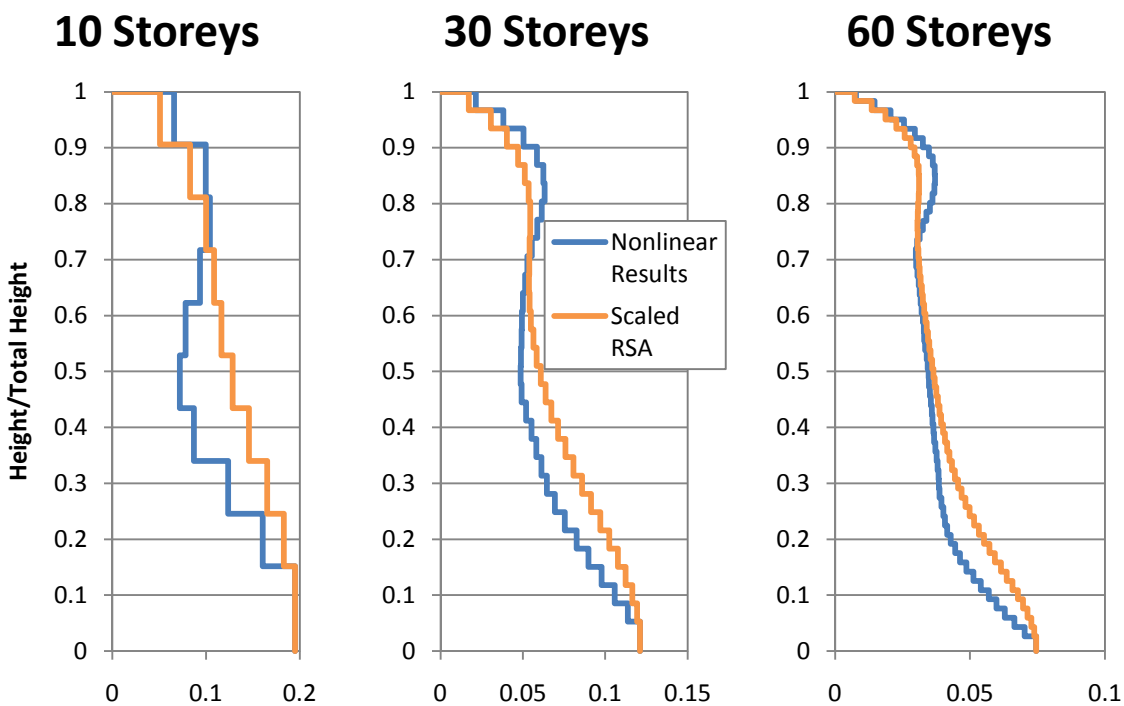


*Figure 5.36: Comparison of increased shear envelope to NLTHA for the 10, 30, and 60 storey structures (x-axis shows base shear/total weight)*

Over most of the height of the structure, using this approach is conservative and overestimates the shear force. Only near the top of the structure does this method become slightly unconservative. Modifications to this approach could be made in order to account for this small issue, but it is an unnecessary complication to an otherwise very simple approach. If the differences were considerably larger, or near the base of the structure where it might be in the plastic hinging range

and therefore more critical it may be necessary to make modifications. Furthermore, it has been shown in Section 5.2.1 that allowing yielding over the height of the structure will reduce the shear demand higher up in the structure, further negating this issue.

Unfortunately the method cannot be applied in the same way to the moment envelope because the RSA has a very different shape than that predicted by the NLTHA. What can be done however is to compare the NLTHA results when yielding is allowed only at the base with the RSA/$R_d$ results added to the pinned moment results. This comparison is shown below:

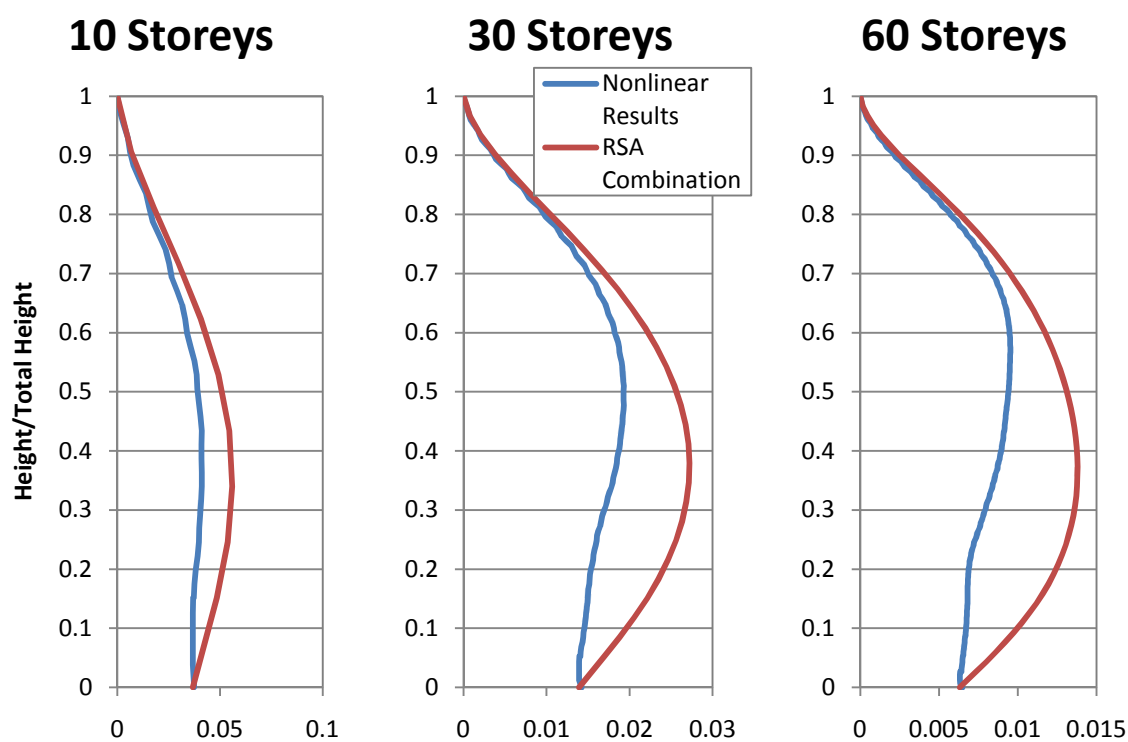


*Figure 5.37: Comparison of moment envelopes from NLTHA and RSA combination for the 10, 30, and 60 storey structures (x-axis shows base moment/[total weight*height])*

The comparison turns out to be quite poor, with the moment at mid-height being over predicted by a large amount. While using the pinned results for the shear at the base gives reasonable results (although slightly conservative), using it in the same proportions for the moment turns out to be excessive. Creating a model for the moment would require using a different proportion of the pinned shear, or perhaps combining the models in a different way.

It must be remembered though that it is unlikely that the moment would actually reach values larger than those at the base without the wall yielding somewhere up the height of the structure first. In this case, the yield moment up the height of the wall completely defines the moment profile, making any kind of model superfluous. Returning to the issue of the shears temporarily, it has been seen that yielding up the height of the structure reduces the shear forces at the base by a very small amount, but up the height of the structure much more. Therefore the model can still be used with confidence, but the user must be aware that if they have chosen to let the structure yield at locations other than the base, scaling the RSA results to the model may result in quite conservative approximations.

# 6 OTHER SHEAR DEMAND ISSUES

So far this thesis has systematically explored the phenomenon of shear amplification, starting with linear response spectrum analysis, through many nonlinear analyses, and finally arrived at a simple method to estimate the shear demand. However, although this process resulted in a good solution considering the assumptions, the shear demand in a cantilever concrete wall is a complicated issue – not only from the perspective of determining the maximum shear force, but even in trying to decide the appropriate design force. Furthermore, the relationship between the capacity and the demand may have some role to play in determining the design shear, and this is something that has not been explicitly addressed.

In this section, two main issues concerning the validity and accuracy of the conclusions reached in Chapter 5 will be addressed. The first is the choice of hysteretic model, as recent research has shown that perhaps a bilinear model is not the best choice for representing a lightly reinforced cantilever wall. The second is the issue of whether the design shear should really be the maximum shear will be considered, and the possibility that the wall may be able to withstand multiple cycles of large shear is raised.

## 6.1 CHOICE OF HYSTERETIC MODEL

In choosing the elastic perfectly plastic (EPP) model to describe the hysteretic behaviour of a reinforced concrete shear wall, this thesis was following what is often done in the analysis of reinforced concrete members. And in fact, for typical sections such as beams and columns with concentrated tension steel, the behaviour can be assumed to be mainly bilinear. This assumption is then often extended to shear walls, without further considerations as to how the behaviour may be different. Furthermore, even if one response (i.e. displacement) can either be assumed to be bilinear or can be modeled as such, that does not necessarily mean that other responses (i.e. moment, shear force) behave the same way.

Unfortunately, real concrete shear walls behave quite differently due to a number of factors. First of all, there is typically a fairly large axial load in a high-rise structure, which has two important effects. The first is to shift the cracking point up to a much higher moment, bringing into question the concept of using a single effective stiffness to represent the behaviour up to the yield point.

Secondly, the high axial load will tend to close cracks in the wall as it cycles back towards zero moment, leading to a rocking behaviour. Another problem is that due to the fact that steel is often distributed along the length of the wall, it is often hard to define a real yield point, as the moment-curvature relationship can be quite rounded. In this case, how real is it to use a bilinear model that requires a well defined yield point?

Work by Dezhdar (2011) has attempted to address these issues by extending the trilinear model for reinforced concrete walls developed by Adebar & Ibrahim (2002) to include hysteretic properties. The three sections of the backbone curve attempt to more accurately represent the uncracked-cracked-yielded behaviour of reinforced concrete walls. Figure 6.1, taken from his work, summarizes the model.

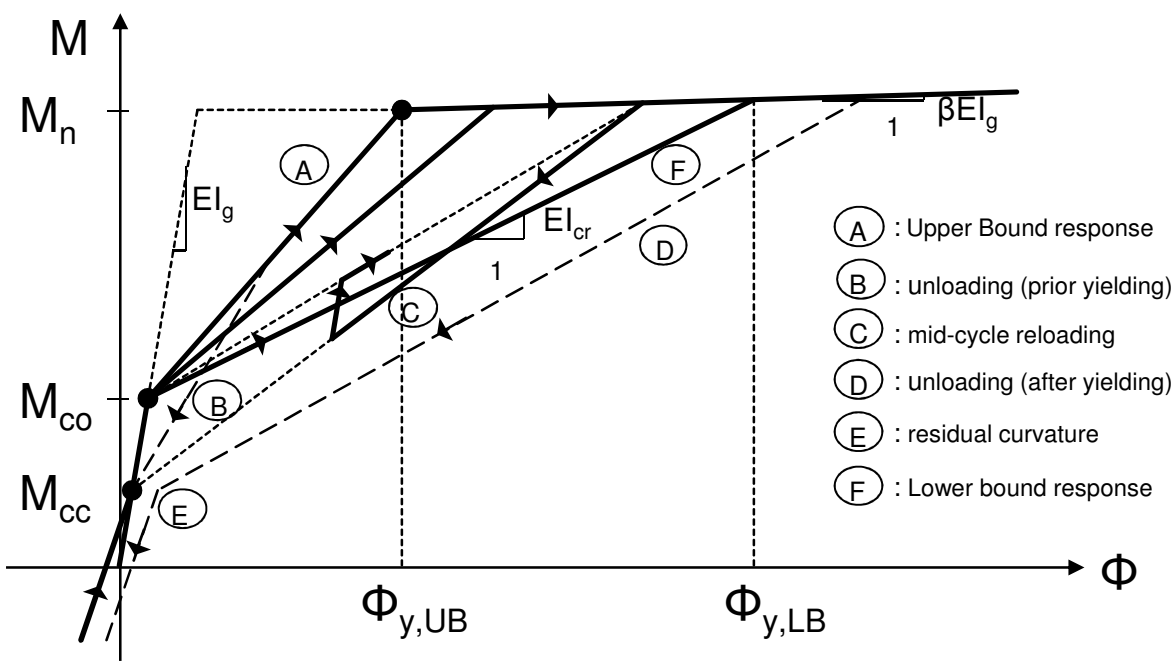


*Figure 6.1: Trilinear moment-curvature model for the hysteretic behaviour of tall reinforced concrete walls (Dezhdar, 2011)*

The next step is to compare the trilinear model with the EPP model used in the rest of the analysis. For this purpose, the 30 storey sample structure was reinforced to achieve 3 different levels of ductility, and analyzed using 25 ground motion records.

### 6.1.1 Comparison to EPP Model

In accurately comparing the EPP and trilinear model, it is important to ensure that the EPP model has been adjusted as well as possible to meet the trilinear model. To this end, a new set of analyses were performed under the same 25 ground motions used to analyze the structures employing the trilinear model. Furthermore, the damping assumed in the trilinear set of results was 3% based on the initial stiffness rather than 5% based on the last-committed stiffness. The yield strength of the EPP model was also changed from the previous RSA/$R_d$ to match the yield strength profile used by the trilinear model over the entire height. Finally, the initial slope of the EPP model was changed from 0.7EIg to 0.5EIg, following recent research by Dezhdar (2011) which found that this was a much better predictor of the top displacement.

The three yield moment profiles provided correspond roughly to base $R_d$ values of 1.2, 2.1, and 2.6 based on RSA results using the average 3% damped spectrum from the set of ground motions. However, the problem with defining an $R_d$ for these models is that it must be back-calculated after the yield strength has already been defined, and using different effective stiffnesses give very different results. Because of this, perhaps the best way to define the three models is to call them high strength (HS, $R_d$ = 1.2), medium strength (MS, $R_d$ = 2.1), and low strength (LS, $R_d$ = 2.6).

The moment envelope results from both analyses, as well as the specified yield moment, are shown in the figures below:

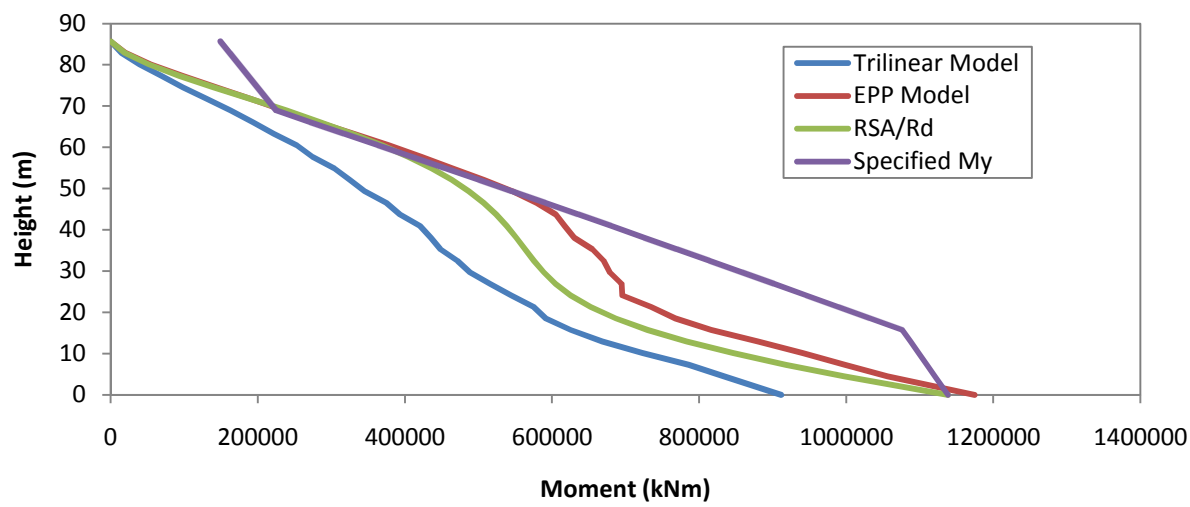


*Figure 6.2: Moment envelopes for the HS structure*

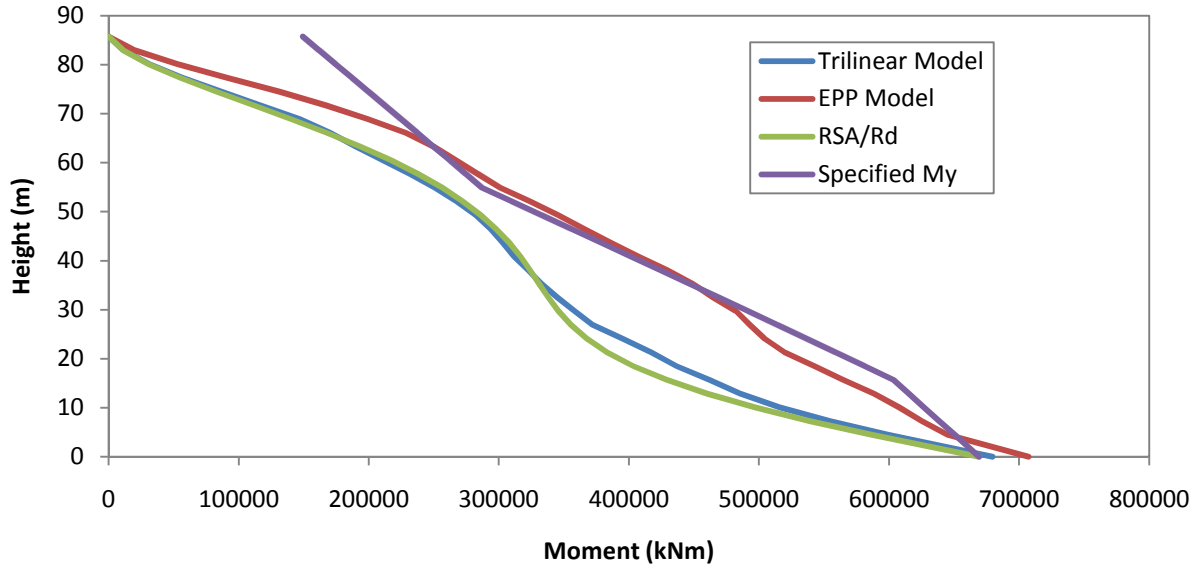


*Figure 6.3: Moment envelopes for the MS structure*

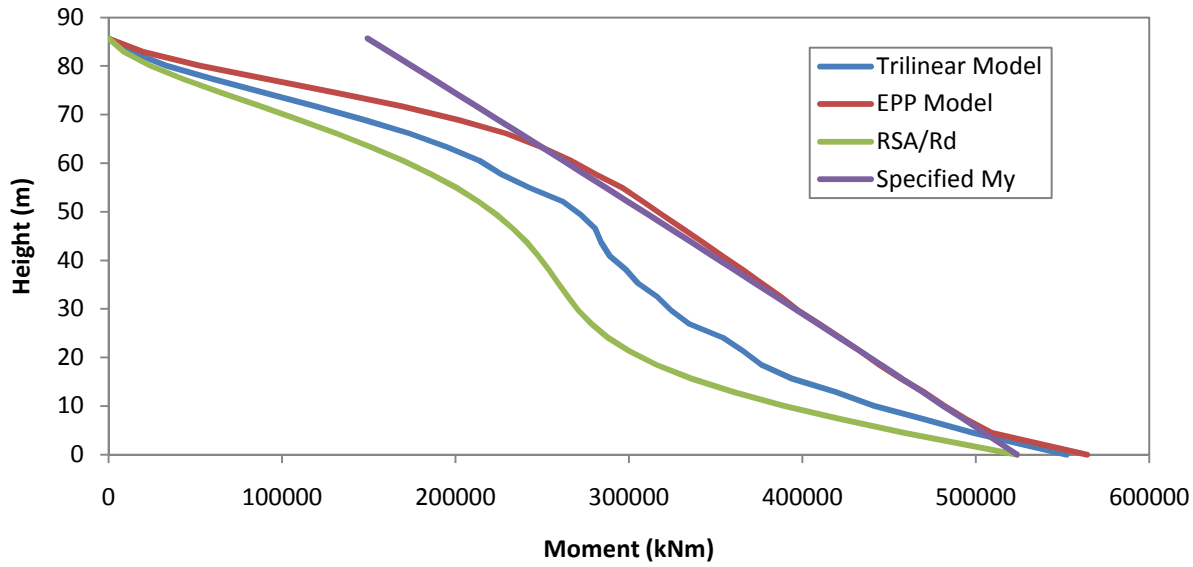


*Figure 6.4: Moment envelopes for the LS structure*

What is immediately clear in these figures is that the trilinear model predicts considerably less demand than the EPP model. In fact, in the HS structure the trilinear model does not even reach the yield point anywhere over the height of the structure, while the EPP model predicts yielding not only at the base but over a considerable range from about 45% of the height of the structure up to 70% of the height. This trend repeats itself in the MS and LS structures, although in these cases the

structure does yield at the base in both models. Notice however that in no case does the structure yield anywhere above the base when a trilinear model is used, in stark contrast to the EPP model which yields over the majority of the height in both cases. Note as in Section 5.2.1 that the increase over the yield moment at the base of the structure is due to the post-yield slope, required for stability of the model.

The explanation for this behaviour lies primarily in the cracked region of the trilinear model. Depending on the characteristics of the structure, this region can have a very shallow slope when compared to the gross stiffness, and is as low as 7% on the LS structure. Essentially, when the structure cracks and transitions into this zone the dynamic characteristics of the structure change and become softer overall, resulting in lower demand. In all of the structures, this cracked region prevents any part of the structure other than the base from yielding in the majority of ground motions.

Given what has been observed in previous sections of this thesis, it would be expected that if there is less inelastic demand then the shears would also be correspondingly less. Figures 6.5 to 6.7 show the shear envelopes from the analysis:

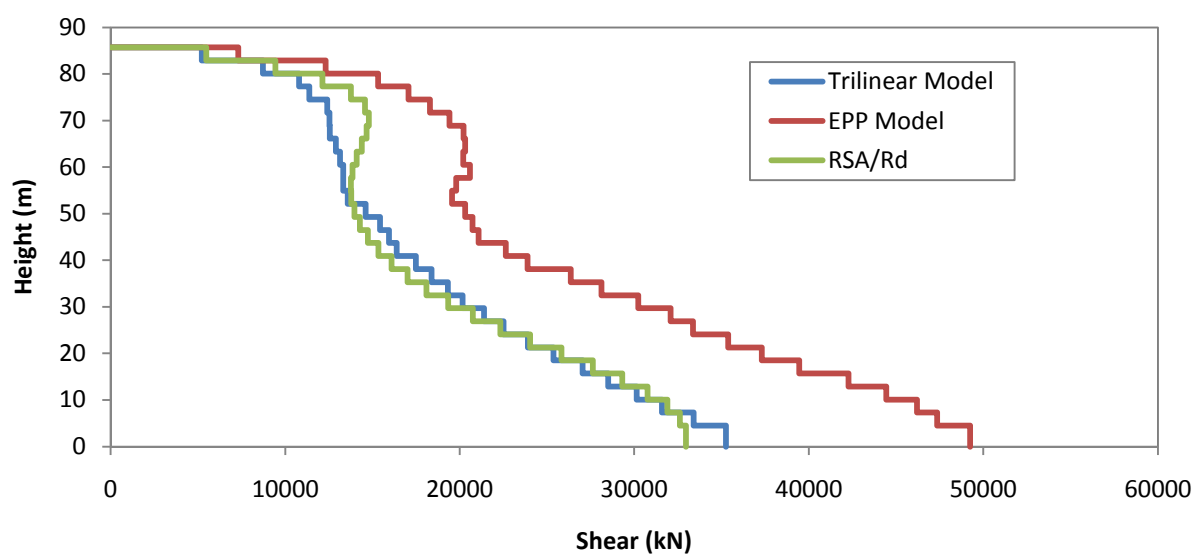


*Figure 6.5: Shear envelopes for the HS structure*

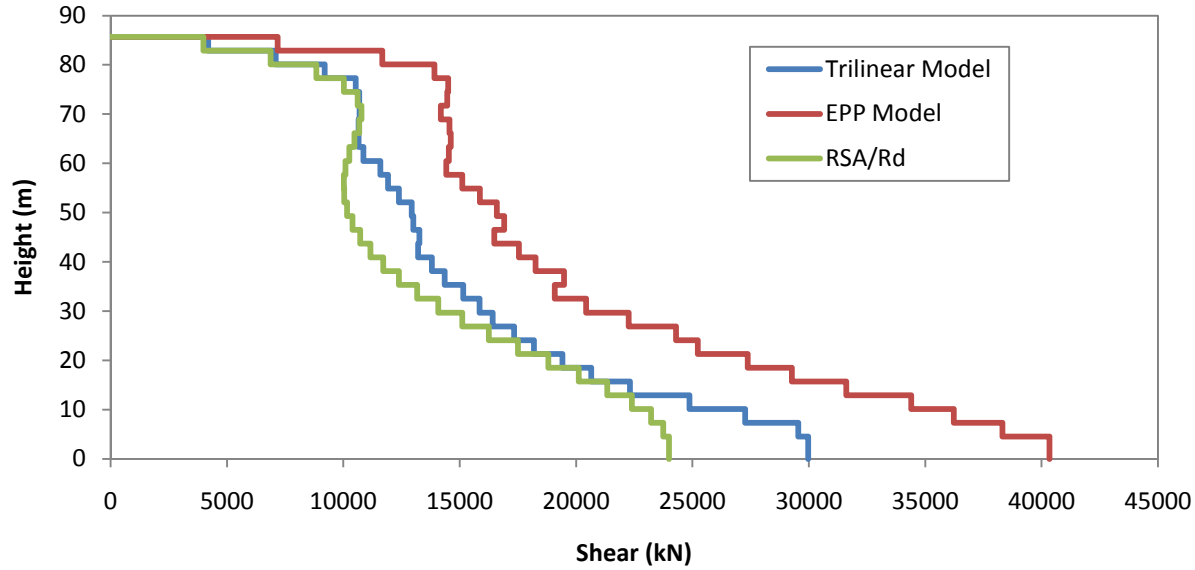


*Figure 6.6: Shear envelopes for the MS structure*

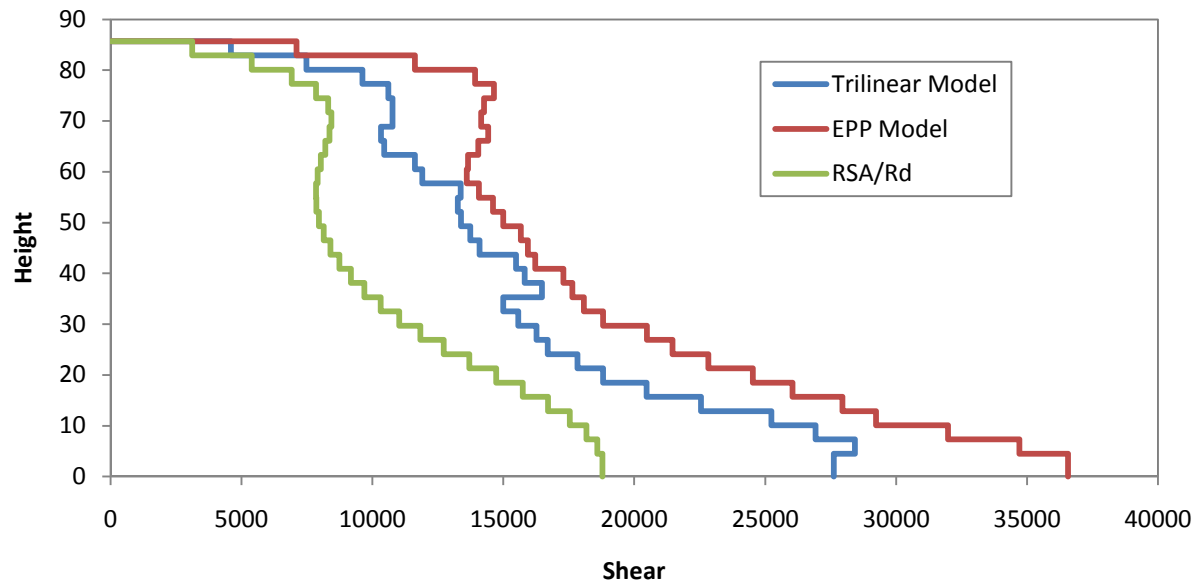


*Figure 6.7: Shear envelopes for the LS structure*

In all cases the shear force resulting from the analysis using the trilinear model is less over than the EPP model over the entire height of the structure. The reason for this is the same as for the moment – even though the shears are not completely controlled by the moment (the RSA/$R_d$ has been plotted for comparison), the softening of the structure due to cracking has reduced the shears considerably.

Further insight into how the trilinear model affects the structural response can be gained by considering the time histories of the moment and the shear. Because there are a total of 25 records, 5 were selected at random and several plots were made from each. The first set that is going to be displayed is from record 21. Figure 6.8 below is the base moment varying with time for the EPP model:

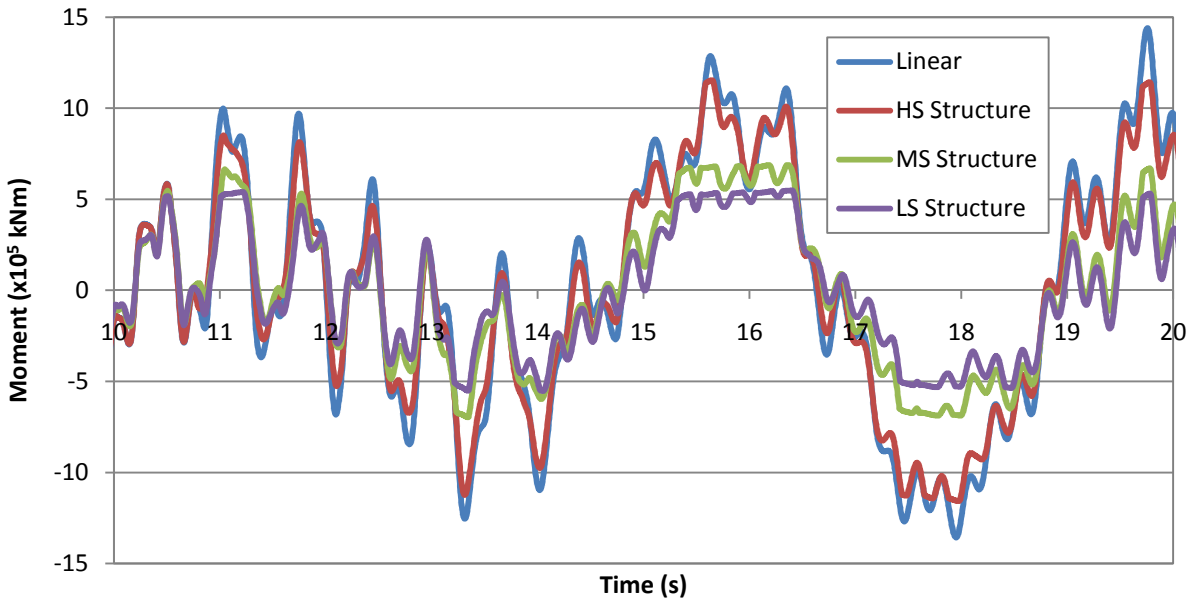


*Figure 6.8: Base moment time history for Record 21 with the EPP model, from 10 seconds to 20 seconds*

The shape of the different strength curves relative to each other is similar to what has been observed before, in that the weaker structures tend to be completely in phase with the stronger structures, with the only difference being that the weaker structures will experience a yield plateau. Contrast the shape of the curves in the EPP diagram with those from the same time period under the same record using the trilinear model:

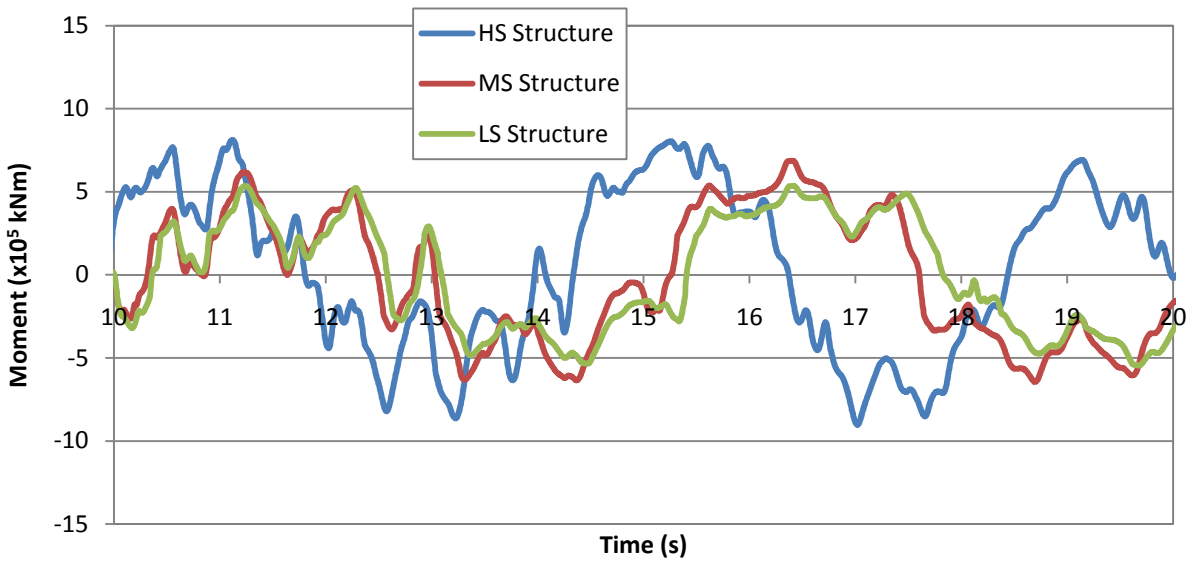


*Figure 6.9: Base moment time history for Record 21 with the trilinear model, from 10 seconds to 20 seconds*

The difference between Figure 6.8 and Figure 6.9 is quite considerable. In the trilinear model the lengthening of the periods due to the cracking of the wall not only causes the responses to be out of phase, but seems to prevent any significant yield plateaus from occurring. It is clear that the similarities in the base moment response are minimal. A similar trend can be seen in the shear response, as seen below:

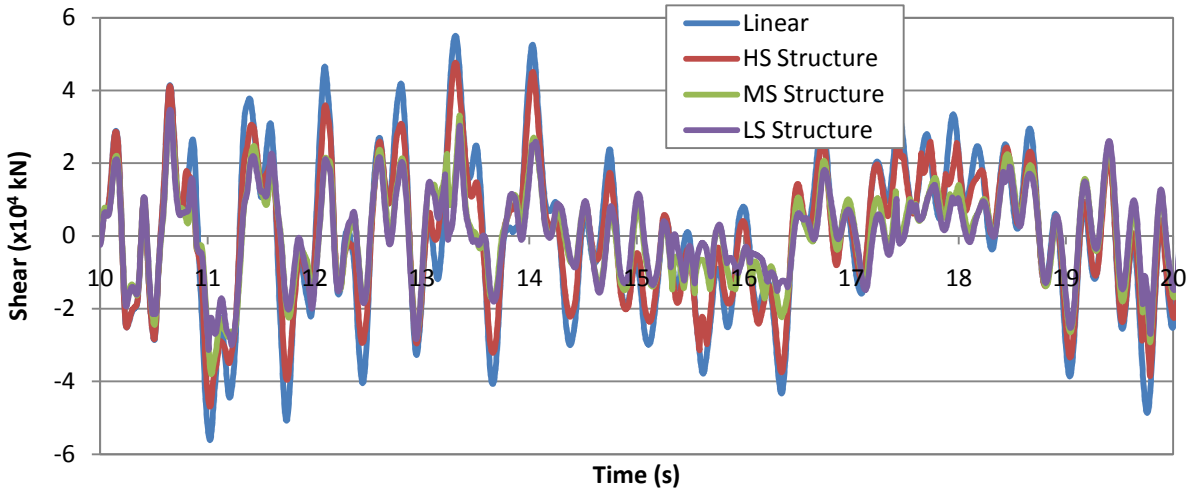


*Figure 6.10: Base shear time history for Record 21 with the EPP model, from 10 seconds to 20 seconds*

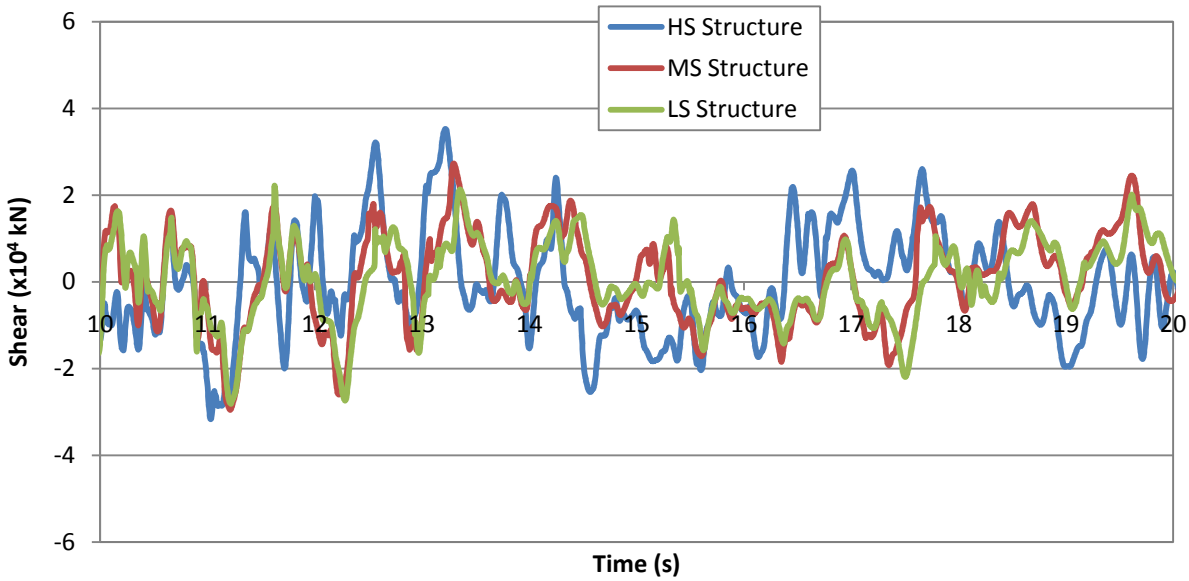


*Figure 6.11: Base shear time history for Record 21 with the trilinear model, from 10 seconds to 20 seconds*

Again, the EPP shear tends to follow the same cycles no matter what the strength, while the different strengths in the trilinear model are out of phase. This highlights the large difference that having secondary slope before yielding has on the response.

While plotting the moment and shear variation with time for each type of hysteretic behaviour is useful, it makes it difficult to compare the two methods. A more useful way to plot the data is to normalize one response by the other, and then show both models together. In this case, both the EPP and trilinear response have been normalized to the maximum EPP response, and both moment and shear have been plotted on the same figure. This gives a clear picture of how the moment and shear vary with each other relative to each model, and also the differences and similarities between the two models. Figure 6.12 below shows the results from record 1 for the LS structure:

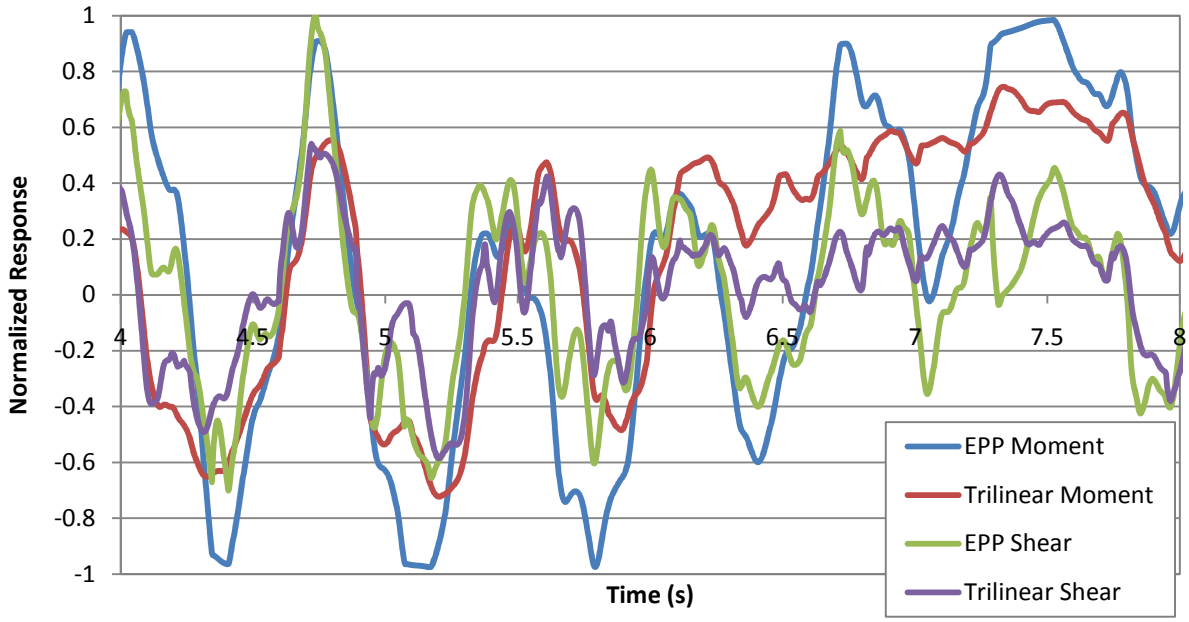


*Figure 6.12: Response time history for Record 1 with the LS structure (moments normalized to maximum EPP moment, shears normalized to maximum EPP shear), from 4 seconds to 8 seconds*

There is a lot of information in Figure 6.12, but there are four main points to address. The first, and perhaps most important, is the tendency in both of the cases for the shear to follow the moment quite closely (or vice versa). It cannot be said that the two are perfectly correlated, but in general it can be seen that the same modes control the response of both, and they cycle together. This follows into the second point – saying that the shear in the trilinear model is less than that in the EPP model due to the softening of the structure in the cracked region is enough in a general sense, but it is worth seeing how much this is tied to the reduction in moment demand. Figure 6.12 seems to indicate so around the 4.75s mark, where it can clearly be seen that both the moment and the shear drop from the EPP results by about the same amount. Unfortunately, this is not always the case. Looking at the same plot for record 12 shows that around 1.5s the moment in the trilinear model falls considerably, and yet the shears stay the same.

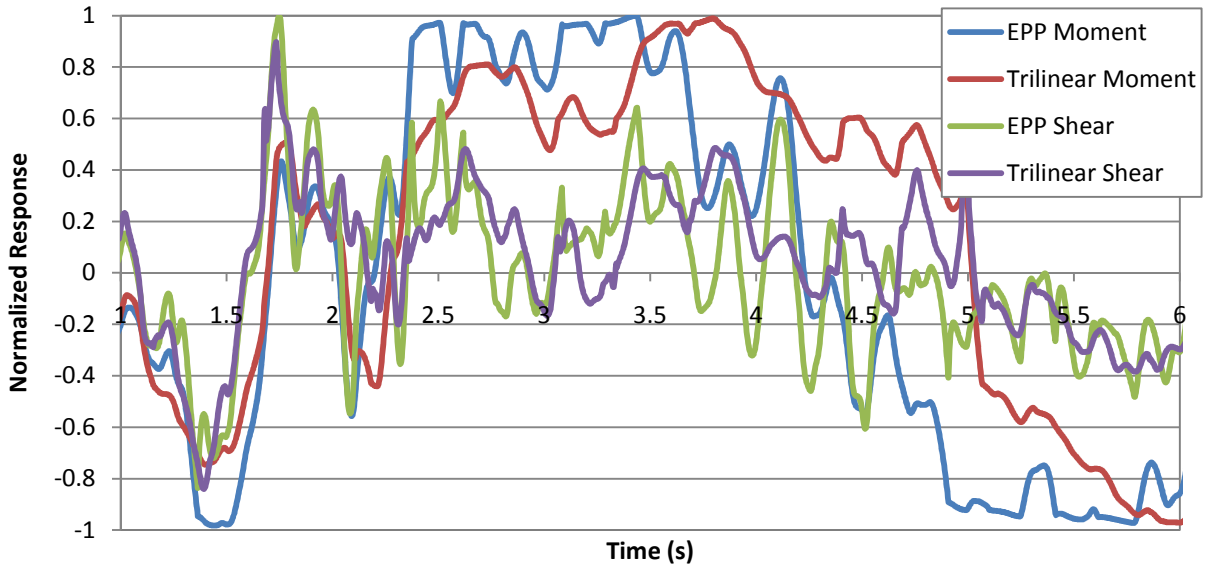


*Figure 6.13: Normalized response time history for Record 12 with the LS structure (moments normalized to maximum EPP moment, shears normalized to maximum EPP shear), from 1 second to 6 seconds*

Even though many points could be found which support or undermine the conclusion that the sole reason for the reduction in shear is due to the smaller moment, the first point made about Figure 6.12 seems the most consistent – that in general the shears follow the moments.

The third and fourth important concepts that can be drawn from figure x are related. As previously observed, the response of the trilinear model and the EPP model differ considerably. It can be seen particularly well in the 6-8s range of the figure, but the 3.5-4s range also shows very different behaviour. These differences in behaviour play a large part in confusing the issue of shear demand – it is difficult to transfer a model for shear behaviour between the different hysteretic shapes when the response is so different. Finally, it is interesting to pick out perhaps the biggest difference between the two models. Because of the cracking region in the trilinear model, the response of this model is much less erratic than that of the EPP model, where as soon as the yielding region is left responds assuming a very large stiffness. Consider the 6-8s region of Figure 6.12. It can be seen that the trilinear model has very small variations about a steadily rising value, whereas the EPP model fluctuates by an order of magnitude more. This applies to both the shears and the moments, and can also be seen in Figure 6.13 any time after about 3s. The only time that this general principle

does not seem to apply is during large “kicks” of the earthquake, such as between about 4.25-5.25s in Figure 6.12. Here both models respond largely in the second mode in a similar way before they diverge again.

It is clear then that unfortunately using an EPP model to predict shears results is overly conservative, and perhaps more importantly, that using an effective stiffness of 0.5EIg is only useful for predicting displacements, and not moments or shears. Problems also arise when trying to apply concepts like $R_d$ to a trilinear model, as was seen earlier. If in fact the cracking stiffness is so low and using a bilinear model cannot capture the full range of behaviour of a real concrete wall, how can concepts like ductility demand be defined precisely?

It is possible that a similar approach as taken in this thesis could potentially capture the behaviour of the trilinear model by performing different analyses for each of the sections, modifying the stiffness of the RSA accordingly. However, this would greatly increase the complexity of the problem and it is not clear how these different results could be combined.

## 6.2 Shear Peaks

Reviewing the literature in Chapter 2, it is common for the researcher to justify the importance of the research by assuming that shear failure is highly brittle and therefore must be protected against. While it is important to estimate any response quantity as well as one can in order to understand the behaviour of the structure, it is not entirely clear whether under dynamic loading the wall will immediately fail in the same brittle way as seen in quasi-static tests. Research (Gerin, 2003) has shown that in fact the shear behaviour exhibits some considerable ductility after diagonal cracking of the concrete, and even after yielding of the horizontal steel. In this light, it is worth discussing whether one sudden pulse of shear which may last for a fraction of a second will actually fail the structure. If it is then acceptable for the structure to undergo some cycling of shear, will there be multiple large peaks of shear during a record, or will the level of shear decrease? And finally, after all of those issues have been considered, what shear force should designers actually be using?

### 6.3.1 Shear Peak Curves

Leaving the issue of shear capacity of the structure under cycling for now, one issue that can be immediately addressed is the question of how much the shear force drops after one or more cycles.

Perhaps the easiest way to display this information is to pick off the points when the shear peaks from the base reaction time history, and then organize this data such that it can be easily seen how many shear peaks are larger than the current one. This way, a curve will be created allowing the reader to easily determine the shear force after any number of cycles. This kind of analysis, although the means will be taken, is likely very dependent on the records used and specifically the duration. For the sake of attempting to characterize the records used, three have been selected at random, and their displacement time histories are shown in Figure 6.14:

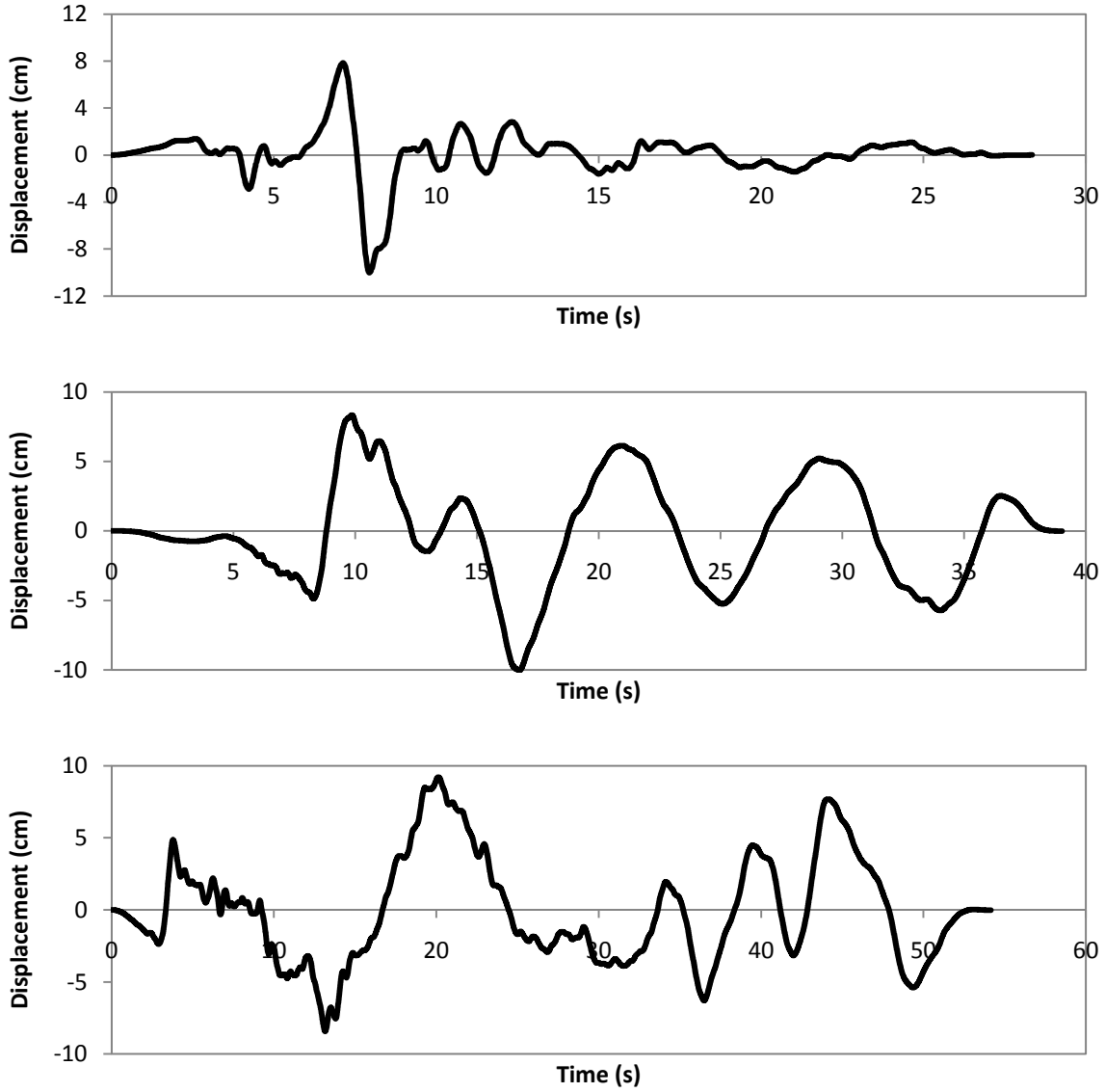


*Figure 6.14: Displacement time histories for 3 records chosen at random*

The 10, 30, and 50 storey structures were analyzed in this way for a number of ground motions and different $R_d$ values, and the results from the 30 storey structure are shown below in Figure 6.15:

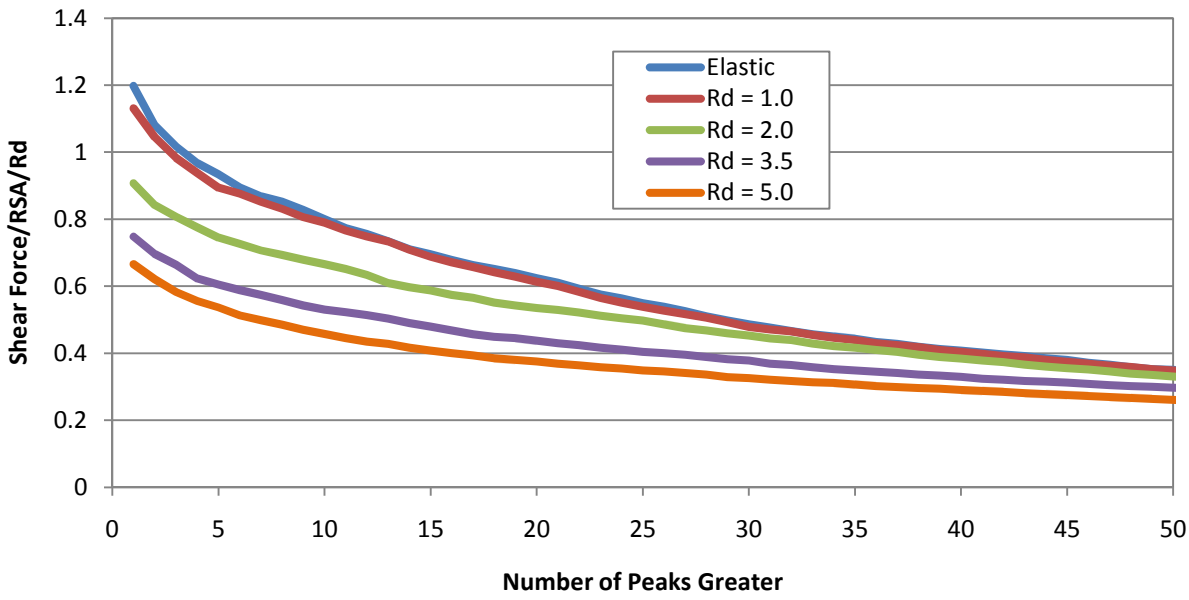


*Figure 6.15: Total shear peaks for the 30 storey structure, normalized by RSA*

At all ductility levels, if the wall is allowed to cycle some there can be considerable reductions in the shear force. For example, if the wall can withstand the shear for 10 cycles, a reduction on the order of 30% can be obtained.

Further insight – and some surprising results – can be gained by separating the shear into those peaks that occur when the structure is yielding versus those peaks that occur when the structures is elastic. This is of particular importance because yielding of the structure is assumed by the code to reduce the ability of the concrete to resist shear to zero. The three different curves – total, non-yielding, and yielding – are plotted below for $R_d$ = 2.0 and 3.5:

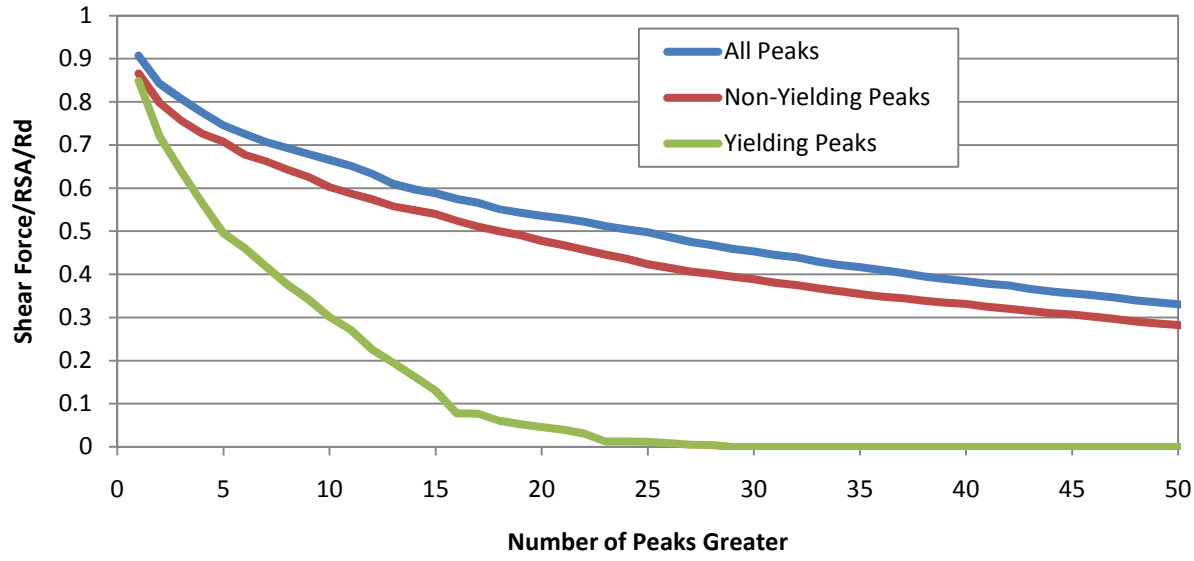


*Figure 6.16: All, yielding, and non-yielding shear peaks for $R_d$ = 2.0 for the 30 storey structure, normalized by RSA*

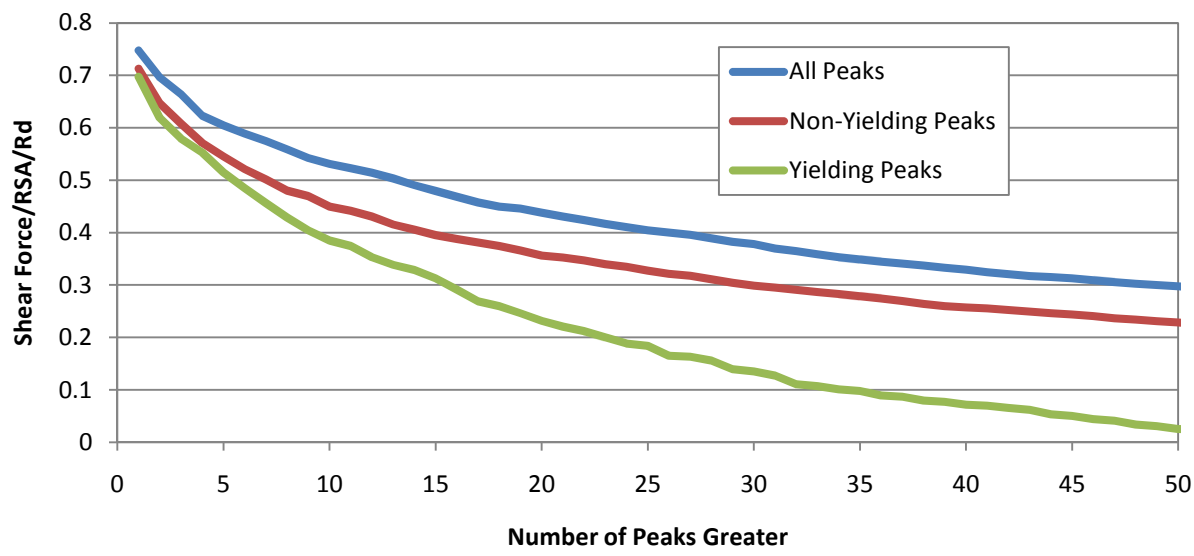


*Figure 6.17: All, yielding, and non-yielding shear peaks for $R_d$ = 3.5 for the 30 storey structure, normalized by RSA*

Several conclusions can be drawn from Figure 6.17. The first is that on average the number of times the maximum shear occurs during a yielding cycle is the same as when it occurs while the base of the wall is not yielding. This is actually rather surprising considering that up until now all of the qualitative explanations for the shear amplification phenomenon have assumed yielding at the base

of the structure. Fortunately, it can be seen that because the two maximum values are the same, the assumption that peak shears can occur because yielding at the base of the structure does not limit higher modes is still correct. Another interesting observation is that the peaks that occur during yielding fall off at a much faster rate than those that are non-yielding. This makes sense, because the structure spends considerably less time yielding than not, as seen from the time history results.

Before an explanation for magnitude of the non-yielding peaks is sought, the issue of reverse shear peaks should be addressed. These are peaks where the shear force is opposing the moment, or in other words when the compression resulting from the diagonal strut action travels to the part of the wall yielding in tension from the moment. If these peaks were found to be significant, they would certainly need to be identified and isolated from the other yielding peaks. However, it was found that in no case were these peaks close to as large as those when the shear is in the same direction as the moment, by an order of magnitude.

The fact that the maximum shear that occurs both during yielding and non-yielding is on average identical makes it easy to predict one force once the other has been calculated, but it is worthwhile to attempt to understand the non-yielding shear phenomenon in the same way that has been done for the yielding phenomenon. Fortunately there is a readily available explanation due to the simplicity of the EPP model. The dynamic properties of the structure, including mode shapes and periods, will be the same as long as the structure is not yielding. The question is whether it is possible that some combination of modes could result in a situation where the base of the structure is not yielding, but at the same time the shear force is much greater than anticipated by a $RSA/R_d$ type procedure.

Answering this question seems quite easy – it is definitely possible to combine modes in such a way that this result occurs, especially if the modes are added together instead of using other modal combination techniques, or some modes are allowed to be negative. The more challenging issue is to come up with a model that can predict these shears. It would be simple to use the results from the NLTHA and come up with some combination of linear modes such that both the moment and the shear match. Unfortunately the solution to this problem is not unique, and furthermore if the solution involves using fractions of modes, how should the combination work? Current modal

combination rules are based on random vibration principles which would not apply in this case, where the concern may not be the one point where the shear is maximum, but entire ranges where the shear is larger than a given amount.

Some attempts were made to predict the shear using a very simplistic algorithm. Essentially, the peak responses from the first ten modes (determined using RSA) were taken, and a factor was applied to each mode such that the moment was equal to the yield moment, but the shear was maximum. In order to meet these criteria, the Solver function in Excel was used. Note that the result, and perhaps the weakness, of this procedure is that all the higher modes will have factors of 1 (meaning that the peaks are used), one mode (usually the second or first) will have some factor between 0 and 1, and any remaining modes will have a factor of 0. This is because each consecutive higher mode has a higher shear to moment ratio. The crux of the problem then comes in determining how to combine the resulting moments and shears. After several methods were tried, such as absolute sum variations and square root sum of the squares (SRSS) variations, it was found that the most accurate predictor of the shears was a method where the higher modes with factors of 1 were combined using the SRSS approach, and then the mode with a factor between 0 and 1 was added to this result. A comparison of the amplification predicted by this method to the results from the NLTHA is shown below:

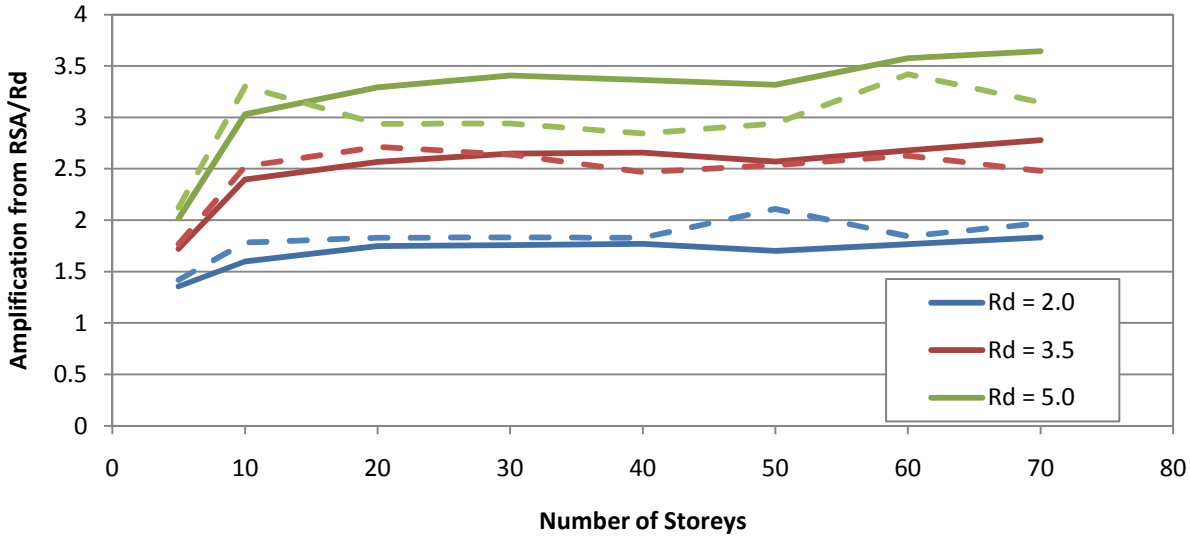


*Figure 6.18: Amplification comparison for the linear peaks model (Vancouver spectrum), solid = NLTHA, dashed = preliminary model*

The explanation of modes interacting in such a way as to not cause yielding at the base seems reasonable, but any further studies would have to look in detail at just how this can be predicted. Ultimately it is questionable how worthwhile it is pursuing a precise model for the non-yielding shear when a good model has already been developed for the yielding shear, and the two are virtually the same.

Returning to the issue of shear peaks in general, examples of the curves for certain structural heights and $R_d$ have been shown, but of particular concern is how they differ between structural heights, different $R_d$, and how the yielding and non-yielding peaks interact. Are the two curves similar only at the peak, or do they match beyond that? Results, broken apart by $R_d$, are shown below that answer these questions:

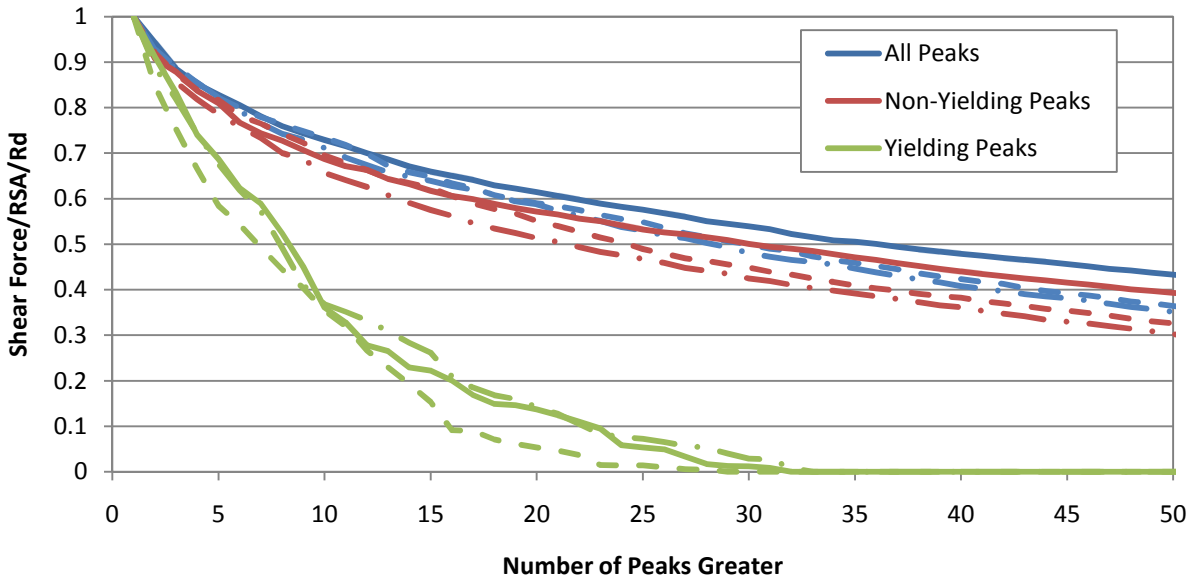


*Figure 6.19: Shear peaks for $R_d$ = 2.0, solid = 10 storeys, dashed = 30 storeys, dash-dot = 50 storeys, normalized to unity at the maximum peak*

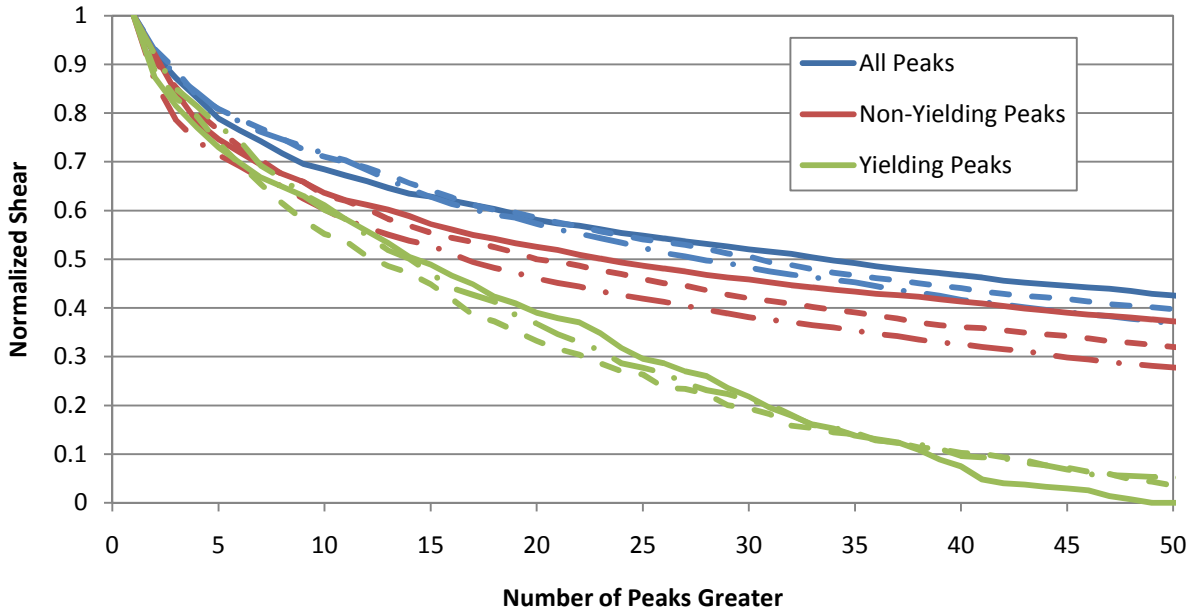


*Figure 6.20: Shear peaks for $R_d$ = 3.5, solid = 10 storeys, dashed = 30 storeys, dash-dot = 50 storeys, normalized to unity at the maximum peak*

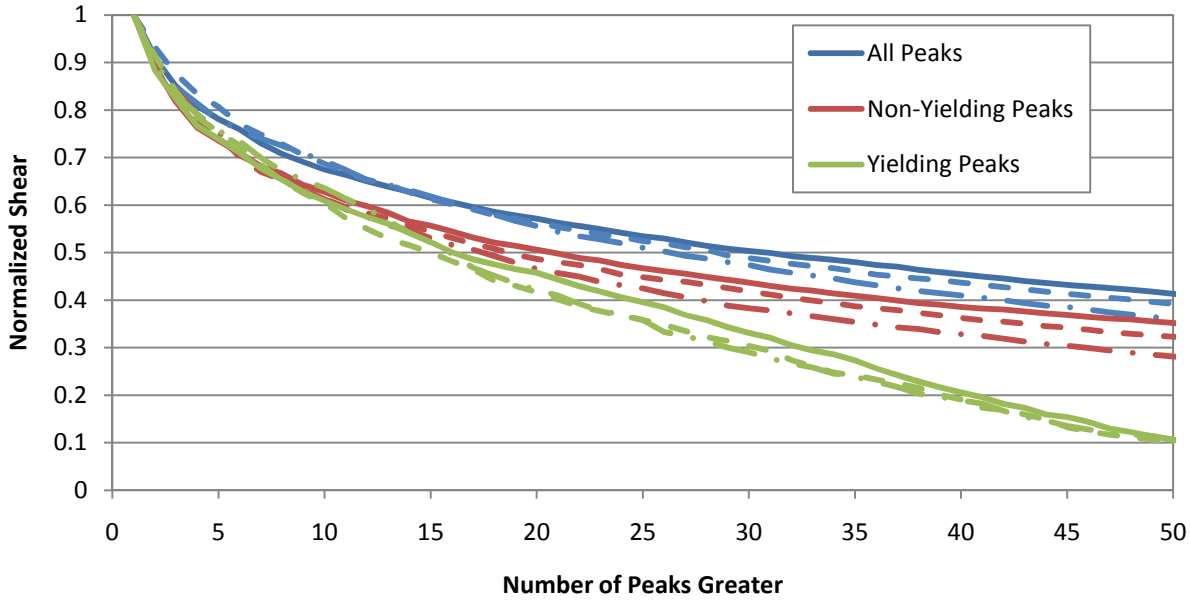


*Figure 6.21: Shear peaks for $R_d$ = 5.0, solid = 10 storeys, dashed = 30 storeys, dash-dot = 50 storeys, normalized to unity at the maximum peak*

These curves are all normalized such that the maximum shear is equal to 1. Part of the reason for this is that it has already been shown in Figures 6.16 and 6.17 that the average maximum peak is identical for all cases. Furthermore, this facilitates comparison between the different storey heights.

Two very important points can then be drawn from this set of figures. The first is that in general the curves are very similar, whether they be the total, yielding, or non-yielding shear peaks curves. It is true that as the number of cycles reaches 50 (or more – not all peaks are shown on these figures for the sake of brevity) there is some difference between the heights, but in the high shear range, which would likely be the most important region, they are very similar. The second point of interest is the tendency for the non-yielding curves in the higher $R_d$ structures to decrease and the yielding curves to increase. This makes sense – because the sum of the two curves horizontally must equal the total shear peak curve, if one increases the other must decrease. Furthermore, it would be expected that in the higher $R_d$ cases there would be more shears in the yielding range, if simply because the structure spends more time yielding. The significance of this result though, is that as the $R_d$ increases, it is not only the maximum shear that is similar, but the shear for several of the next largest cycles as well. Just visually assessing the data, it can be seen that for $R_d = 2.0$, the shears are about the same for 2 cycles, for $R_d = 3.5$ they are the same for about 8 cycles, and for $R_d = 5.0$ they are similar for about 12 cycles. This information could be of importance if walls are to be designed to a lower shear, because the design is much different when the wall is yielding.

Finally it is interesting to note that the total shear curves are very similar no matter the hysteretic model. The same analysis was performed on the trilinear results from Section 6.1.1, and Figure 6.22 below shows that while there are differences in the curves, it is still the case that if some cycling is allowed the shear drops off considerably.

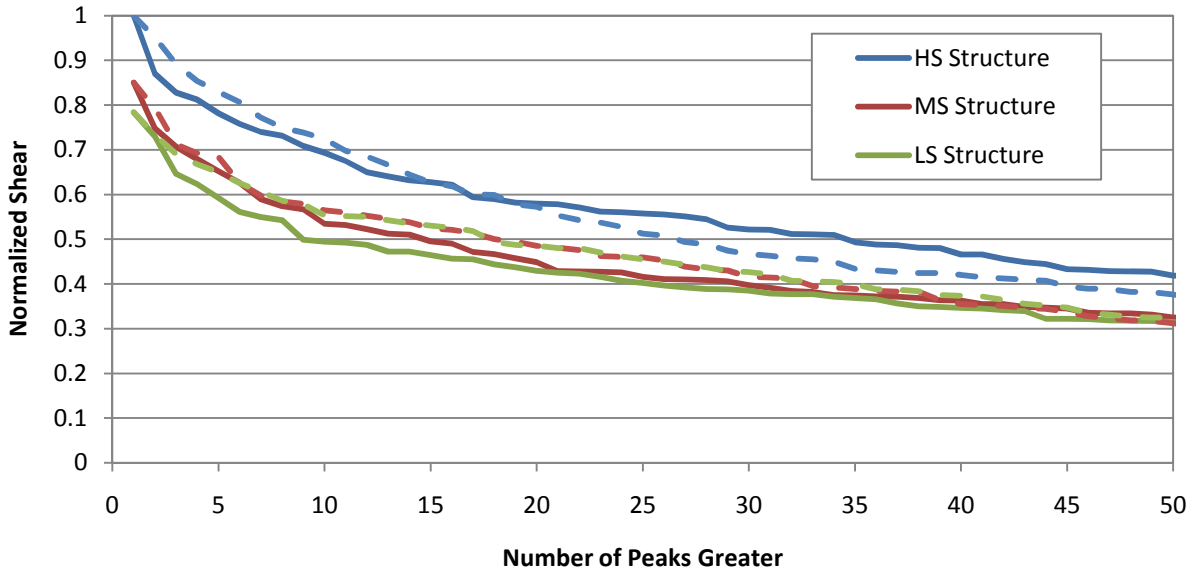


*Figure 6.22: Shear peaks normalized to the EPP maximum shear for each $R_d$ value, solid = trilinear model, dashed = EPP model*

Unfortunately separating the trilinear results into yielding/non-yielding would not tell the whole story because of the cracking region. And due to the fact that the behaviour changes with cycling, it would not even be clear how to separate the data into 3 categories.

### 6.3.2 Capacity Side

So far all of the discussion has focused on the demand side of the equation – what can be said about the shear force in relation to the next highest peak. However if one is trying to assess which shear peak should be designed for, or even if looking at the shear peaks in this way is a valid method, the capacity of the wall section under cyclic/seismic loading must be considered. Unfortunately, there is a dearth of information regarding this topic when it comes to walls. There are many quasi-static tests, and even some full scale tests, but out of those not many have focused on looking at potential shear failure modes. The focus of this section is thus not on trying to answer any questions, but rather to raise possible issues that must be addressed.

The first set of issues is related to the behaviour of the wall under multiple shear cycles. So far all the modeling has made a number of implicit assumptions, namely that the direction of the shear does not matter, and that the order of peaks does not matter. It is not at all clear whether this is

true. For example, it is true that shear loading in opposite directions will not close shear cracks, but the cracks will only open further if the shear is in one direction. As well, is it worse for the wall if several large cycles occur before the largest shear, or will large cycling after the peak shear result in more damage? There are all relevant questions that do not have clear answers.

A related problem is trying to understand exactly how the wall can fail in shear. As alluded to previously, a wall undergoing shear deformations actually has a fair amount of ductility built in due to cracking and yielding (Gerin, 2003). This would suggest that the failure of a wall would not be sudden, but would rather be after strain has accumulated over some length of time. It is this property which brings into question the notion that as soon as the shear resistance of the wall is reached it will fail in a sudden brittle manner. So then, how many cycles would it take for the wall to accumulate this amount of strain?

A corollary to this question is should shear yielding even be accepted? In capacity design philosophy, one mechanism is chosen to be ductile, and the other mechanisms are designed to remain elastic. If shear yielding is a mechanism to be prevented, then how many cycles could the wall potentially go through before any yielding of the reinforcing occurred?

These are issues which will require considerably more research, and perhaps testing, to answer.

# 7 CONCLUSION

This thesis has dealt extensively with the concept of shear amplification –the tendency for the shear force developed in a cantilever reinforced concrete wall to be greater than predicted by current linear code methods. Out of the possible sources of increases in the shear, the effect of higher modes in both the elastic and inelastic structure was identified as the primary source of the increases in shear observed by researchers. Through the use of response spectrum analysis (RSA), linear time history analysis (LTHA), and nonlinear time history analysis (NLTHA), the phenomenon has been explained both qualitatively and quantitatively.

It was seen from RSA models that yielding at the base of the structure did not limit shear forces from increasing, and from NLTHA that even when the base of the structure does not yield, it is still possible to develop large shear forces. A simple model was developed that relied only on the results of the typical RSA a designer would perform to predict the shear force at the base of the wall (Equation 5-3). Furthermore, although the equation is universal in that it can be adapted to fit within the design code of any region, it was written here in the terminology used in the Canadian design codes, such as NBCC 2005 (NRC, 2005) and CSA A23.3 (CSA, 2004). In this regard it is immediately useful, as neither code provides any guidance on how to account for this increase in shear force. Without any modifications it is ready to be presented to Canadian designers.

The model also proved to be instructive with regards to explaining the phenomenon. Several different models were initially proposed, but it was found that using the full RSA shear for the capacity component, and adding the pinned base shear was the best model. Physically, this can be interpreted as two different systems acting simultaneously – the pre-yielding and post-yielding parts. Within the yielding part of the model, two factors explain what is happening. The first, called $R_{pf}$, describes the ratio of maximum fixed base shear to the maximum pinned base shear. This can be thought of as the theoretical maximum amount of shear available in the yielding region. The second factor, called $H_f$, takes this theoretical maximum shear and applies a factor to it to account for the actual amount of yielding expected in a structure (represented by $R_d$ in this case). As expected, a structure that yields less would not have as many opportunities to develop the full pinned shear, and therefore the factor $H_f$ is less.

Chapter 2 of this thesis covered previous research in the other done by other practitioners, and it was found that often the methods proposed varied considerably. Further analysis of the results found that in general the researchers lacked a comprehensive picture of the problem – they either neglected to consider certain variables or had an incomplete or inadequate set of analysis results to work with. In that sense, this work can be seen as the most complete and in depth work on this subject to date, with a comprehensive analysis consisting of 8 structures, 40 ground motions, 2 different spectra, and various levels of yielding. A comparison to both the previous work and the NLTHA has shown that the method proposed here is superior.

In addition to providing a thorough solution to the problem when an elastic perfectly plastic (EPP) hysteretic model was assumed, possible issues with the assumptions made were explored. These included issues with the hysteretic model, and identification of the design shear force. With regards to the hysteretic model, it was found that when a trilinear shape was used the shear force demand reduced considerably. Another factor which would negate the increased shear force was the idea of allowing the wall to undergo several shear cycles, effectively reducing the shear force that needs to be designed for.

Future research in the field can be divided into three main sections:

- Selection and scaling of ground motions for tall structures. There are groups working on this topic, most notably the PEER Tall Building Initiative, but so far no conclusions have been reached. Until this matter is resolved, studies concerning tall structures will have to rely on the judgment of the researcher, which may or may not be adequate.
- Continuing to refine the models for estimating the shear demand. As discussed in Section 6.1, newer and better models for the flexural behaviour of concrete shear walls are being developed, and they may change the results. Furthermore, the effect of a good nonlinear shear model has not been studied in depth.
- The relationship between shear demand and shear capacity. It has been shown that in general if a number of cycles of shear are considered, the demand reduces. However, it is unclear how the wall would respond to such excitations and whether it is a benefit to consider multiple cycles.

# BIBLIOGRAPHY


Abrahamson, N. (1993). *RSPM – Spectral Matching Program*.

Adams, J. & Halchuk, S. (2003). Fourth generation seismic hazard maps of Canada: Values for over 650 Canadian localities intended for the 2005 National Building Code of Canada. *Geological Survey of Canada Open File 4459, Ottawa.*

Adebar, P. & Ibrahim, A. (2002). Simple nonlinear flexural stiffness model forconcrete structural walls. *Earthquake Spectra, 18,* 407-426.

Aoyama, H. (1987). Earthquake resistant design of reinforced concrete frame buildings with "flexural" walls. *Journal of the Faculty of Engineering, The University of Tokyo, 39,* 87-109.

ASCE. (2005). *ASCE 7 - Minimum Design Loads for Buildings and Other Structures.* USA: American Society of Civil Engineers.

ATC. (2005). *FEMA 440 – Improvement of nonlinear static seismic analysis procedures*. California: Applied Technology Council.

Blakely, R.W.G., Cooney, R.C., & Megget, L.M. (1975). Seismic shear loading at flexural capacity in cantilever wall structures. *Bulletin of the New Zealand Society for Earthquake Engineerin, 8,* 278-290.

Boivin, Y. & Paultre, P. (2010). Seismic performance of a 12-storey ductile concrete shear wall system designed according to the 2005 National building code of Canada and the 2004 Canadian Standard Association standard A23.3. *Canadian Journal of Civil Engineering, 37,* 1-16.

CEN. (2004). *Eurocode 8: Design of structures for earthquake resistance*. Brussels: Comite Europeen de Normalisation.

Chaallal, O. & Gauthier, D. (2000). Seismic shear demand on wall segments of ductile coupled shear walls. *Canadian Journal of Civil Engineering, 27,* 506-522.

Chopra, A. (2007). *Dynamics of Structures: Theory and Applications to Earthquake Engineering.* New Jersey: Prentice Hall.

CSA. (1994). *A23.3-94: Design of Concrete Structures.* Mississauga: Canadian Standards Association.

CSA. (2004). *A23.3-04: Design of Concrete Structures*. Mississauga: Canadian Standards Association.

Dezhdar, E. (2011). *Estimating of seismic demands on high-rise cantilever shear walls.* Vancouver: UBC Press.

Eberhard, M.O. & Sozen, M.A. (1993). Behavior-based method to determine design shear in earthquake-resistant walls. *Journal of Structural Engineering, 119,* 619-940.

Filiatrault, A., D'Aronco, D., & Tinawi, R. (1994). Seismic shear demand of ductile cantilever walls: a Canadian code perspective. *Canadian Journal of Civil Engineering, 21,* 363-376.

Fischinger, M., Rejec, K., & Isakovic, I. (2010). Seismic behavior of RC structural walls and Eurocode 8 provisions. *Proceedings of the 9th U.S. National and 10th Canadian Conference on Earthquake Engineering, Toronto, Paper 1824.*

Gerin, M.C. (2003). *Reverse-cyclic shear in reinforced concrete elements.* Vancouver: UBC Press.

Ghosh, S.K. (1992). Required shear strength of earthquake-resistant reinforced concrete shearwalls. In H. Krawinkler & P. Fajfar (Ed.), *Nonlinear Seismic Analysis and Design of Reinforced Concrete Buildings* (pp. 171-180). New York: Elsevier.

Ghosh, S.K., and Markevicius, V.P. (1990). Design of earthquake resistant shearwalls to prevent shear failure. *Proceedings of Fourth U.S. National Conference on Earthquake Engineering (Volume 2), USA,* 905-913.

Hamburger, R.O. & Moehle, J. (2010). Guidelines for seismic design of tall buildings. *Proceedings of the 9th U.S. National and 10th Canadian Conference on Earthquake Engineering, Toronto, Paper 954.*

Kabeyasawa, T. & Ogata, K. (1984). Ultimate-state design of R/C wall-frame structures. *Japan Concrete Institute,* 629-636.

Keintzel, E. (1992). Advances in the design for shear of RC structural walls under seismic loading. In H. Krawinkler & P. Fajfar (Ed.), *Nonlinear Seismic Analysis and Design of Reinforced Concrete Buildings* (pp. 171-180). New York: Elsevier.

NRC. (2005). *National Building Code of Canada 2005*.

NZS. (1982). *Part 1: Code of practice for the design of concrete structures*. Wellington: Standards Association of New Zealand.

Panneton, M., Leger, P., & Tremblay, R. (2006). Inelastic analysis of a reinforced concrete shear wall building according to the National Building Code of Canada 2005. *Canadian Journal of Civil Engineering, 33,* 854-871.

Priestly, N. & Amaris, A. (2003). Dynamic amplification of seismic moments and shear forces in cantilever walls. *Proceedings, FIB Symposium, Concrete Structures in Seismic Regions, Athens.*

Rajaee Rad, B. (2009). *Seismic shear demand in high-rise concrete walls.* Vancouver: UBC Press.

SEAOC. (2009). Reinforced concrete stuctures. In SEAOC, *Blue Book – Seismic Design Recommendations*. California: Structural Engineers Association of California.

Senevratna, G.D. & Krawinkler, H. (1994). Strength and displacement demands for seismic design of structural walls. *Proceedings of the 5th U.S. National Conference on Earthquake Engineering, Chicago,* 181-190.

Sullivan, T.J., Priestly, M.J.N., Calvi, G.M. (2006). Shear forces in RC walls of frame-wall structures. *Proceedings of the 8th U.S. National Conference on Earthquake Engineering, USA, Paper 1188.*

UC Berkeley. (2009). *OpenSees – Open System for Earthquake Engineering* (version 2.1.0). Retrieved December 2009, from http://opensees.berkeley.edu/index.php

# APPENDIX A – EXAMPLE CORES

**Cores at 1:100 Scale**

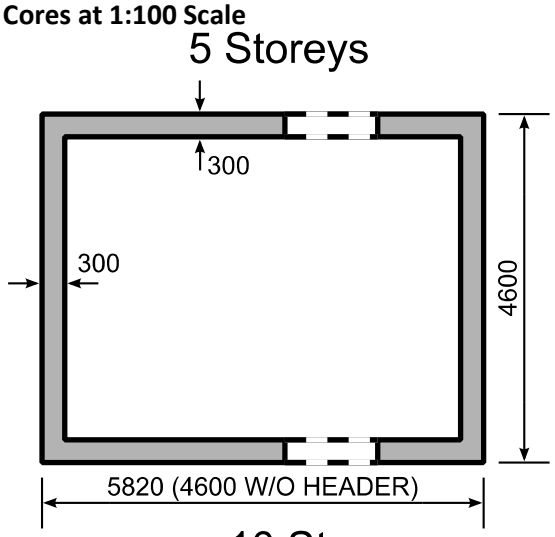


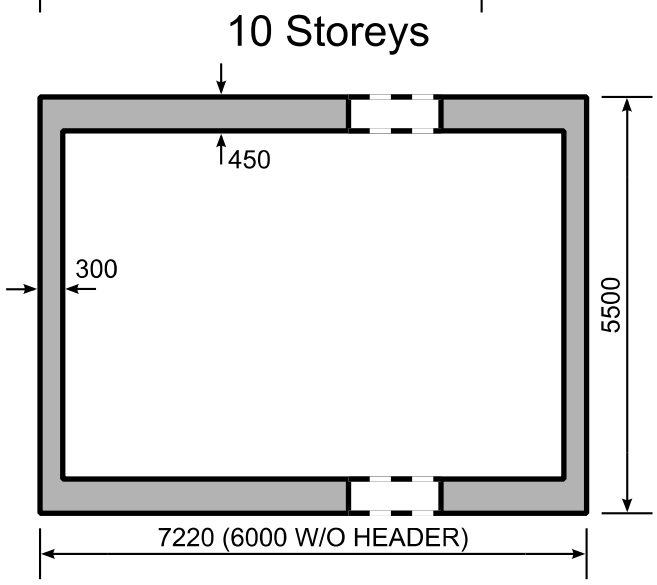

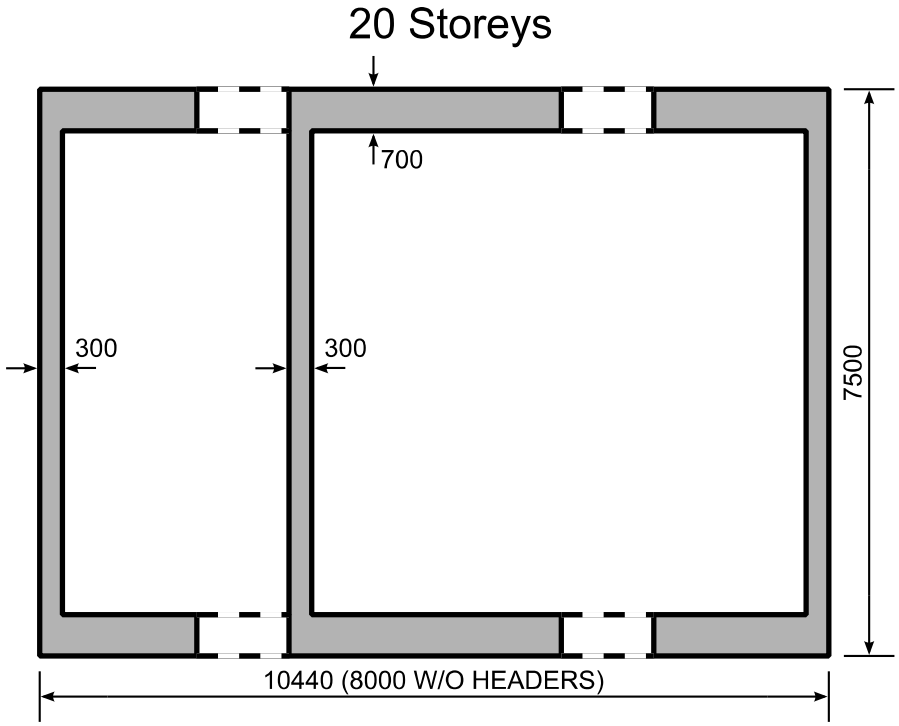


**Cores at 1:200 Scale**

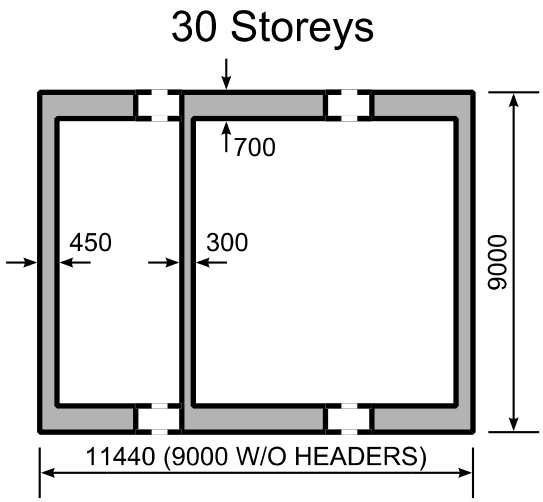


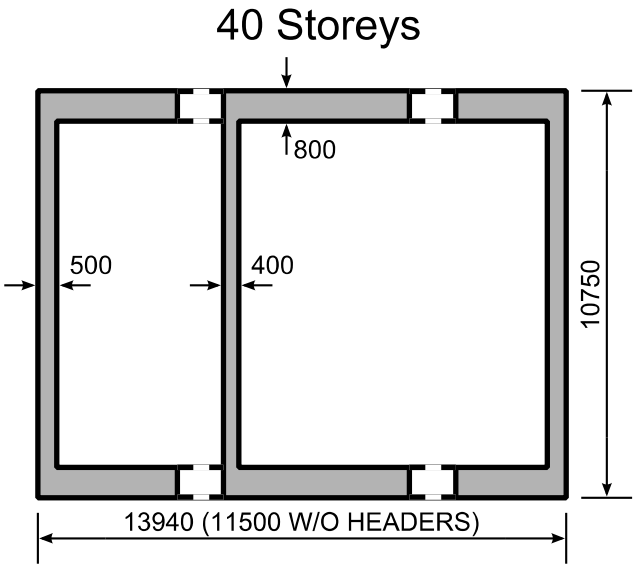

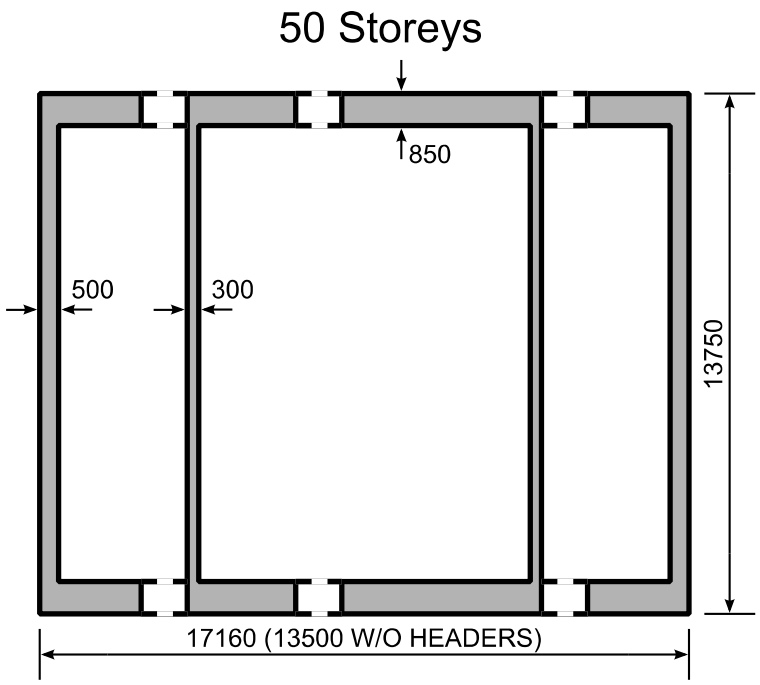
50 Storeys
850
500
300
13750
17160 (13500 W/O HEADERS)

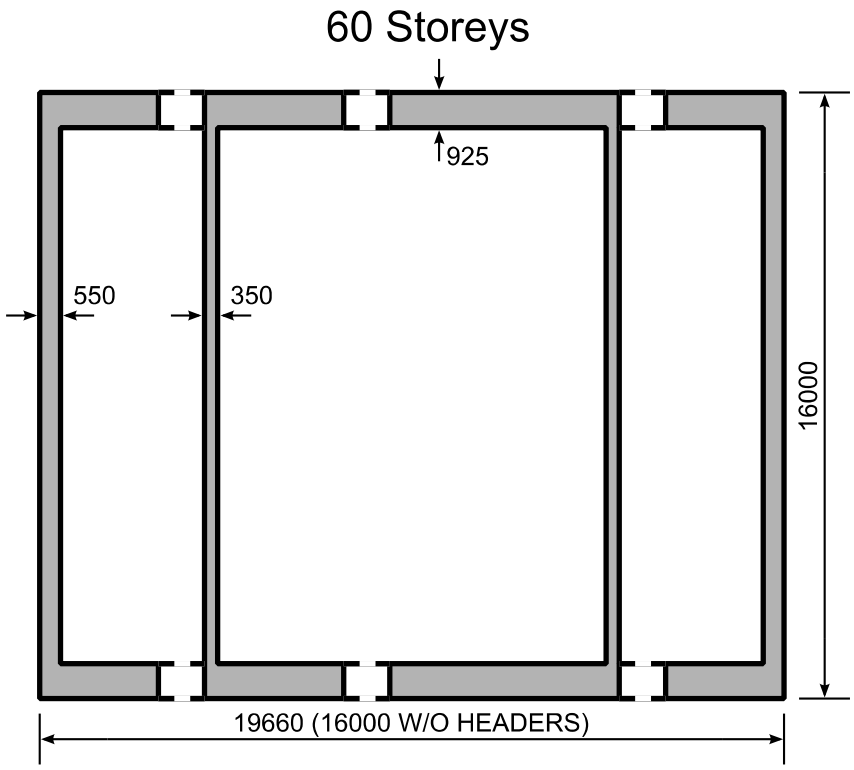
60 Storeys
925
550
350
16000
19660 (16000 W/O HEADERS)

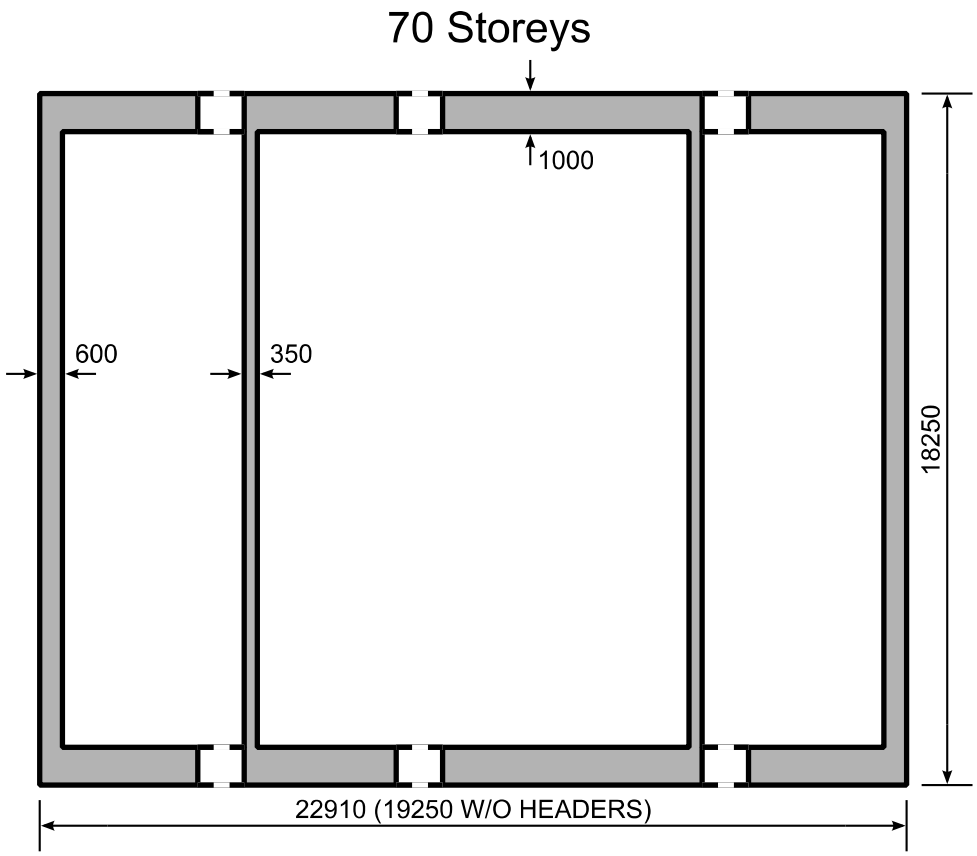
70 Storeys
1000
600
350
18250
22910 (19250 W/O HEADERS)

# APPENDIX B – FEMA 440 GROUND MOTIONS

**Site Class B Records**

| Date | Earthquake Name | Magnitude (Ms) | Station Name | Station Number | Component (deg) | PGA ($cm/s^2$) |
|---|---|---|---|---|---|---|
| 6/28/1992 | Landers | 7.5 | Silent Valley, Poppet Flat | 12206 | 0 | 48.9 |
| 6/28/1992 | Landers | 7.5 | Twentynine Palms Park Maintenance Bldg | 22161 | 0 | 78.7 |
| 6/28/1992 | Landers | 7.5 | Amboy | 21081 | 90 | 146 |
| 10/17/1989 | Loma Prieta | 7.1 | Point Bonita | 58043 | 297 | 71.4 |
| 10/17/1989 | Loma Prieta | 7.1 | Piedmont, Piedmont Jr. High Grounds | 58338 | 45 | 81.2 |
| 10/17/1989 | Loma Prieta | 7.1 | San Francisco, Pacific Heights | 58131 | 270 | 60.2 |
| 10/17/1989 | Loma Prieta | 7.1 | San Francisco, Rincon Hill | 58151 | 90 | 88.5 |
| 10/17/1989 | Loma Prieta | 7.1 | San Francisco, Golden Gate Bridge | 1678 | 360 | 228.6 |
| 10/17/1989 | Loma Prieta | 7.1 | Hollister-SAGO vault | 1032 | 360 | 60.1 |
| 10/17/1989 | Loma Prieta | 7.1 | South San Francisco, Sierra Point | 58539 | 205 | 102.7 |
| 10/17/1989 | Loma Prieta | 7.1 | Berkeley, Lawrence Berkeley Lab. | 58471 | 90 | 114.8 |
| 10/17/1989 | Loma Prieta | 7.1 | Coyote Lake Dam, Downstream | 57504 | 285 | 175.6 |
| 1/17/1994 | Northridge | 6.8 | Mt Wilson, CIT Seismic Station | 24399 | 90 | 228.5 |
| 1/17/1994 | Northridge | 6.8 | Antelope Buttes | 24310 | 90 | 99.7 |
| 1/17/1994 | Northridge | 6.8 | Los Angeles, Wonderland | 90017 | 285 | 168.7 |
| 1/17/1994 | Northridge | 6.8 | Wrightwood, Jackson Flat | 23590 | 90 | 54.5 |
| 1/17/1994 | Northridge | 6.8 | Littlerock-Brainard Can | 23595 | 90 | 7.2 |
| 1/17/1994 | Northridge | 6.8 | San Gabriel, E. Grand Ave. | 90019 | 180 | 256 |
| 10/1/1987 | Whittier Narrows | 6.1 | Los Angeles, Gritfith Park Observatory | 141 | 0 | 133.8 |
| 10/15/1979 | Imperial Valley | 6.8 | Superstition Mountain | 286 | 135 | 189.2 |

**Site Class C Records**

| Date | Earthquake Name | Magnitude (Ms) | Station Name | Station Number | Component (deg) | PGA ($cm/s^2$) |
|---|---|---|---|---|---|---|
| 10/15/1979 | Imperial Valley | 6.8 | El Centro, Parachute Test Facility | 5051 | 315 | 200.2 |
| 2/9/1971 | San Fernando | 6.5 | Pasadena, CIT Athenaeum | 80053 | 90 | 107.9 |
| 2/9/1971 | San Fernando | 6.5 | Pearblossom Pump | 269 | 21 | 133.4 |
| 6/28/1992 | Landers | 7.5 | Yermo, Fire Station | 12149 | 0 | 167.8 |
| 10/17/1989 | Loma Prieta | 7.1 | APEEL 7, Pulgas | 58378 | 0 | 153 |
| 10/17/1989 | Loma Prieta | 7.1 | Gilroy #6, San Ysidro Microwave site | 57383 | 90 | 166.9 |
| 10/17/1989 | Loma Prieta | 7.1 | Saratoga, Aloha Ave. | 58065 | 0 | 494.5 |
| 10/17/1989 | Loma Prieta | 7.1 | Gilroy, Gavilon College Phys Sci Bldg | 47006 | 67 | 349.1 |
| 10/17/1989 | Loma Prieta | 7.1 | Santa Cruz, University of California | 58135 | 360 | 433.1 |
| 10/17/1989 | Loma Prieta | 7.1 | San Francisco, Diamond Heights | 58130 | 90 | 110.8 |
| 10/17/1989 | Loma Prieta | 7.1 | Fremont, Mission San Jose | 57064 | 0 | 121.6 |
| 10/17/1989 | Loma Prieta | 7.1 | Monterey, City Hall | 47377 | 0 | 71.6 |
| 10/17/1989 | Loma Prieta | 7.1 | Yerba Buena Island | 58163 | 90 | 66.7 |
| 10/17/1989 | Loma Prieta | 7.1 | Anderson Dam, Downstream | 1652 | 270 | 239.4 |
| 4/24/1984 | Morgan Hill | 6.1 | Gilroy, Gavilon College Phys Sci Bldg | 47006 | 67 | 95 |
| 4/24/1984 | Morgan Hill | 6.1 | Gilroy #6, San Ysidro Microwave site | 57383 | 90 | 280.4 |
| 7/8/1986 | Palmsprings | 6 | Fun Valley | 5069 | 45 | 129 |
| 1/17/1994 | Northridge | 6.8 | Littlerock, Brainard Canyon | 23595 | 90 | 70.6 |
| 1/17/1994 | Northridge | 6.8 | Castaic, Old Ridge Route | 24278 | 360 | 504.2 |
| 1/17/1994 | Northridge | 6.8 | Lake Hughes #1, Fire Station #78 | 24271 | 0 | 84.9 |

# APPENDIX C – LINEAR SCALING FACTORS ($T_1$ TO $T_2$)

**VANCOUVER**

| Height | B01 | B02 | B03 | B04 | B05 | B06 | B07 | B08 | B09 | B10 |
|---|---|---|---|---|---|---|---|---|---|---|
| 5 | 3.16 | 2.27 | 6.66 | 9.28 | 2.33 | 6.32 | 5.94 | 5.86 | 7.55 | 3.20 |
| 10 | 2.98 | 4.31 | 4.73 | 12.68 | 2.28 | 9.19 | 4.38 | 5.13 | 8.92 | 7.25 |
| 20 | 4.03 | 6.83 | 4.80 | 13.08 | 1.91 | 12.57 | 4.98 | 5.86 | 8.55 | 13.76 |
| 30 | 5.55 | 7.81 | 5.17 | 12.52 | 1.68 | 12.76 | 6.22 | 5.73 | 10.18 | 19.66 |
| 40 | 7.95 | 7.95 | 5.33 | 11.44 | 1.59 | 11.06 | 8.28 | 6.05 | 10.90 | 23.31 |
| 50 | 10.91 | 7.68 | 5.47 | 10.67 | 1.55 | 10.07 | 10.03 | 6.69 | 11.32 | 27.21 |
| 60 | 14.08 | 7.62 | 5.65 | 9.55 | 1.60 | 9.65 | 12.78 | 7.71 | 11.37 | 32.25 |
| 70 | 17.97 | 7.53 | 5.25 | 9.09 | 1.67 | 9.03 | 15.79 | 8.60 | 11.78 | 39.99 |

| Height | B11 | B12 | B13 | B14 | B15 | B16 | B17 | B18 | B19 | B20 |
|---|---|---|---|---|---|---|---|---|---|---|
| 5 | 5.61 | 8.69 | 6.38 | 5.61 | 3.79 | 2.68 | 1.80 | 3.70 | 1.74 | 2.07 |
| 10 | 3.62 | 4.71 | 4.39 | 5.20 | 3.40 | 2.34 | 1.98 | 2.13 | 1.72 | 1.30 |
| 20 | 2.16 | 3.13 | 3.26 | 4.55 | 3.83 | 2.58 | 2.49 | 1.79 | 1.63 | 0.92 |
| 30 | 2.23 | 2.76 | 2.90 | 4.91 | 4.36 | 2.96 | 3.06 | 1.95 | 1.77 | 0.96 |
| 40 | 2.32 | 2.65 | 2.98 | 4.80 | 4.57 | 3.54 | 3.64 | 2.12 | 1.91 | 1.00 |
| 50 | 2.44 | 2.75 | 3.06 | 4.61 | 5.18 | 4.27 | 3.99 | 2.37 | 1.98 | 1.08 |
| 60 | 2.69 | 2.93 | 3.15 | 4.58 | 5.84 | 5.15 | 4.38 | 2.81 | 2.02 | 1.22 |
| 70 | 3.12 | 3.05 | 3.19 | 4.66 | 6.29 | 6.26 | 4.86 | 3.27 | 2.02 | 1.40 |

| Height | C01 | C02 | C03 | C04 | C05 | C06 | C07 | C08 | C09 | C10 |
|---|---|---|---|---|---|---|---|---|---|---|
| 5 | 2.63 | 5.52 | 3.46 | 1.80 | 1.13 | 3.50 | 0.76 | 2.37 | 1.35 | 2.99 |
| 10 | 2.98 | 4.10 | 2.67 | 1.97 | 1.03 | 2.83 | 1.13 | 1.83 | 1.29 | 2.78 |
| 20 | 3.01 | 4.46 | 2.67 | 2.11 | 0.81 | 2.73 | 1.54 | 2.02 | 1.40 | 2.77 |
| 30 | 2.94 | 5.17 | 3.08 | 2.30 | 0.77 | 2.92 | 2.17 | 2.19 | 1.65 | 2.93 |
| 40 | 2.74 | 5.82 | 3.53 | 2.55 | 0.81 | 3.16 | 2.47 | 2.20 | 1.95 | 3.15 |
| 50 | 2.51 | 6.86 | 4.11 | 2.66 | 0.86 | 3.44 | 2.70 | 2.38 | 2.16 | 3.16 |
| 60 | 2.43 | 9.22 | 4.94 | 2.82 | 0.91 | 3.70 | 3.08 | 2.64 | 2.30 | 3.17 |
| 70 | 2.45 | 11.88 | 6.22 | 3.19 | 0.98 | 3.95 | 3.64 | 2.80 | 2.40 | 3.25 |

| Height | C11 | C12 | C13 | C14 | C15 | C16 | C17 | C18 | C19 | C20 |
|---|---|---|---|---|---|---|---|---|---|---|
| 5 | 4.31 | 0.93 | 4.33 | 6.78 | 1.17 | 0.63 | 2.61 | 3.23 | 6.17 | 1.90 |
| 10 | 3.64 | 1.17 | 3.81 | 10.43 | 0.95 | 0.59 | 2.40 | 5.30 | 4.51 | 1.29 |
| 20 | 4.29 | 1.28 | 3.78 | 13.03 | 0.89 | 0.64 | 2.52 | 7.22 | 3.86 | 0.88 |
| 30 | 5.01 | 1.65 | 3.81 | 14.40 | 0.98 | 0.73 | 2.70 | 8.67 | 3.62 | 0.86 |
| 40 | 6.36 | 1.80 | 4.07 | 15.82 | 1.10 | 0.80 | 2.84 | 9.60 | 3.79 | 0.87 |
| 50 | 9.21 | 1.90 | 4.14 | 17.27 | 1.29 | 0.93 | 2.92 | 10.20 | 3.88 | 0.86 |
| 60 | 12.06 | 2.04 | 4.30 | 19.40 | 1.57 | 1.07 | 3.10 | 11.02 | 3.94 | 0.85 |
| 70 | 15.16 | 2.23 | 4.62 | 21.63 | 2.00 | 1.18 | 3.31 | 12.01 | 4.01 | 0.83 |

**MONTREAL**

| Height | B01 | B02 | B03 | B04 | B05 | B06 | B07 | B08 | B09 | B10 |
|---|---|---|---|---|---|---|---|---|---|---|
| 5 | 2.00 | 1.43 | 4.21 | 5.88 | 1.47 | 4.00 | 3.76 | 3.71 | 4.78 | 2.03 |
| 10 | 1.60 | 2.31 | 2.54 | 6.80 | 1.22 | 4.93 | 2.35 | 2.75 | 4.78 | 3.89 |
| 20 | 1.77 | 3.00 | 2.11 | 5.75 | 0.84 | 5.53 | 2.19 | 2.58 | 3.76 | 6.05 |
| 30 | 2.12 | 2.99 | 1.98 | 4.79 | 0.64 | 4.88 | 2.38 | 2.19 | 3.89 | 7.52 |
| 40 | 2.75 | 2.75 | 1.84 | 3.95 | 0.55 | 3.82 | 2.86 | 2.09 | 3.76 | 8.05 |
| 50 | 3.45 | 2.43 | 1.73 | 3.37 | 0.49 | 3.18 | 3.17 | 2.12 | 3.58 | 8.60 |
| 60 | 4.13 | 2.23 | 1.66 | 2.80 | 0.47 | 2.83 | 3.75 | 2.26 | 3.34 | 9.46 |
| 70 | 4.94 | 2.07 | 1.44 | 2.50 | 0.46 | 2.48 | 4.34 | 2.36 | 3.24 | 10.99 |

| Height | B11 | B12 | B13 | B14 | B15 | B16 | B17 | B18 | B19 | B20 |
|---|---|---|---|---|---|---|---|---|---|---|
| 5 | 3.55 | 5.50 | 4.04 | 3.55 | 2.40 | 1.69 | 1.14 | 2.34 | 1.10 | 1.31 |
| 10 | 1.94 | 2.53 | 2.36 | 2.79 | 1.83 | 1.26 | 1.06 | 1.14 | 0.92 | 0.70 |
| 20 | 0.95 | 1.37 | 1.43 | 2.00 | 1.68 | 1.13 | 1.09 | 0.78 | 0.72 | 0.40 |
| 30 | 0.85 | 1.06 | 1.11 | 1.88 | 1.67 | 1.13 | 1.17 | 0.75 | 0.67 | 0.37 |
| 40 | 0.80 | 0.92 | 1.03 | 1.66 | 1.58 | 1.22 | 1.26 | 0.73 | 0.66 | 0.35 |
| 50 | 0.77 | 0.87 | 0.97 | 1.46 | 1.64 | 1.35 | 1.26 | 0.75 | 0.62 | 0.34 |
| 60 | 0.79 | 0.86 | 0.92 | 1.34 | 1.71 | 1.51 | 1.29 | 0.82 | 0.59 | 0.36 |
| 70 | 0.86 | 0.84 | 0.88 | 1.28 | 1.73 | 1.72 | 1.34 | 0.90 | 0.56 | 0.38 |

| Height | C01 | C02 | C03 | C04 | C05 | C06 | C07 | C08 | C09 | C10 |
|---|---|---|---|---|---|---|---|---|---|---|
| 5 | 1.66 | 3.50 | 2.19 | 1.14 | 0.71 | 2.22 | 0.48 | 1.50 | 0.85 | 1.89 |
| 10 | 1.60 | 2.20 | 1.43 | 1.06 | 0.55 | 1.52 | 0.61 | 0.98 | 0.69 | 1.49 |
| 20 | 1.32 | 1.96 | 1.17 | 0.93 | 0.36 | 1.20 | 0.68 | 0.89 | 0.62 | 1.22 |
| 30 | 1.12 | 1.98 | 1.18 | 0.88 | 0.30 | 1.11 | 0.83 | 0.84 | 0.63 | 1.12 |
| 40 | 0.95 | 2.01 | 1.22 | 0.88 | 0.28 | 1.09 | 0.85 | 0.76 | 0.67 | 1.09 |
| 50 | 0.79 | 2.17 | 1.30 | 0.84 | 0.27 | 1.09 | 0.85 | 0.75 | 0.68 | 1.00 |
| 60 | 0.71 | 2.70 | 1.45 | 0.83 | 0.27 | 1.08 | 0.90 | 0.77 | 0.67 | 0.93 |
| 70 | 0.67 | 3.26 | 1.71 | 0.88 | 0.27 | 1.09 | 1.00 | 0.77 | 0.66 | 0.89 |

| Height | C11 | C12 | C13 | C14 | C15 | C16 | C17 | C18 | C19 | C20 |
|---|---|---|---|---|---|---|---|---|---|---|
| 5 | 2.73 | 0.59 | 2.74 | 4.29 | 0.74 | 0.40 | 1.65 | 2.05 | 3.90 | 1.20 |
| 10 | 1.95 | 0.63 | 2.04 | 5.59 | 0.51 | 0.32 | 1.29 | 2.84 | 2.42 | 0.69 |
| 20 | 1.89 | 0.56 | 1.66 | 5.73 | 0.39 | 0.28 | 1.11 | 3.17 | 1.70 | 0.39 |
| 30 | 1.92 | 0.63 | 1.46 | 5.50 | 0.38 | 0.28 | 1.03 | 3.32 | 1.38 | 0.33 |
| 40 | 2.20 | 0.62 | 1.41 | 5.47 | 0.38 | 0.28 | 0.98 | 3.32 | 1.31 | 0.30 |
| 50 | 2.91 | 0.60 | 1.31 | 5.46 | 0.41 | 0.30 | 0.92 | 3.23 | 1.23 | 0.27 |
| 60 | 3.54 | 0.60 | 1.26 | 5.69 | 0.46 | 0.31 | 0.91 | 3.23 | 1.16 | 0.25 |
| 70 | 4.17 | 0.61 | 1.27 | 5.95 | 0.55 | 0.32 | 0.91 | 3.30 | 1.10 | 0.23 |